Combining Rock Slope Ranking Methods and Performance Monitoring Techniques for Rockfall Geohazards to Advance Geotechnical Asset Management in Alberta

by

Taylor Del Gerhard Wollenberg-Barron

A thesis submitted in partial fulfillment of the requirements for the degree of

Master of Science

in

Geotechnical Engineering

Department of Civil and Environmental Engineering
University of Alberta

Abstract

Alberta Transportation and Economic Corridors (TEC) are currently working towards the development and implementation of a formalized Geotechnical Asset Management (GAM) program to manage the diverse range of both geotechnical and transportation assets present along Alberta's roadway infrastructure. This requires the assessment of available tools to effectively collect and manage data for both funding forecasting and evidence-based decision making.

The Geohazard Risk Management Program (GRMP) is TEC's current system for the assessment, monitoring, and prioritization for mitigation of geohazard sites identified along the Province's roadway infrastructure. The objectives of this thesis were to develop a methodological basis for combining the results of initial condition assessment tools, including the GRMP Risk Level Rating, and slope performance monitoring techniques to provide an additional tool for the prioritization of resource allocation for rockfall geohazards. This included this assessment of applicable initial condition assessment tools, quantifying the results of performance monitoring techniques, and correlating these the results across multiple sites in a practical and repeatable way that TEC could implement as part of a formalized GAM program.

A suite of potential condition assessment tools was selected from the results of a literature review. The intent of the study was to focus on practical assessment tools which could be applied relatively quickly and without the need for specialized equipment, following the methodology of TEC's current Regional Slope Tours. The condition assessment tools were applied to several rockfall geohazard sites which existed within TEC's current asset inventory. The sites were selected to cover a wide range of documented hazard levels to test the effectiveness of each condition assessment tool in Alberta's geological setting. The results of the field assessment were compiled and correlated against the GRMP Risk Level rating system,

comprising a Probability Factor and a Consequence Factor. From the results of this comparison, select condition assessment tools were short-listed for use based on their effective correlation with the GRMP rating system components. Three of the rockfall geohazard sites included in the study had pre-existing remote sensing databases. This information was built upon, and change detection analysis was performed as a means to quantify each slope's performance. The shortlisted condition assessment results of these three slopes were then compared to two performance metrics derived from the change detection results. The selected performance metrics were the estimated annual failure volumes and frequency of events greater than or equal to 1 m^3 from failure volume-frequency plots developed for each site.

From the results presented in this thesis, the GRMP rating system was determined to be a viable condition assessment tool as part of the formalized GAM program. The GRMP rating system components correlated well with industry accepted and rigorously tested slope rating and rock mass rating systems such as the Rockfall Hazard Rating System (RHRS), Q-Slope, and Geological Strength Index (GSI). Strong correlations were subsequently developed between these short-listed condition assessment tools and the rockfall metrics derived from the change detection results. A practicable and repeatable methodology was successfully developed to directly compare the results of condition assessment tools with the results of rock slope performance monitoring techniques. The analysis presented in this thesis provides a basis for which TEC, or other transportation agencies, can build upon with data from additional rockfall geohazards to improve the prioritization of maintenance and remedial measures, based on a quantified level of hazard.

Preface

A version of Chapter 3 from this thesis is being prepared for submission to the MDPI

Geosciences journal with the following citation:

Wollenberg-Barron, T.D.G., Macciotta R., Gräpel, C., Tappenden, K.M., and Skirrow, R.K. 2023. Comparison of Rating Systems for Alberta Rock Slopes, and Assessment of Applicability for Geotechnical Asset Management. University of Alberta Geotechnical Centre [Unpublished].

A version of Chapter 4 from this thesis is being prepared for submission to the Landslides

Journal with the following citation:

Wollenberg-Barron, T.D.G., Macciotta R., Mirhadi, N., Gräpel, C., Tappenden, K.M., and Skirrow, R.K. 2023. Combining Change Detection and Slope Condition Assessment Tools to Enhance Geotechnical Asset Management in Alberta. University of Alberta Geotechnical Centre [Unpublished].

Dedication

This work is dedicated to my parents, Marlene, Dan, and Sandra for their unwavering support along the journey getting here and my partner Rebecca for her constant reassurance and understanding as I worked towards the completion of this document.

Acknowledgements

Table of Contents

List of Tables

List of Figures

List of Abbreviations

AADT – Average Annual Daily Traffic

AASHTO – American Association of State Highway and Transportation Officials

ACIS – Alberta Climate Service

AVR – Average Vehicle Risk

C2C – Cloud-to-Cloud Comparison

C2M – Cloud-to-Model Distance

CF – Consequence Factor

CRHRS – Modified Colorado Rockfall Hazard Rating System

DoD – DEM of Difference

DOT – Department of Transportation

FHWA – Federal Highway Administration

FIP – Field Implementation Plan

GAM – Geotechnical Asset Management

GCP – Ground Control Point

GRMP – Geohazards Risk Management Program

GSI – Geological Strength Index

KCB – Klohn Crippen Berger

LiDAR – Light Detection and Ranging

LoD – Limit of Detection

LS – Length of Slope

M3C2 – Multiscale Model to Model Cloud Comparison

PF – Probability Factor

PSL – Posted Speed Limit

R^2 – Coefficient of Determination

RHRS – Rockfall Hazard Rating System

RL – Risk Level

RMR – Rock Mass Rating

RQD – Rock Quality Designation

SMR – Slope Mass Rating

SOR – Statistical Outlier Removal

TAM – Transportation Asset Management

TEC – Alberta Transportation and Economic Corridors

UAV – Unmanned Aerial Vehicle

vpd – Vehicles per Day

WAADT – Weighted Average Annual Daily Traffic

Chapter 1

Introduction

1.1 Background

Asset management is a concept that emerged in the transportation industry to address the need for a system to monitor, optimize, and upgrade infrastructure cost effectively (FHWA 1999). Transportation assets refers to constructed infrastructure such as pavements, bridges, or railway tracks. These assets rely, quite literally, on the performance of the underlying geotechnical assets (Bernhardt et al. 2003). This highlights the importance of the performance of geotechnical assets on transportation infrastructure. While not all geotechnical assets are exclusively linked to transportation assets and highway or railway subgrades; embankments, slopes, and retaining structures are also considered geotechnical assets. The implementation of Transportation Asset Management (TAM) programs has become part of national requirements in North America and Europe and Geotechnical Asset Management (GAM) emerged from TAM to manage complex risk uncertainty introduced by the natural variability and/or knowledge uncertainty of geotechnical assets. Deterioration curves are often used in TAM to track and forecast the condition of assets, such as pavements, and have been shown to significantly extended their service life (Stanley and Pierson 2013). Deterioration curves for geotechnical assets, such as rock slopes, within the same transportation corridor will vary based on several geologic and climatic factors and must be uniquely tailored for each site (Vessely 2013).

Alberta Transportation and Economic Corridors (TEC) monitors geohazard sites across Alberta through the departments Geohazard Risk Management Program (GRMP).

The GRMP was established as the Province's program to identify and monitor geotechnical assets and determine strategies for risk management, maintenance, and rehabilitation (Tappenden and Skirrow 2020). TEC is currently working towards the development of a formalized GAM program to enhance their ability to monitor the condition and deterioration of geotechnical assets. This requires the assessment of available tools to effectively collect and manage data for both funding forecasting and evidence-based decision making (Tappenden and Skirrow 2020).

The most prominent condition assessment tool used in GAM programs throughout the United States is the Rockfall Hazard Rating System (RHRS). The RHRS was introduced in the early 1990s by Pierson (1992) and initially implemented by the Oregon Department of Transportation (DOT) and subsequently by 2012, 28 transportation agencies in North America have adopted rockfall management systems based on the RHRS (Pierson 2012). One of the modified RHRS adopted by the Colorado DOT was reviewed as a possible candidate for TEC's GAM program. The modified Colorado RHRS (CRHRS) (Santi et al. 2008) was considered in this research as a modernized version of the RHRS tailored for use in the Rocky Mountains in Colorado, sharing some geological characteristics of those found in Alberta. Other more widely accepted geological characterization tools, such as the Geological Strength Index (GSI) (Hoek 1994), the Rock Mass Rating (RMR) system (Bieniawski 1993) and the Q-Slope system (Barton and Bar 2015) were also considered even though they have no capacity to quantify the consequence of slope failure.

In addition to the initial condition assessment of a rockfall geohazard, continued monitoring of a slope's performance is critical to prioritize the allocation of resources for

high-risk slopes and for the development of site-specific deterioration curves. Especially considering it takes years of monitoring to estimate a geotechnical assets life expectancy (Stanley and Pierson 2013). Slopes performance of rockfall geohazards may be measured with the aid of remote sensing techniques. Surveys of slopes using remote sensing techniques, such as Unmanned Aerial Vehicle (UAV) photogrammetry or Light Detection and Ranging (LiDAR), can be used to generate temporally independent point clouds which can be compared to calculate slope changes. This process, known as change detection, and the use of point clouds generated through remote sensing techniques has seen significant use in geotechnical engineering for rock slope to assess rock mass characteristics (Sturzenegger and Stead 2009, Gigli and Casagli 2011, Lato et al. 2009, Riquelme et al. 2016, Riquelme et al. 2017), identify rockfall hazards and precursors (Abellán et al. 2010, Kromer et al. 2015, Kromer et al. 2017), and determine failure kinematics (Oppikofer et al. 2009, Maerz et al. 2012, Justice 2015, Rodriguez et al. 2020, Woods et al. 2021). The challenge that departments of transportation face is how to relate slope condition assessment tools that are practicable to deploy along extensive transportation corridors, with the actual performance of the slopes, in order to optimize resource allocation.

1.2 Problem Description

Transportation agencies lack a systematic way of assessing the condition of rockfall geohazards, monitoring their performance, and combining the two in a way that improves their prioritization for resource allocation. TEC can benefit from research which works towards standardizing the integration of rock slope rating systems with monitoring for rock slopes in a practicable and repeatable manner. This requires the assessment of

3

available tools to effectively collect and manage data for both funding forecasting and evidence-based decision making (Tappenden and Skirrow 2020), as well as the development of the correlations between condition assessments and slope performance. This further requires development of slope performance metrics that reflect the economic and safety requirements of the transportation agency.

1.3 Thesis Objectives

The overarching objective of this research is to develop a methodological basis for leveraging the results of initial condition assessment tools and slope performance monitoring techniques to assist transportation agencies with an additional tool to prioritize the allocation of resources for rockfall geohazards. This requires the development of correlations between rock slope initial condition assessment tools to assess the viability of each. Quantifiable metrics must also be derived from slope performance techniques to provide a means to correlate with the condition assessment results. The study sites selected for the application of initial condition assessment tools and remote sensing techniques were focused on Alberta's geological setting so that the results could be integrated into TEC's developing GAM program.

The specific objectives of this thesis are:

1. Summarize the state of practice of geotechnical asset management in a literature review covering the development and application of asset management programs for transportation infrastructure and subsequently, geotechnical assets.

2. Provide recommendations on rock slope and rock mass rating systems as initial condition assessment tools on the basis of their practicability for use on rock slopes in Alberta, apply them to existing rockfall geohazards in Alberta, and

provide a shortlist of viable condition assessment tools which may be used by TEC as part of a formalized GAM program.

3. Propose a methodology to develop correlations between initial condition assessment tools and metrics derived from measured slope performance techniques for a practicable and efficient allocation of resources for rock slope maintenance.

4. Illustrate the application of the proposed methodology on a number of existing rockfall geohazard sites within TEC's asset inventory and provide initial correlations to initiate a database for combining the ratings of viable condition assessment tools and the results of performance monitoring through change detection analysis which may be applied to rockfall geohazards across Alberta to form a basis for the prioritization of resources to relatively high-risk rockfall geohazards.

1.4 Overview of the Methodology

The first step taken to complete this thesis was to conduct a narrative literature review. The synthesis of the literature review led to the selection of six initial condition assessment tools for application to rockfall geohazard sites in Alberta, including TEC's GRMP Risk Level (RL) rating. The other rock slope and rock mass rating systems were selected considering time restrictions imposed during a standard annual slope inspection tour conducted by TEC and their consultants. The selected rating systems included: the RHRS, the CRHRS, Q-Slope, GSI, and RMR. A Field Implementation Plan (FIP) was developed which outlined the individual application methodologies of each of the selected rating systems to support the application of each in the field.

The first three Albertian rock slopes which were selected for inclusion in this research were the C018 site, the S020 site, and the S042 site. These sites were included since remote sensing databases had already been initiated for each of these sites. To assist in the selection of additional rockfall geohazards, Klohn Crippen Berger (KCB) was contacted to request recommendations for active and expired rockfall geohazard sites within TEC's asset inventory. The additional slopes included were selected based on their existing GRMP RL ratings to ensure the group of study sites would cover a wide range of hazard levels. The remaining study sites included are the S018 site, the S057 site, the S070 site, and the S074 site. Detailed descriptions for each of the study sites are presented in Chapter 3.

The first application of the rating systems was conducted at the C018 site on November 12, 2021. The rating systems were applied at the remainder of the study sites between September 24 and 25, 2022. Site visits were conducted annually as part of this thesis to collect LiDAR data of the S042 site, beginning in 2021. All previous scans of the S042 site were completed by previous or concurrent members of the University of Alberta Geotechnical Centre. The 2022 data collection of the S042 site coincided with the application of the rating systems on September 25, 2022. UAV surveys of the C018 site and the S020 site and generation of point clouds through photogrammetry were completed by others including Renato Macciotta, Nima Mirhadi, and Jorge Rodriguez. The compilation of point clouds generated via remote sensing and subsequent change detection analyses of the S020 site and S042 site was completed as part of this thesis utilizing the CloudCompare V2.12 software (CloudCompare 2022). A detailed change

detection methodology is presented in Chapter 4. Change detection for the C018 site was completed by Nima Mirhadi and included in the analysis presented in Chapter 4.

1.5 Outline of the Thesis

This thesis is structured into five chapters, including this introduction chapter, following a paper-based format. Chapter 2 comprises a narrative literature review conducted on relevant topics to provide context for the subsequent chapters. Chapters 3 and 4 are manuscripts submitted for publication. Chapter 3 (Manuscript 1) titled "Comparison of Rating Systems for Alberta Rock Slopes, and Assessment of Applicability for Geotechnical Asset Management" provides the evaluation of several possible initial condition assessment tools, including TEC's current method, the GRMP RL rating. Chapter 4 (Manuscript 2) titled "Combining Change Detection and Slope Condition Assessment Tools to Enhance Geotechnical Asset Management in Alberta" presents the results of change detection analyses for three rockfall geohazards in Alberta and a methodological basis for combining their results with those of viable initial condition assessment tools. The change detection analyses for the C018 site were prepared by Nima Mirhadi (Ph.D. candidate at the University of Alberta) and included in this research as an additional data set. Finally, Chapter 5 provides the general conclusions of this thesis and recommendations for future research.

Chapter 2

Literature Review

2.1 Introduction

The content of this literature complements the literature review presented in the introductory sections of Chapter 3 and Chapter 4. Sections covering rock slope and rock mass rating systems, including the GRMP RL rating, Q-Slope, RMR, and GSI, as well as remote sensing techniques, including UAV photogrammetry, Light Detection and Ranging (LiDAR), and change detection, are presented in Chapter 3 and Chapter 4, respectively.

2.2 Asset Management

Asset management is a concept that has been around for many years with the implementation of programs dating back to the 1980s and 1990s in Canada, Australia, New Zealand, and Europe (Wolf et al. 2015). Asset management is defined by the Federal Highway Administration (FHWA 1999) as "*... a systematic approach of maintaining, upgrading, and operating physical assets cost effectively. It combines engineering principles with sound business practices and economic theory, and it provides tools to facilitate a more organized, logical approach to decision making. Thus, asset management provides a framework for handling both short- and long-range planning*".

To understand the management of any kind of asset, one must first grasp the key concepts of asset management, including inventory, condition, life-cycle costs, risk, performance, and prioritization (Vessely et al. 2019). Understanding these concepts in

conjunction with knowledge pertaining to the owned assets in question provides major benefits to the managing agency. These benefits include the reduction in asset life-cycle costs, defined service level requirements, performance tracking improvements, transparency in decision making, consequence prediction feasibility, and decreased financial and operational risk (Shah et al. 2014).

In TAM the development of performance measures has been an important area of research. Performance measures help to summarize the condition of an asset and indicate the need for additional service to maintain functionality (Dehghanisanij et al. 2012). Difficulties in this process arise when connecting performance measures with allocation of resources. Traditionally, performance measures have been technical in nature to capture the engineering and/or operational attribute of the system it is measuring. More recently, the use of a more diverse range of performance measures has been implemented to capture the increasingly complicated and wider range of problems present in the transportation industry (Cambridge Systematics et al. 2006). Performance measures should quantifiably communicate the condition of an asset but must also be based on an agency's goals so that policy makers can monitor the effectiveness of the systems in place and effectively improve policies.

An important asset management concept and area of research pertaining to the life-cycle cost of a particular asset is the development of deterioration models. Since the lifespan of any asset is a finite value, analyses of asset condition and reliability must be conducted to determine how proper operation, maintenance, and repairs affect the service life of an asset (Grussing et al. 2006). In addition, environmental factors, improper operations, and lack of maintenance also impact the service life of an asset.

2.2.1 Geotechnical Asset Management

Geotechnical Asset Management (GAM) has emerged from TAM as a necessity due to the importance of the performance of geotechnical assets on transportation infrastructure. The adverse performance of a geotechnical asset may threaten the performance of other transportation assets, such as a retaining wall adjacent to a roadway. The resulting impact on higher-level TAM performance objectives merits the development of more specific GAM programs to target this performance of geotechnical assets.

The framework for a GAM program is generally defined by its governing agency's goals which are often predetermined by agency policies and strategic goals. A clear relationship must be established between an agency's objectives and GAM decisions (Thompson 2017). These goals usually include the management of risk within a transportation system. The next step in GAM development is the collection of data to create an asset inventory. Each asset identified within a target area must be catalogued with its physical characteristics but also some measure of its cost, performance, and impact of failure (Bernhardt et al. 2003). An assessment of the asset's condition is necessary in determining how the agency's limited resources will be used to the greatest benefit. This is particularly difficult for slopes due to the lack of empirical knowledge regarding their anticipated service life, therefore monitoring over several years is necessary to estimate their life expectancy (Stanley and Pierson 2013). Deterioration curves are often used in TAM to track and forecast the condition of assets. This approach has been applied to GAM but with greater uncertainty. Deterioration curves for rock slopes within the same transportation corridor will vary based on geology, microclimate, vegetation, and exposure and must be uniquely tailored for each site (Vessely 2013).

Often program alternatives must be considered to account for uncertainties in funding, costs, and emerging hazards. Standardized performance measurements must be established so that cost/benefit relationships can be used to optimize the program's efficiency (Thompson 2017). This in turn gives rise to the need for robust analytical tools capable of measuring and monitoring the performance of a geotechnical asset. The development of an asset inventory is a continuous process; following the initial assessment and identification of an unstable asset, continued monitoring is required to maintain adequate allocation of resources. Figure 2-1 provides an outline for a typical GAM process.
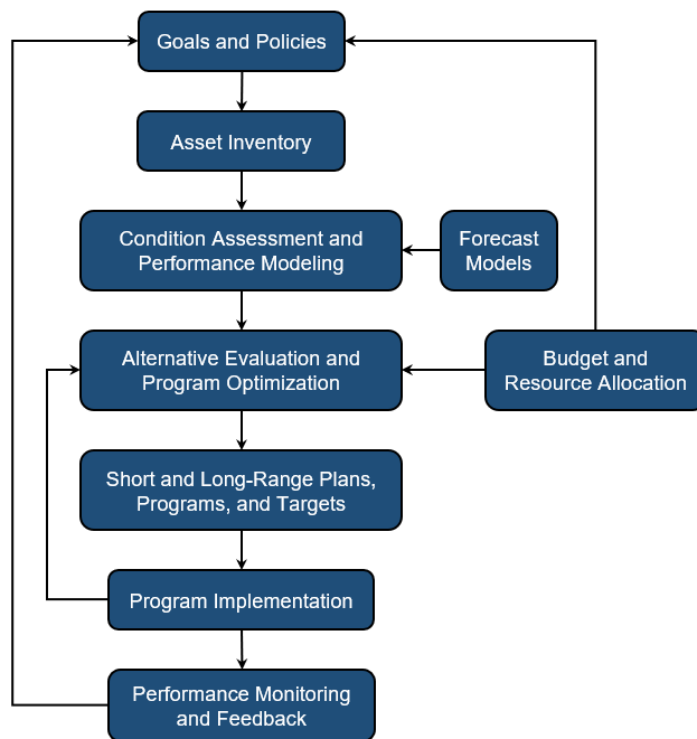
Figure 2-1: Geotechnical Asset Management process (modified from Thompson 2017)

In TAM, research towards integrated performance measurement framework has made it possible to compare different types of assets based on key performance and asset

health indicators. One methodology is to apply individual asset heath ratings and an overall corridor health rating (Dehghanisanij et al. 2012). For GAM however, additional sources of uncertainty are introduced with the variability in soil and rock geology. Similar assets with varying geological condition may require completely different performance measures to acquire a rating for an asset's health.

2.3 Rockfalls

Rockfalls are a geomorphic process in which gravity carries a rock block or mass downslope after it detaches from a slope (Higgins et al. 2012). The initiation of a rockfall event may be the result of several factors. Higgins et al. (2012) broke down these factors into two main influence categories: internal and external. Internal influences include lithology, discontinuities, and groundwater. External influences include climatic conditions (Macciotta et al. 2017, Macciotta 2019, Pratt et al 2019), weathering, anthropogenic causes, earthquakes, and stress relief. Regardless of the influences, rockfalls from slopes comprising competent rock generally result from the characteristics of its discontinuities (Wyllie 2014). The four basic failure types for rockfalls are planar sliding, wedge sliding, toppling, and circular sliding. Planar sliding occurs when a discontinuity dips out of the slope and gravitational kinematics drives rockfall block downslope. Hoek and Bray (1981) outline the following four conditions that must be satisfied for planar sliding to occur:

1.   The plane of sliding is within 20° of the slopes dip direction.

2.   The failure plane "daylights" out of the slope face.

3.   The friction angle of the failure plane is less than its dip angle.

4.	The lateral extents of the failing rock block provide negligible resistance to

sliding.

If two discontinuities intersect obliquely to the slope face, wedge sliding may occur. This

often occurs in rock masses, typically comprising sedimentary rock, with orthogonal joint

sets, bedding planes, or foliations that form a V shaped wedge between them. For

toppling, there are several sub-categories of failure, but it essentially occurs when

subvertical discontinuities form slabs and columns which rotate around their base

(Higgins et al. 2012). Circular sliding is the least structurally controlled of the four basic

failure types and typically occurs in highly weathered or weak rock masses. A circular

failure surface develops along the path of least resistance similar to soil and is not

typically associated with rockfall detachment mechanisms. Regardless of the failure

mechanisms governing rockfall events, they are particularly severe in areas with heavy

precipitation, frequent freeze thaw cycles, and seismic events (Wyllie 2015)

2.4 Rock Slope and Rock Mass Rating Systems

2.4.1 Rockfall Hazard Rating System

The origin of the Rockfall Hazard Rating System (RHRS) dates back to the early 1970s

following train derailments in British Columbia, Canada, when the Canadian government

began to no longer accept slides as an "Act of God" (Brawner and Wyllie 1976). The

goal being to produce a procedure to quantify slopes for prioritization based on the

potential hazard of rockfalls occurring along a transportation corridor. A comprehensive

participants manual for the RHRS was published in the early 1990s by a collaboration of

United States transportation agencies including the Oregon Department of Transportation

and the National Highway Institute (Pierson and Van Vickle 1993).

Following its conception, several US Departments of Transportation (DOT) and other

agencies outside the United States have adopted and modified this RHRS to suit their

specific needs (Russell et al. 2008). Some of the agencies using modified versions of

RHRS include but are not limited to New York DOT (Hadjin 2002), New Hampshire

DOT (Fish and Lane 2002), Missouri DOT (Maerz et al. 2005), Idaho DOT (Miller

2003), Ohio DOT (Shakoor 2005), Tennessee DOT (Vandewater et al. 2005), University

of Naples (Budetta 2004), and Colorado DOT (Stover 1992). Additional details

pertaining to the RHRS, and its scoring categories can be found in Chapter 3.

2.4.2 Colorado Rockfall Hazard Rating System

The Colorado DOT opted to implement a slightly modified version of the RHRS to

address some of the weaknesses identified within the original RHRS (Stover 1992). This

in combination with the Colorado Rockfall Accidents in State Highways (CRASH)

database allowed the Colorado DOT to match mile markers with accidents caused by

rockfalls and focus on the sections of highway most prone to rockfalls. In more recent

years, the modified Colorado RHRS (CRHRS) was developed with additional parameters

validated through use by other state DOTs. The developers of the CRHRS attempted to

further the removal of subjective scoring criteria within the RHRS while incorporating

additional geologic and climatic factors recognized in literature to contribute to rockfalls

(Russell et al. 2008). The CRHRS was tested on 355 Colorado slopes followed by a

statistical analysis of the results to determine the dominating factors controlling rock

slope stability (Santi et al. 2008). The differences between the CRHRS and RHRS along

with descriptions of the added scoring categories is presented in Chapter 3.

2.4.3 Slope Mass Rating System

The Slope Mass Rating (SMR) system was developed by Romana (1985) as an addition to the RMR system specifically for the classification of rock slopes. The SMR system was intended for use as a preliminary assessment for slopes since the RMR lacked clear guidelines for slopes and therefore left a high degree of uncertainty and limited viability for design. The SMR system uses four additional parameters to the RMR system to address the range of failure modes that impact slopes. These parameters were added to an earlier version of the RMR system prior to the introduction of the 'Orientation of discontinuities' factor. Equation 2-1 shows the relationship between RMR and SMR.

$$SMR = RMR + (F_1 \cdot F_2 \cdot F_3) + F_4 \qquad (2\text{-}1)$$

Adjustment factors F1, F2, and F3 are calculated using the dip and dip directions of the slope and individual joints. Measurements must be gathered for each of the major discontinuity planes to determine which is most likely to result in a planar or toppling failure. The final adjustment factor F4 is selected for the excavation method used to construct the slope with 'natural slope' as an option. Romana (1985) empirically determined limit values between different stability classes of SMR for different failure modes. Guidelines for slope support design are available for each SMR stability class which are intended for use in preliminary design and require both detailed field data and significant engineering judgement to apply (Romana et al. 2015).

The SMR system was considered for use in this research but ultimately was not included in the suite of rating systems due to the required discontinuity and slope orientation data required. Detailed rock mapping was considered outside the scope of TEC's standard slope inspection tour. This does not in itself discredit SMR as a valuable

tool for assessing rock slopes. SMR has seen success worldwide as a tool for preliminary slope assessment (Romana et al. 2015). With the help of modern remote sensing techniques, joint and slope orientations can be extracted from surface or point cloud files to determine SMR parameters.

2.5 Extraction of Rock Mass Characteristics

In recent years software has been developed for the semi-automated extraction of rock mass joint and discontinuity information from remote sensing data (Haneberg et al. 2006, Lato et al, 2009, Gigli and Casagli 2011, Otoo et al. 2011, Riquelme et al. 2014, Riquelme et al. 2015, Riquelme et al. 2017). Joint orientation data for slopes may then be applied to the SMR system as another comparative tool to assess the condition of slopes. When applying these techniques, it is important to note the limitations of how the point cloud was derived. LiDAR is better suited to detect discontinuity facets i.e., the discontinuity surfaces exposed on the rock face, while photogrammetry better captures fracture traces i.e., the intersections between discontinuities on the rock face (Otoo et al. 2011).

Although the extraction of discontinuity information is not pursued further in the course of this research, there exists an opportunity for the integration of monitoring, in particular remote sensing, with slope rating and quantification to correlate slope ratings to slope performance. This can be achieved through correlations between slope rating and rockfall intensity and slope deformations, without the necessity to wait for a significant instability. This would allow more insight into the critical range of a particular rating system implemented for a GAM program.

Chapter 3

Comparison of Rating Systems for Alberta Rock Slopes, and Assessment of Applicability for Geotechnical Asset Management

Contributions made to this Chapter:

The work presented in this chapter, which includes literature review, collection of field data, methodology, analysis, discussion of results, and writing of the text was carried out by the M.Sc. Recipient.

Dr. Renato Macciotta reviewed all parts of the work and provided guidance during the development of the methodology and its application. The other authors reviewed the text and provided recommendations for edits and additional discussion.

A version of this Chapter is being prepared for submission to the MDPI Geosciences journal with the following citation:

Wollenberg-Barron, T.D.G., Macciotta R., Gräpel, C., Tappenden, K.M., and Skirrow, R.K. 2023. Comparison of Rating Systems for Alberta Rock Slopes, and Assessment of Applicability for Geotechnical Asset Management. University of Alberta Geotechnical Centre [Unpublished].

Abstract

In 1999, Alberta Transportation and Economic Corridors (TEC) implemented the Geohazard Risk Management Program (GRMP) to identify, assess, monitor, and prioritize the mitigation of risk resulting from geohazard events at specific sites along the provincial highway network. Engineering design and construction supervision services are retained under the GRMP for existing and emerging geohazard sites that are

programmed for capital repairs. The GRMP was developed to address a variety of geohazard types including rockfall hazards that occur at natural and constructed (cut) highway backslopes. The analysis methods described in this paper are intended to assist TEC in the development of a framework to provide the basis for robust morphological inspection and monitoring of rockfall geohazards. An evaluation of various methods for condition assessment of rockfall geohazards, including TEC's current GRMP risk rating system, has been completed with the intent of better understanding the suitability of each method as TEC transitions to a formalized GAM program (Tappenden and Skirrow 2020). The GRMP risk rating values for selected rockfall geohazard sites along highway corridors in Alberta were compared to values developed from results of five established rock mass and rock slope rating systems. Diligent evaluation and ongoing review of asset condition and risk assessment tools is an essential part of GAM. This provides valuable feedback to policy makers for the advancement and optimization of their monitoring programs and prioritization for resource allocation. The results of this study demonstrate that TEC's current GRMP risk rating system is a viable tool for condition assessment and performance monitoring of rockfall geohazards, which could be utilized within a formalized GAM program, further benefitting from years of recorded application in Alberta. Of the other rating systems tested, the rockfall hazard rating system (RHRS) showed a strong correlation with the GRMP risk rating while Q-Slope, the Geological Strength Index (GSI) and Rock Mass Rating (RMR) correlation were marginal but displayed a potential for use as condition assessment tools.

3.1 Introduction

The concept of asset management, in a formalized sense, has been present in the minds of civil engineers for nearly half a century, with the earliest implementation of Transportation Asset Management (TAM) programs dating back to the 1980s and 1990s (Wolf et al. 2015). One definition of asset management by the American Association of State Highway and Transportation Officials (AASHTO 2020) is a "strategic and systematic process of operating, maintaining, upgrading, and expanding physical assets effectively throughout their life cycle." Although the definition may differ depending of the types of assets present, the goal of an asset management program is to build, operate, and maintain assets in a cost-effective manner in hopes to inevitably improve asset performance (Wolf et al. 2015).

Geotechnical Asset Management (GAM) has emerged from TAM due to the impact and interrelated performance of geotechnical assets on transportation infrastructure. Geotechnical assets may range from inclusive to completely exclusive of transportation assets. Examples of inclusive assets are culverts, drainage ditches, bridge foundations, and pavement subgrade. Exclusively or partially exclusive geotechnical assets comprise both natural and constructed assets, including rock and soil slopes, embankments, retaining structures, and tunnels (Bernhardt et al. 2003). These lists are not exhaustive and often vary depending on the GAM owner requirements.

GAM includes an undeniable degree of increased uncertainty when compared to TAM. This uncertainty may be attributed to natural variability and/or knowledge uncertainty. Natural variability can be both spatial and temporal, e.g., changes in soil and rock stratigraphy, material strengths, and presence of groundwater. Knowledge

uncertainty is associated with a lack of data regarding past events, or lack of understanding of the physical laws or processes taking place within a particular geotechnical asset (Christian and Baecher 2003). For GAM, this means similar assets with varying geological conditions may require different measures to quantify and evaluate asset performance.

Alberta Transportation and Economic Corridors (TEC) is currently working towards the development of a formalized GAM program to enhance the Province's ability to monitor the condition and deterioration of geotechnical assets, and to effectively prioritize candidate mitigation projects based on the risk an asset poses to highway safety and efficiency. This requires the assessment of available tools to effectively collect and manage data for evidence-based decision making when prioritizing investments and advocating for future funding needs (Tappenden and Skirrow 2020). TEC has documented approximately 500 geohazard sites, 250 of which are actively monitored through the department's Geohazard Risk Management Program (GRMP) (Tappenden and Skirrow 2020). The GRMP inventory includes soil and rock slopes, highway embankments, retaining walls, and highway subgrades, adopting the terminology of Anderson et al. (2016). These sites are assessed using TEC's GRMP risk level rating methodology, presented in Section 3.2.1, which allows the direct comparison of relative risk level for earthflow and debris flow, rockfall, and erosion geohazards. Geotechnical asset management programs include several asset classes, as described above, and may encounter difficulty when cross-asset comparisons are undertaken to establish capital funding distributions. The concept of risk can be useful to determine which sites are in more urgent need of remediation. In the interests of furthering a risk-based GAM

20

program TEC can benefit from research that progresses the development of a framework to provide a morphological inspection and monitoring basis for rockfall geohazards.

This study focuses on the tools available to assess and monitor rockfall geohazards which are some of the more frequent geohazards encountered along highways in Alberta (Macciotta and Martin 2019, Macciotta et al. 2020). Rockfalls are a geomorphic process in which a rock block or mass travels downslope after it detaches from a slope (Higgins et al. 2012). The initiation of a rockfall event may be the result of several factors. Higgins et al. (2012) describe two main influence categories: internal and external. Internal influences include lithology, discontinuities, and groundwater. External influences include climatic conditions (Macciotta et al. 2018, Macciotta 2019, Pratt et al 2019), weathering, anthropogenic causes, earthquakes, and stress relief. Regardless of the influences, rockfalls from slopes comprising competent rock generally result from the characteristics of its discontinuities (Wyllie 2015).

In this paper, rock slope and rock mass rating systems, including TEC's GRMP risk rating system, are compared to evaluate their consistency and provide insight into the suitability of these methods as basis for a future GAM program. The study involved application of the various rating systems to several rockfall-prone slopes along the Alberta highway network, to test their practicability while considering future integration and consistency with monitored slope performance (e.g., deformation monitoring, rock fall frequencies). The paper presents the results of five rock mass and rock slope rating systems applied to eight rockfall geohazard sites in Alberta, compared against the documented GRMP risk rating values for each site. Although some of the selected rating systems are not intended to quantify risk, they were included regardless as widely

accepted industry tools for characterizing rock slopes or rock masses that can provide a measure of slope condition within a GAM framework. The sites were selected with the intention of capturing a wide range of risk levels. Three of the included sites with relatively high GRMP risk ratings have existing remote sensing data that will be incorporated with the results of this study for future evaluation of slope rating tools. A brief description of each geohazard site including geologic context, available history of geohazard occurrences, and difficulties encountered during application of each of the rating systems are also presented herein.

3.2 Rock Slope and Rock Mass Rating Systems

3.2.1 GRMP Risk Level Rating

TEC's GRMP was established in 1999 with the objective of supporting and maintaining the safety and reliability of the province's highway network (Tappenden and Skirrow 2020). The GRMP is TEC's method for documenting unstable geohazard sites, assessing their relative risk, and determining strategies for both short-term and long-term risk management, maintenance, and rehabilitation (Tappenden and Skirrow 2020).

The GRMP uses field inspection observations and instrumentation readings to assign a relative risk level (RL) rating on a scale of 1 to 200 for each geohazard site. The RL is calculated utilizing a multiplication-based rating system presented in Equation (3-2. A probability factor (PF) ranging on a scale from 1 to 20 and a consequence factor (CF) ranging on a scale of 1 to 10 are selected for each geohazard site, based upon the likelihood of a highway service disruption due to a geohazard occurrence, and the attendant consequences. The product of these factors results in the RL of the site. The PF, CF, and resulting RL are determined through a workshop style discussion on site between

consultant representatives, TEC engineers, and local highway operations staff. This ensures the selected parameters reflect an aggregate of opinions from various perspectives.

$$\text{Risk Level (RL)} = (\text{Probability Factor, PF}) \times (\text{Consequence Factor, CF}) \qquad (3\text{-}2)$$

TEC has four tables of probability and consequence factors for (a) earth slides and debris flows, (b) rockfalls, (c) erosion, and (d) voids-dispersive soil sites to address the majority of geohazards that affect transportation corridors in Alberta. Table B, covering rockfall geohazards, is available in Appendix A to this paper (AMEC 2006). TEC and their consultants use these factors and corresponding RL to prioritize sites for intervention. The reliability of the GRMP risk rating system requires thoughtful deliberation when selecting appropriate parameter values. The scorers must consider the limitations imposed by visual inspection and the GRMP's qualitative categories, such as limited access to the slope, height and distance from the slope, and information (or lack thereof) regarding historical geohazard activity for each site. Tappenden and Skirrow (2020) acknowledge that the current GRMP risk rating system does not include a direct measure of risk exposure; low traffic volume highways can have the same RL as analogous feature on a high traffic volume highway. Tappenden and Skirrow (2020) suggest that this shortcoming could be mitigated for rock slopes with the inclusion of additional components incorporating a measure of the average annual daily traffic (AADT), similar to the Rockfall Hazard Rating System (RHRS) discussed further in Section 3.2.2.

3.2.2 Rockfall Hazard Rating System (RHRS)

The RHRS was published in the early 1990s following an extensive development and testing program, involving over 3,000 sites, by the Oregon Department of Transportation in collaboration with several other United States transportation agencies and the Federal Highway Administration (Pierson L.A. 1992). Their goal was to provide transportation departments with a rational way to make informed decisions on where and how to spend construction funds to reduce the risk associated with rockfall (Pierson L.A. 1992).

The RHRS uses an exponential scoring system of 12 categories, 10 of which are summed together to generate a hazard score. Categories cover a range of slope characteristics (slope height, geological character, and volume of rockfall/block size), environmental factors (climate and presence of water on slope), rockfall history, and traffic vulnerability (ditch effectiveness, average vehicle risk (AVR), decision sight distance, and road width) (Pierson and Van Vickle 1993). AVR is a value developed to estimate the amount of time a vehicle spends within a rockfall prone area. AVR is calculated using Equation (3-3 based on the AADT, posted speed limit (PSL), and length of a slope (LS) (Pierson and Van Vickle 1993). With the inclusion of categories which cover rockfall consequences, the RHRS may be directly compared to the GRMP RL.

$$\text{AVR} = 100\% \times (\text{ADT} \left(\frac{vehicles}{day}\right) \times \frac{LS \ (km)}{24 \ (hrs/day)} \ )/ \ \text{PSL (km/hr)} \qquad (3\text{-}3)$$

Slopes with scores below 300 may be considered as low priority while slopes with scores over 500 are considered urgent priority for remedial action (Justice 2015; Budetta 2004). After its conception, the RHRS has been directly adopted or modified for use by at least 25 Departments of Transportation (DOT) of US states (Pierson et al. 2012). Through its extensive use it has proven to be a capable tool for preliminary risk

assessment of rock slopes and the development of asset inventories to facilitate the implementation of GAM programs. The simplicity of the RHRS allows for the categorization of vast slope databases without requiring specialized training, equipment, or subsurface exploration. The simplicity of the RHRS doesn't come without some downfalls, including: the subjective terminology for several of the RHRS categories may introduce inconsistency between different scorers (Rose 2005), some of the internal and external influences known to contribute to rockfalls are not captured, and only two parameters exist to gauge the impact of geologic conditions which may lead to high scoring when the geological conditions are unlikely to produce rockfalls. (Russel et al. 2008).

3.2.3 Modified Colorado Rockfall Hazard Rating System

The current version of Colorado's RHRS was developed at the Colorado School of Mines (Russel et al. 2008, Santi et al. 2008). The significantly increased complexity of the modified Colorado RHRS (CRHRS), compared to its predecessor, mitigates some of the limitations present in the original RHRS. While the original RHRS uses the sum of 10 parameters to determine the slope score, the CRHRS increases the number of parameters to 21. The CRHRS breaks down the geologic character of a slope into 3 categories: sedimentary rock, crystalline rock, and block-in-matrix, e.g., conglomerates and till, each with differing hazard morphology and trigger characteristics. These additions help the scorer distinguish between failure mechanisms and structural influences. For the sedimentary rock categories, Jar Slake test (Walkinshaw and Santi 1996) results are required for scoring. A modified Jar Slake testing procedure was proposed by Santi et al. (2008) to improve the consistency of the results and make the test more "field friendly".

This testing procedure was reviewed, along with the Colorado Department of

Transportation (2020) published testing procedures to determine the Jar Slake category

scores for each of the applicable Alberta study areas.

The CRHRS also incorporates three additional parameters to better account for

climatic factors, including score ranges for annual precipitation, annual freeze thaw

cycles, and slope aspect. Collection and review of weather data is required to address the

categories pertaining to average yearly precipitation and number of freeze thaw cycles.

For this study, the Alberta Climate Service (ACIS 2022) database was used to collect

daily and monthly precipitation and air temperature data near the project sites. The

CRHRS also revised several other parameters from the original RHRS to reduce the

subjectivity by providing specific ranges for scoring. The goal for these modifications

was to ultimately improve the consistency of the scoring system while increasing its

complexity and requiring more specific geotechnical training and measurement tools to

properly implement. Considering its advantages and disadvantages, the CRHRS was

accepted in this study as a refined RHRS model developed in a similar geologic and

climatic setting as Alberta's transportation corridors, and suitable for direct comparison

to the GRMP RL.

3.2.4 Q-Slope

The original Q-system introduced by Barton et al. (1974) is a rock mass classification

method with the capability of providing tunnel support and reinforcement design

recommendations. After nearly 60 years of use, the Q-System remains a staple tool in

geotechnical engineering, having been applied in thousands of civil and mining

engineering projects around the world (Barton and Grimstad 2014). The Q-Slope System,

introduced by Barton and Bar (2015), is intended for use on slope cuts adjacent to roads or railways, and benches of open pit mines (Bar et al. 2016). Q-Slope uses the same six parameters as the original Q-System with some modifications to account for different structurally controlled failure mechanisms, a wider range of environmental conditions, and additional reduction factors relevant to slopes (Bar et al. 2016). The Q-Slope system is essentially a function of three parameters: Block size (RQD/J_n); shear strength of the least favourable joint set or average shear strength for potential wedge failure ($(J_r/J_a)_0$); and external influences including environmental and in-situ stress (J_{wice}/SRF_{slope}) (Bar and Barton 2017). Equation (3-4 presents the modified parameters to determine the Q-Slope value.

$$Q_{slope} = \frac{RQD}{J_n} \cdot \left(\frac{J_r}{J_a}\right)_0 \cdot \frac{J_{wice}}{SRF_{slope}} \tag{3-4}$$

Equation (3-5 then allows the calculated Q-Slope value to be converted into a theoretical steepest slope angle (β) not requiring support by reinforcement (Barton and Bar 2015).

$$\beta = 20 \cdot \log_{10} Q_{slope} + 65° \tag{3-5}$$

The input parameters for Q-Slope are amenable to visual slope inspections, with the exception of the Rock Quality Designation (RQD) which requires direct measurement from rock cores. Applicability through visual inspection alone has positive implications for Q-Slope's viability when applied to GAM, although more specialized training and geological experience is required to select appropriate rock mass and discontinuity parameters. A major limitation of Q-Slope, which appears as a common limitation for many rock mass rating systems, is that it was not developed as a tool to quantify risk and

can only rationally be correlated to the GRMP PF and not the overall RL. Values of Q-slope range from 0.001 (exceptionally poor) to 1000 (exceptionally good).

3.2.5 Geological Strength Index

The Geological Strength Index (GSI) was first introduced by Hoek (1994) and Hoek et al. (1995) as a system to estimate the reduction in rock mass strength for various geological conditions (Hoek and Brown 1997). The parameters of the generalized Hoek-Brown failure criterion incorporate GSI so that rock mass strength can be estimated for larger scales on the basis of intact rock samples and rock mass characteristics (Marinos et al. 2007). The GSI was established as a rock mass characterization tool which accounts for the two principal factors influencing the mechanical properties of a rock mass: the structure and condition of its joints (Hoek and Brown 2018). The two categories required to determine the GSI of a rock mass reflect the principal factors discussed above, i.e., structure and surface condition of joints/discontinuities. Both categories can be assessed through visual inspection of slopes or outcrops for a variety of rock masses. It should be noted that the GSI is a qualitative approach that requires specialized geological experience to implement in a repeatable and reliable manner. Furthermore, it was originally envisioned for different degrees of "blockiness" of the rock mass, and not for addressing near-intact ranges or very sheared and altered masses, where soil-like behaviour exerts significant influence. Even so, experienced practitioners should expect a range of potential values and avoid isolating a single value. Typical GSI ranges for a variety of rock types have been published by Marinos and Hoek (2000) to assist practitioners in the application of GSI.

GSI has no capability to quantify risk or assist in support/reinforcement design like Rock Mass Rating (RMR) or the Q-System (Marinos et al. 2005). With only two categories required to determine GSI, it is an efficient tool for the assessment of rock that can be applied quickly in the field via visual inspection, and therefore implemented at multiple sites during highway inspections covering hundreds of kilometers. For this study GSI will be compared against the GRMP PF as it cannot directly quantify risk or consequence. Theoretically, GSI does not measure likelihood of failure either, i.e., two slopes with the same geology but vastly different likelihood of failure would score the same. For these reasons, the applicability of GSI with regards to GAM implementation remains unclear. Since GSI is not intended for rock masses with a clearly defined dominant structural orientation (Marinos et al., 2005) or with structurally dependent gravitational instability (Marinos et al., 2007), it has limited applicability as a GAM assessment tool in the context of Alberta's geohazards comprising sedimentary deposits. Marinos et al. (2005) noted that GSI can still be applied, with caution, if the rock's anisotropy does not control its failure.

3.2.6 Rock Mass Rating

The Rock Mass Rating (RMR) system was originally introduced by Bieniawski (1973) and refined over the next 15 years through successful application to many civil and mining engineering related projects. A commonly used version of the RMR system was published in 1989 (Bieniawski 1989). The RMR system utilizes six rock mass parameters for individual structural regions:

1.   Uniaxial compressive strength of the rock.

2.   Rock Quality Designation (RQD).

3.   Spacing of discontinuities.

4.   Condition of discontinuities.

5.   Groundwater condition.

6.   Orientation of discontinuities.

Values are assigned to ranges of the six parameters and summed to determine the RMR

score. RMR was originally developed for the tunnelling and mining sectors for which it is

widely used (Aksoy 2008) but is also applicable to slopes (Bieniawski 1993). Since the

RMR requires measured values to fall within specified ranges for each of the six input

parameters, it is very challenging and subjective when applied to a slope using visual

inspection alone. The method requires additional time, laboratory and field resources, and

specialized geotechnical training. This is exacerbated by the lack of published guidelines

for the definition of each class of the orientation of discontinuities factor. Romana et al.

(2015) notes that this parameter was very difficult to apply due to the extreme range of

this factor.

The viability of RMR as an economically feasible asset condition assessment

method as part of a GAM plan remains in question, especially since it does not account

for the consequence of failure. Therefore, the resulting RMR score, similarly to Q-Slope

and GSI, should only be compared with the GRMP PF, not the overall RL. Equation (3-6

was established as a correlation between GSI and the 1989 version of RMR by Hoek and

Brown (1997).

$$GSI = RMR_{89}' - 5 \qquad\qquad (3\text{-}6)$$

Hoek and Brown (1997) note that RMR is unreliable for very poor-quality rock masses

(GSI < 25). The use of this relationship increases the viability of RMR for use in this

30

study as a means of verifying GSI values gathered through visual inspection alone. Note that the RMR$_{89}$' indicates that the groundwater rating parameter is set to 15 and the orientation of discontinuities parameter is set to zero.

3.3 Study Sites

Rock slopes were selected for inclusion in this study primarily based on their GRMP RL to provide a broad range of values for comparison. Three sites included in this research were previously recommended for additional monitoring and have several years of remote sensing data. Some selected sites with corresponding low RL are categorized by TEC as 'expired', meaning they have not been recently active and are no longer being regularly inspected. The historical records are limited for some of these sites with more than a decade since their last official inspection. This issue is compounded over time, as institutional memory of these sites fades. The sites with higher RL ratings, which remain unmitigated due to funding limitations and hence are subject to continued rockfall activity, are inspected annually as part of TEC's Geohazard Risk Management Program.

The slope inspections and application of rating systems were completed on November 12, 2021 for site C018 in Central Alberta, and between September 24 to 25, 2022 for sites S018, S020, S042, S057, S070, and S074, in Southern Alberta. Limited tools were required for the application of the selected rating systems, which included: a range finder with built-in clinometer, a 2-m-long measuring stick, and two measuring tapes with lengths of 6 m and 30 m. Preliminary ratings developed for C018 were published by Wollenberg-Barron et al. (2022) and have been updated for inclusion in this study. The locations of the study sites and representative photographs are shown in Figure 3-1.
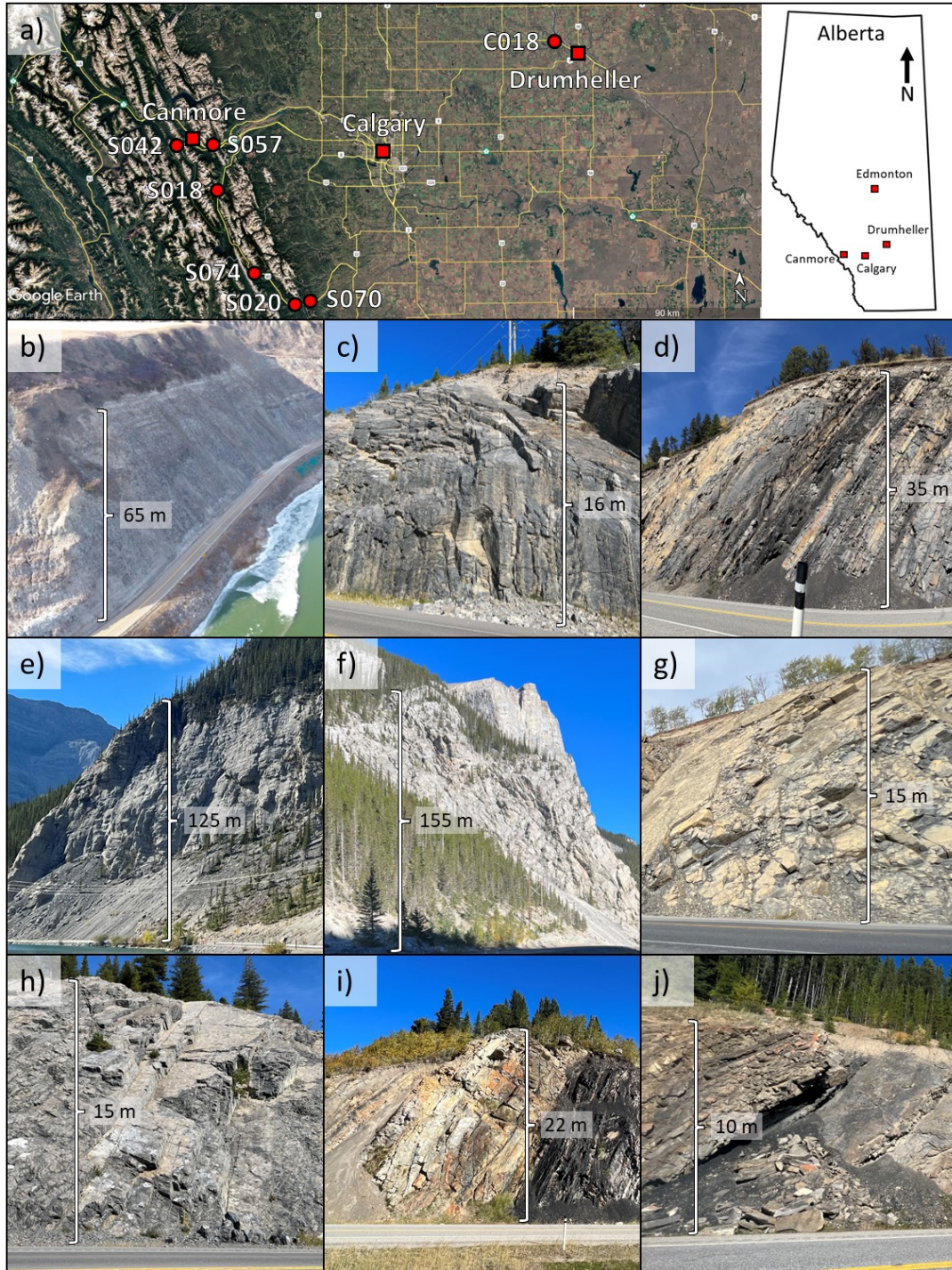
31

Figure 3-1: a) Location of rock slope study areas with Alberta map reference (Google Earth 2022). Site photos and approximate slope heights of b) C018, c) S018, d) S020, e) S042-North, f) S042-South, g) S057-A, h) S057-B, i) S070, and j) S074.

3.3.1 C018 – Red Deer River Valley Slope Instability

Site C018, the Red Deer River Valley Slope Instability, is located along Highway 837:02 approximately 14 km Northwest of Drumheller, Alberta. The AADT at this location is 294 vehicles per day (vpd). The slope bedrock is part of the Horseshoe Canyon formation comprising feldspathic sandstone interbedded with siltstone, bentonitic mudstone, carbonaceous mudstone, concretionary sideritic layers, and laterally continuous coal seams (Roustaei et al 2020). The highly disaggregated nature of the sedimentary deposits at C018 lead to a variety of complex failure mechanisms on the backslope above the highway. The active portion of C018 is approximately 60 m high and extends approximately 500 m along the highway adjacent to the Red Deer River.

From TEC's records, Highway 837 was constructed in the 1980's and was identified early on as a geohazard site that may require reinforcement or protective measures. A nominal ditch was constructed along the highway, at the toe of the backslope, but no other improvement work was undertaken at that time (Klohn Crippen Consultants Ltd. 2001. C018 has been included in TEC's annual Central Region geohazards inspection tour since 2001. Up until 2017, riverbank erosion and instability on the downslope side of the highway embankment was the primary concern at C018; this was mitigated by reconstructing the slope with geogrid reinforcement and armoring the toe of the slope with riprap. An annual to biannual remote sensing program utilizing drone photogrammetry was implemented at C018 in 2017 following a rockfall of blocky frozen material from the backslope above the highway. Other major events occurred through 2017 and 2018 including an earthflow, translational slide, and additional rockfalls. These hazards resulted in the installation of jersey barriers to contain the fallen

33

debris, reducing Highway 837 to one-lane-alternating traffic. Change detection analysis

for C018 between 2017 and 2019 was previously published by Rodriguez et al. (2020)

and Roustaei et al. (2020). Additional details regarding the initial slope ratings from the

November 12, 2021 inspection and difficulties encountered during the inspection of C018

are presented in Wollenberg-Barron et al. (2022).

3.3.2 S018 – Galatea Creek Rock Cut

Site S018, the Galatea Creek Rock Cut, is located along Highway 40, approximately 32

km south of the junction between Highway 40 and Highway 1, in southwest Alberta. This

portion of Highway 40 has an AADT of 2530 vpd. The slope consists of dark grey shale

to siltstone with some white quartz inclusions (AMEC 2009a). The S018 backslope is

approximately 18 m high and 310 m long along the highway.

The highway through-cut at S018 was originally constructed in the 1970's.

According to TEC's records, the S018 backslope rock cut was initially inspected in 2004

and has been included in TEC's annual Southern Region geohazards inspection tour since

2007. Rock bolts were installed at the site, possibly during the original highway

construction. In 2016, additional rockfall mitigation, comprising a high tensile strength

mesh drape was installed, covering most of the eastern slope. This analysis focuses on the

eastern portion of the cut due to its historically higher RL recorded via the GRMP.

During the time of the inspection numerous fallen rocks were present in the

eastern ditch along the highway. Most of the observed debris had accumulated at three

locations along the toe of the backslope but had not reached the highway due to the

effectiveness of the wire mesh rockfall drape. The unfavourable orientation of the

sedimentary bedding plane daylighting out of the slope at S018 leads to planar sliding,

while wedge failures were observed where a perpendicular joint set, sub-parallel to the slope face, intersects the bedding plane. Rockfall blocks noted at the site ranged from gravel to boulder sizes. Due to the high volume of traffic at the time of the inspection, some slope and highway measurements could not be collected due to safety considerations. It was necessary to estimate the highway width using a range finder with a built-in clinometer.

3.3.3 S020 – Highwood House Rockfall Hazard

Site S020, the Highwood House Rockfall Hazard, is located along Highway 541:02, approximately 800 m east of the junction between Highways 40, 541, and 940. This portion of Highway 541 has an AADT of 647 vpd. The backslope above the highway comprises interbedded coal, shale, mudstone, and sandstone with a sub-vertical bedding plane. The mudstone and sandstone are notably less weathered than the coal and shale (KCB 2018a). Geological maps corroborate this assessment, indicating the slope is composed of Mesozoic sandstone, shale, and coal (Stewart et al. 1924). S020 measures approximately 150 m long and 35 m high, with an erosion gully at the west end of the site extending beyond the crest of the backslope (approximately 50 m in length).

Highway 541 and the rock cut at S020 was originally constructed in the 1970's. TEC records indicate S020 was initially inspected in 2004 and has been included in TEC's annual Southern Region geohazards inspection tour since 2007. Remote sensing data, via drone photogrammetry, has been collected at S020 between 2020 and 2022, which provides a database for calculating slope surface change that can be used to correlate visual inspections and slope performance.

At the time of the inspection, rockfall debris had collected at the toe of the cut slope across nearly the entire length of the slope. The largest quantity of rockfalls had accumulated below the western portion of the slope, underneath an erosion gully which extends above the rock slope. This is likely attributed to both erosion of the surficial soils and higher degree of differential weathering leading to undercutting of the rock mass within the gully. The gully has formed above the slope leaving loose blocks and boulders within the soil at the brow of the slope that will eventually fall. Other failure mechanisms present include the raveling of coal layers, which acts to reduce the confinement of the surrounding rock and leads to further rockfalls. Block toppling is also marginally possible along the slope face with joints nearly parallel to the slope face. Rockfall block sizes noted during the inspection ranged from sand to boulder sizes. Due to the high degree of activity at S020, with small rockfalls of sand to gravel sizes occurring during the inspection, approaching the slope for RQD measurements was deemed unsafe. Estimates of the rock masses RQD had to be taken at less active portions of the slope and later corroborated with slope imagery.

3.3.4 S042 – Spray Lakes Rockfall

Site S042, the Spray Lakes Rockfall, is located on Highway 742 (Spray Lakes Road) approximately 5 km southwest of Canmore, Alberta. This portion of Highway 742 is gravel surfaced and has an AADT of 1468 vpd. S042 is located in the Mount Rundle range which comprises Paleozoic limestones, dolomitic limestones, dolostones, and shales which have been thrust onto the sedimentary rocks present in the Bow Valley (Macciotta et al. 2019). The north portion of S042 (S042-North), with an eastern slope aspect, extends approximately 200 m while the south portion (S042-South), with a

southern slope aspect, extends approximately 110 m. The slope has a maximum height of approximately 165 m. A broad talus slope has developed along the base of the slope which narrows significantly at the transition between the two opposing slope aspects.

From the information available, S042 was identified as a rockfall geohazard before 2009 and included multiple locations along a 2.3 km section of Highway 742 which includes the S042 – Spray Lakes Rockfall site. A call-out inspection was conducted in 2013 following a relatively large rockfall event that narrowly missed a vehicle and group of people travelling along Highway 742 (AMEC 2015). Since then, S042 has been included in TEC's annual Southern Region geohazards inspection tour. An annual remote sensing program utilizing ground-based LiDAR was initiated in 2018 for the S042 site, which has initiated a database for calculating slope surface change that can be used to correlate visual inspections and slope performance.

Slope ratings were developed for both the S042-North and S042-South to accommodate the opposing slope aspects and capture the relative difference in rock mass quality and rockfall potential. At the time of inspection, rockfall debris appeared to have recently been cleared from the roadway by highway maintenance staff and was concentrated across the base of the talus slope forming a small berm. The majority of rockfall was concentrated towards the centre of the slope, coinciding with the decrease of the talus slope height and presence of a catch fence installed at that location between 2016 and 2017. It is difficult to determine if the accumulation of rockfalls at the base of the broad talus slope are a result of detachment from the rock slope above the talus, or attenuation and sloughing of talus slope itself. A kinematic analysis presented in Macciotta et al (2019) found that wedge failure is the most probable failure mechanisms

at S042, and planar sliding is possible along the northern slope. To estimate the RQD of the rock mass, measurements were made on a rock outcrop adjacent to the highway. The distance from the highway to the rock slope introduces some uncertainty when transposing road-side outcrop rock mass properties to the upper rock slope.

3.3.5 S057 – Highway 1A, Exshaw

Site S057, Hwy 1A, Exshaw, consists of two rock cut-slopes, Site A and Site B. This portion of Highway 1A has an AADT of 3781 vpd. The sites comprise the cut backslopes along Highway 1A:02 between km 12:52 and km 11.91, approximately 2 km northwest of the Hamlet of Exshaw, Alberta. Geological maps of the area indicate S057 is part of the Exshaw and Banff formations, comprising Paleozoic silty limestone, calcareous siltstone, shale, and siltstone (Price 1970). While both sites have similar geology, Site A is in a more advanced state of weathering. Both slopes have a height of approximately 15 m. Site A and Site B extend approximately 210 m and 300 m, respectively, along the eastbound lane of the highway.

TEC Records of S057 date back to a rock slope scaling program carried out along Highway 1A in the early 2000's. Although identified as a potential rockfall geohazard, S057 was not included in the annual Southern Region geohazards inspection tour until 2019, when the highway maintenance contractor reported an unusually high amount of rockfall debris had accumulated in the catchment ditch (KCB 2019a). Prior to 2019, periodic clearing of rockfalls from the ditches and road surface at S057 was carried out as part of routine road maintenance.

3.3.5.1 Site A

At the time of the inspection at S057 – Site A, the majority of rockfall debris was present at the toe of the backslope, concentrated in three primary locations where the bedding plane adversely dips out of the slope and intersects another joint set creating collection chutes. This intersection leads to rockfalls via planar sliding and wedge failure. Most of rockfall blocks contained in the catchment ditches were relatively small, gravel to cobbles sizes, while there were larger blocks present with multiple boulders in one of the chutes. No notable difficulties were encountered at S057 Site A when applying the rating systems.

3.3.5.2 Site B

When inspecting S057 – Site B, rockfall blocks present were, on average, larger than those at Site A, ranging up to from cobble and boulder sizes. Accumulation of rockfall debris along the toe of the backslope was more evenly distributed than Site A, apart from two locations where boulder-sized rockfall blocks were concentrated. These locations displayed evidence of structurally controlled wedge failures related to intersecting joint sets and possible planar sliding along a prominent bedding plane. A small berm of rockfall debris was present off the shoulder of the highway, indicating recent highway maintenance efforts to remove rockfall blocks from the highway shoulder. During the inspection, mountain goats were seen traversing the crest of the slope, while appearing to bypass Site A, which could be attributed to the higher degree of rockfalls present at this site. Similar to Site A, no notable difficulties were encountered when applying the rating systems.

3.3.6 S070 – East of Fir Creek Rock Cut

Site S070, East of Fir Creek Rock Cut, is situated along Highway 541:02 approximately 7 km east of the junction between Highways 40, 541, and 940 at Highwood House. This portion of Highway 541 has an AADT of 647 vpd. Geology maps for the area are dated but indicate the slope is comprised of Mesozoic sandstone, shale, and coal of the Kootenay and Blairmore formations (Stewart et al. 1924), additionally, conglomerates were noted within the slope during the field inspection. The varying stratum are interbedded with a sub-vertical bedding plane. The slope has a measured height of approximately 22 m and extends approximately 70 m along the highway.

Slope history for S070 as a geohazard site is limited. The first available inspection report dates back to a 2005 Highway 40/Highway 541 corridor review. The next inspection of S070 was conducted in 2009 and the consultant recommended that S070 presented minimal risk to highway operations and could be discontinued from the annual GRMP inspection tour (AMEC 2009b).

At the time of the inspection, significant accumulation of rockfalls and sediment was concentrated at the base of an erosion channel near the western extent of the slope. The channel appears to be facilitating the transport of eroded surficial soils from the crest of the slope, accelerating the erosion of the rock slope at this location. Coal dominates the east portion of the slope where raveling leads to the loss of confinement around more competent sedimentary layers, which leads to further weakening and rockfalls along the slope face. This mechanism also presents itself along the western portion of the slope, where differential weathering of weaker layers is evident. Block toppling is also marginally possible along the western slope with joints nearly parallel to the slope face.

Gravel- to cobble-sized rockfalls have accumulated at the toe below this portion of S070. Other rockfalls ranging from gravel to boulder sizes were present along the toe of the slope, just off the shoulder of the highway. There were boulders noted resting at the brow of the slope that are likely to fall in the future and may impact the road surface.

3.3.7 S074 – Lipsett Ridge Rock Cut

Site S074, the Lipsett Ridge Rock Cut, is located along Highway 40:12, approximately 28 km south and 26 km north of the junction with Highway 742 and Highway 40, respectively. This portion of Highway 30 has an AADT of 560 vpd. The slope comprises Mesozoic sandstone, siltstone, coal, mudstone, and shale (McHechan 1995). The slope has an adverse bedding plane orientation, dipping towards the highway. The slope is approximately 10 m high and extends approximately 210 m along the highway.

Limited information regarding S074 is available from TEC records. One inspection was conducted as part of a 2005 Highway 40/Highway 541 corridor review (AMEC 2006). At the time of the inspection, significant differential erosion between the interbedded weak coal and other sedimentary deposits has resulted in large overhangs and accumulation of rockfalls at five locations along the toe of the slope. This appears to be the dominant mechanism leading to rockfalls at this site. Planar sliding and wedge failure are also possible due to the very unfavourable bedding plane orientation and intersecting joint sets. The rockfall blocks range from sand to boulder sizes. Although no rockfalls are known to have reached the road surface, the effectiveness of the ditch has been significantly diminished. At the most prominent overhang, a large rock block has released from the rock face and will eventually release from the slope, possibly impacting the road surface.

3.4 Rating System Results and Discussion

To quantify the varying risk associated with different slope failure mechanisms and rockfall block volumes, multiple GRMP RLs have been published for C018 and S042. KCB (2018b) introduced three separate RLs for C018 following the major events in 2017 discussed in Section 3.3.1. RLs were generated to cover the varying failure mechanisms present at the site. For event volumes greater than 0.5 m^3 (C018-L), less than 0.5 m^3 (C018-S), and for earth slide events. To capture the impact of increased failure event volume on the applicable rating systems, a volume of 10 m^3 was selected to represent an event greater than 0.5 m^3. With historical event volumes upwards of 500 m^3 recorded at C018, this is considered conservative for a major event while having a significant impact on the applicable rating systems. For this study, the RL for an earthside event was not included as the rating systems selected are intended to assess rockfall events. Similar to C018, AMEC (2015) introduced two RLs for S042 following the rockfall event in 2013 which was applied to both the north and south slopes, resulting in four individual S042 ratings. These distinguished the relative difference in RL for small (S042-North-S and S042-South-S), or frequent, and large (S042-North-L and S042-South-L), or infrequent, rockfall block volumes corresponding to isolated rockfalls from block detachment and larger wedge failures, respectively. Large rockfall blocks volumes were defined by KCB (2019b) as greater than 15 m^3. The small rockfall block volume was selected as less than 0.3 m^3 following the observations and analysis presented in Macciotta et al. (2018) and Macciotta et al. (2019) for S042. Subsequently, for the changes in rockfall event volumes, the Rockfall History and Rockfall Frequency categories pertaining to the RHRS and CRHRS, respectively, were adjusted to reflect the likelihood of the varying volumes.

Note that small and large rockfall block volumes were applied to both the north and south

slope portions of S042. The varying RLs associated with different failure mechanisms

were incorporated into this study as additional data points to analyze the effectiveness of

each rating system at capturing the change. The inclusion of the additional RL data

increased the total number of slopes to 12 for each of the following comparative analyses.

The GRMP ratings, estimated slope angles, and results of each other rock slope and rock

mass rating system for each study area are presented in Table 3-1 and may be inspected

together with the slope photos presented in Figure 3-1.

Table 3-1: Slope details and results of rock slope and rock mass rating systems

Slope ID	GRMP			RHRS	CRHRS	Slope Angle (°)	Q-Slope	β Angle (°)	GSI	RMR$_{89}$'
	PF	CF	RL							
C018-S	15	6	90	413	777	42*	0.000833	3.4	15 - 25	29
C018-L	16	9	144	512	801	42*	0.000833	3.4	15 - 25	29
S018	13	3	39	292	729	85	0.133	47.5	35 - 50	49
S020	14	5	70	394	759	60*	0.0357	36.1	20 - 35	37
S042-East-S	13	4	52	293	747	60*	0.983	64.8	55 - 70	69
S042-East-L	7	7	49	358	777	60*	0.983	64.8	50 - 65	66
S042-West-S	13	4	52	287	819	60*	0.986	64.9	55 - 70	69
S042-West-L	7	7	49	352	849	60*	0.986	64.9	50 - 65	66
S057-A	11	1	11	275	735	40	0.0844	43.5	30 - 45	39
S057-B	11	3	33	285	753	45	0.133	47.5	30 - 45	39
S070	15	2	30	234	759	55	0.0605	40.6	15 - 30	35
S074	15	1	15	242	735	50	0.0195	30.8	20 - 35	38

*Slope angle approximated in the field and corroborated with remote sensing data when available

3.4.1 RHRS and CRHRS

With categories to assign values for both probability and consequence, as discussed in

Sections 3.2.2 and 3.2.3, RHRS and CRHRS were compared directly against the GRMP

RL. Traffic data to determine the AVR for both the RHRS and CRHRS was gathered for

each of the study areas using the weighed annual average daily traffic (WAADT) published by TEC (2022).

The minimum and maximum possible scores for the RHRS are 20 and 905, respectively. The RHRS scores for the sites range from 234 to 512; seven sites scored below 300 indicating low priority, four were between 300 and 500 indicating moderate priority, and one was over 500: C018-L, indicating urgent priority. The slopes scoring well below 300, i.e., S070 and S074, are currently "expired" sites and were last assigned GRMP RLs in 2009 and 2006, respectively. The resulting low RHRS scores gives credence to TEC's decision to retire these sites. The other 4 sites scoring below 300 only did so by a small margin and due to the subjectivity of the RHRS categories, may fall above 300 if conditions encountered during scoring were interpreted differently. Slopes scoring between 300 and 500 included: C018-S, S020, and both S042-North-L and S042-South-L. A linear trendline was applied to Figure 3-2a to measure the degree of correlation between the prescribed GRMP RL and RHRS scores. The resulting coefficient of determination (R^2) was quite high with a value of 0.87 for the 12 data points.

The CRHRS scores ranged from 735 to 849 for the sites. The minimum and maximum possible scores for the CRHRS are 63 and 1701, respectively. The CRHRS system is more complex to implement and the is no provision for determining site priority. It is therefore not a simple matter to determine a rock slope's priority level on an individual basis. The method developers' intentions were to have CRHRS results stand out more so that high rockfall hazard sites would be more easily identifiable (Russel et al. 2008). The results of this study seem contradictory to this intention with the total range of

CRHRS scores much less than that of the RHRS scores. This is likely an effect of selecting slopes with pre-existing rockfall potential which inherently score higher. A total of 9 Jar Slake tests were conducted, 3 tests for samples collected from S057-A, S057-B, and S070 as representative geologic samples to estimate the Jar Slake results for S018, S020, and S074. All 9 samples were non-reactive after 30 minutes of submersion. The slaking potential of samples from C018 was previously tested by Roustaei et al. (2020) where two out of three samples began to disaggregate after 24 hours of submersion.

The resulting R^2 value of 0.20 indicates a poor correlation between GRMP RL and CRHRS. The suspected reasoning for the low R^2 value is attributed to the complexity of the CRHRS and relatively low range of scores between the study areas. The summation of 21 category scores provides ample opportunity to deviate from the GRMP RL, and potentially diminish or mask features that could have a marked influence on the probability of rockfalls. The most significant CRHRS outliers were S042-South-L, S042-South-S, and S018.

S042-South-S and S042-South-L resulted in the highest CRHRS scores of all the slopes included in this study as well as the greatest deviations from the GRMP RL trend. Between S042-South-L and S042-South-S, the only change in scoring is attributed to Block Size / Volume and Rockfall Frequency. The deviation is largely attributed to the Slope Aspect CRHRS category. The change in slope aspect from the northern to southern slope portions increase the overall S042-South CRHRS scores by 72 points. The rockfall mitigation measures installed at S018, while not captured by the RHRS categories, reduced the CRHRS Ditch Catchment category which stipulates scoring of 3 (lowest

45

possible score) if mitigation measures exist. Without the mesh drape the CRHRS score for S018 would have been 24 points higher.

The RHRS and CRHRS scores were compared directly (Figure 3-2c) to review the impact of the additional parameters at each of the rock slopes. The significant deviation from the trend of S042-South-L, S042-South-S, and S018 resulted in an overall poor correlation between the two rating systems, with an R^2 value of 0.20. Excluding S042-South-S and S042-South-L from Figure 3-2b and Figure 3-2c increase the R^2 to 0.72 and 0.69, respectively. While having less than half of the total summed parameters, the relative risk of a slope is well predicted through the RHRS categories alone, when taking the GRMP RL as a good proxy for the documented risks at these sites. A similar conclusion was reached via the statistical analysis conducted for the CRHRS (Russel et al 2008 and Santi et al. 2008), indicating that the total scores could be reasonably estimated measuring only 4 to 6 key parameters.
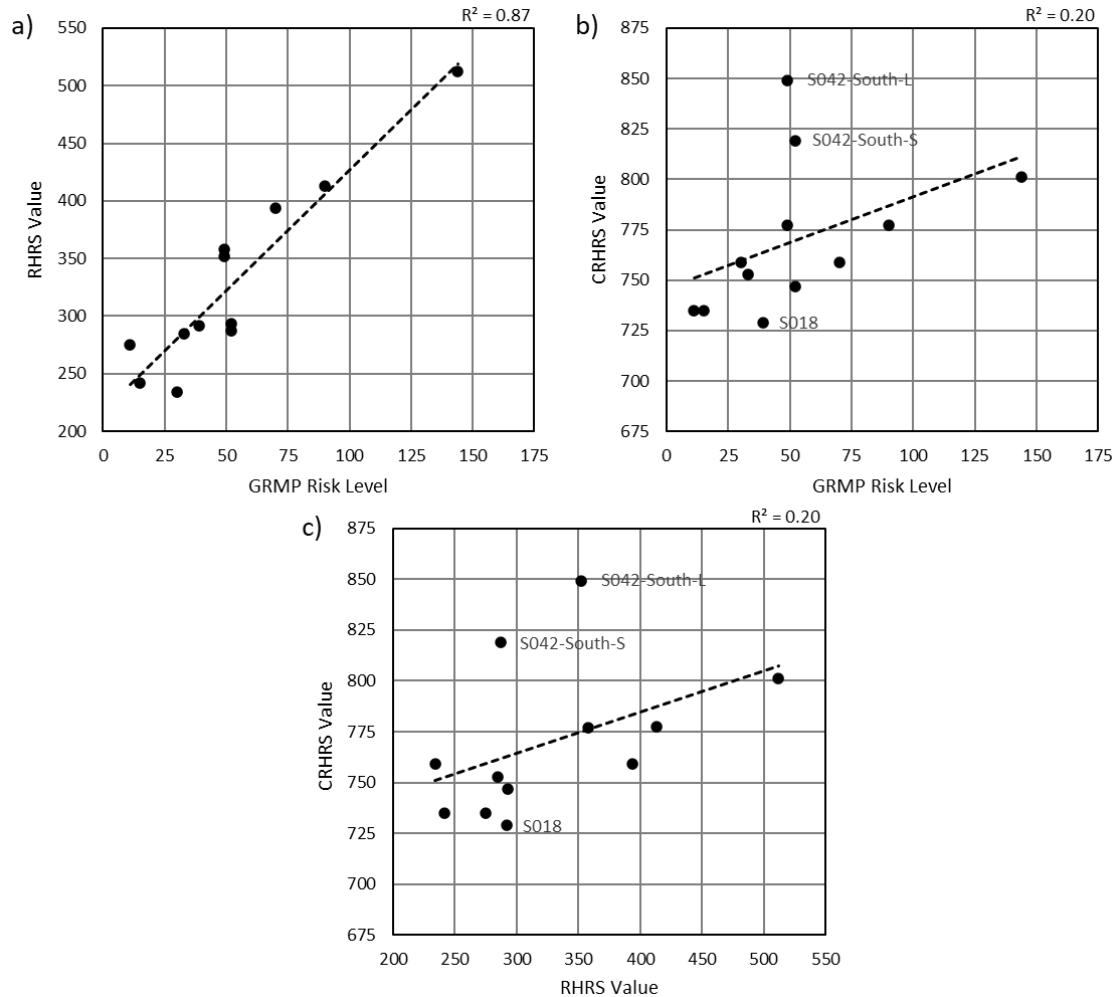
Figure 3-2: Correlation between a) RHRS and GRMP risk level, b) CRHRS and GRMP risk level, c) CRHRS and RHRS. Slope scores with greatest deviation from correlation trendline identified.

3.4.2 Q-Slope

The calculated Q-Slope values were directly plotted against the GRMP PF in Figure 3-3a with a corresponding R^2 value of 0.40. Equation (3-4 was applied to each Q-slope value, and the difference from the actual slope angle and calculated β angle was plotted against the GRMP PF (Figure 3-3b) where the resulting R^2 value was 0.48. Finally, each Q-Slope value was plotted on the Q-Slope stability chart (Figure 3-3c) to see where they lay

within the published ranges of stable slopes, unstable slopes, or uncertain stability as a preliminary indicator for slope stability (Barton and Bar 2015). Although Q-Slope was developed to allow engineers to assess changing stability of a slope in the field during construction, parameter selection is generally supplemented with borehole data (Barton and Bar 2015). Q-Slope values in this study were determined successfully via basic measurements and visual inspection with some engineering judgement and deployment of the field RQD measuring technique proposed by Hutchinson and Diederichs (1996) for exposed rock walls. Due to the limited accuracy in measuring the actual slope angle at each site using a range finder with a digital clinometer, a general error range was applied to the values shown in Figure 3-3b and Figure 3-3c of ± 5 degrees. For the sites with remote sensing data (C018, S020, and S042), the range was determined through direct measurement of slopes with virtual surface models generated from available remote sensing data.

S042-North-S and S042-South-S were identified as outliers in the Q-Slope analysis while S042-North-L and S042-South-L fit reasonably well. This is likely attributed to Q-Slope not accounting for rockfall event sizes, only through the mechanism in which it occurs by application of appropriate O-factors. The increased GRMP PF between the two failure mechanisms results in a large deviation from the trend in Figure 3-3a and Figure 3-3b. Additionally, it's worth noting that the Q-Slope Equation (3-5 was developed only for slope heights less than 30 m (Bar and Barton 2017). Considering S042 extends over 125 m high, a deviation from the trend of Figure 3-3b is not unexpected. The Q-Slope results of C018-S and C018-L plot well below the trend in Figure 3-3a and Figure 3-3b. This is a product of highly disaggregated sedimentary rock

present at the site. Furthermore, C018 is approximately 65 m high and, like S042, is beyond the intended slope height to apply Equation (3-5. The resulting Q-Slope value yields uncertain slope stability plotting outside the range of Figure 3-3c. S018 is an interesting case for Q-Slope since multiple rockfall mitigation measures exist at the site (mesh drape and rock bolts). The Q-Slope adjustment factor for slope reinforcement measures utilized for this case does not appear to fully capture the reinforcement impact. No factor exists for mesh drapes, which theoretically diminishes the consequence of a rockfall event, but which is not captured by Q-Slope. While the S018 Q-Slope value shows good correlation with the trend in Figure 2a, it deviates significantly from the trend of Figure 2b. This is attributed to the definition of the β angle as the steepest slope angle not requiring reinforcement (Bar and Barton 2017). The fact that the β angle calculated more closely resembles the approximate dip angle of the bedding plane at S018 rather than the vertical slope cut gives credit to this reasoning. The same reasoning can be applied to explain why S018 plots well into the unstable slope range in Figure 3-3c. It is interesting to note that while S070 and S074 consistently correlate well with a relatively low RL and PF they plot within the unstable slope portion of Figure 3-3c. The inclusion of these slopes in this study and their existence within TEC's rockfall geohazard database serves as an indicator that they are, or have previously been, unstable. This logic applies to each of the nine slopes in this study since none plot well inside the stable slope portion of Figure 3-3c.
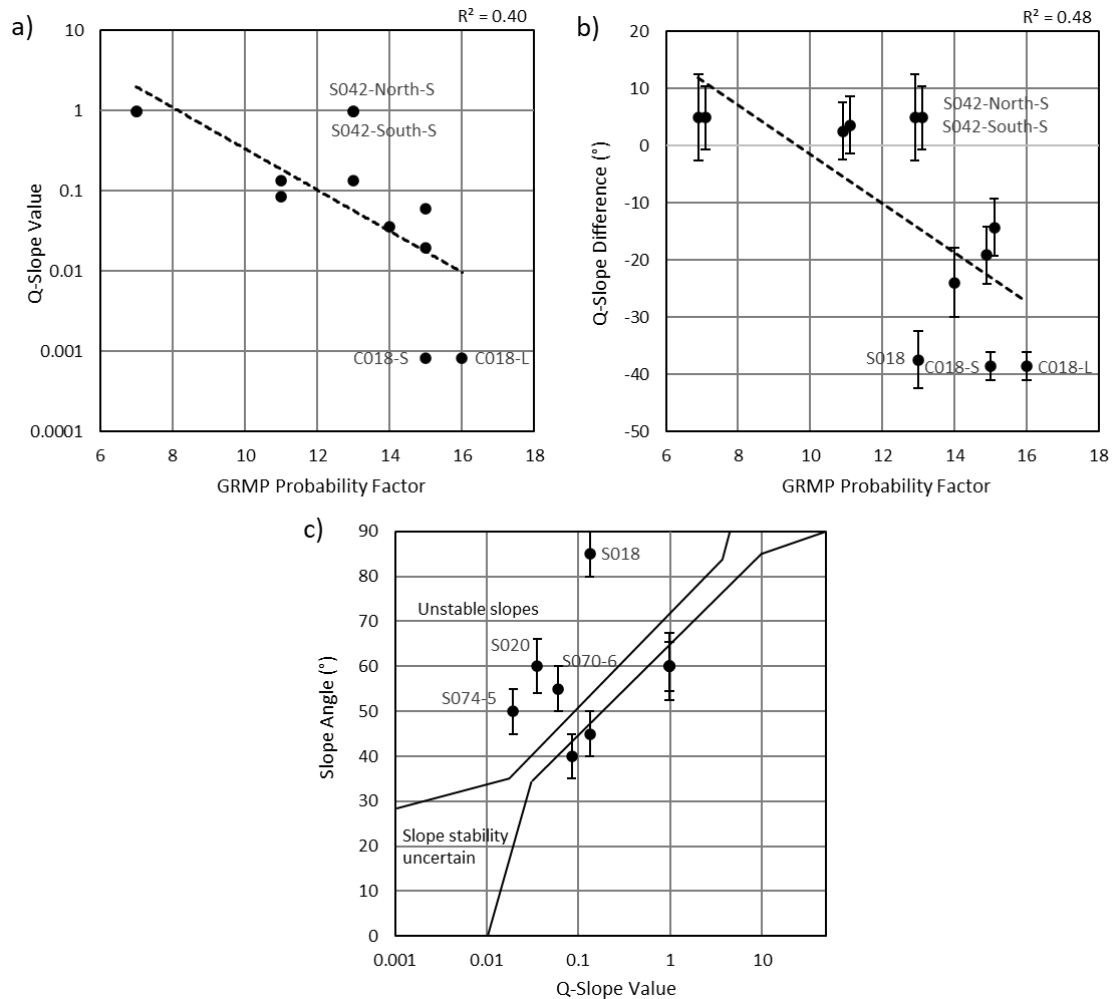
Figure 3-3: Developed correlation between GRMP probability factor and a) Q-Slope on Log scale and b) difference between Q-Slope β and actual slope angle; c) Slopes plotted on Q-Slope stability chart from Barton and Bar (2015). Unstable slopes and scores with greatest deviation from correlation trendline identified.

3.4.3 GSI and RMR

A representative GSI range was assigned to each of the study sites based on visual

inspection and detailed review. Due to the subjectivity of GSI's categories and reliance

on geological expertise of the scorer for selection of values, the GSI values were selected

in the field and later reviewed by experienced practitioners in a workshop setting. Visual

50

records are presented as material supplementary to this manuscript (as Appendix B). Another challenge was encountered when applying GSI to slopes comprising varying rock mass characteristics, i.e., S070 where coal dominates the eastern portion of the slope. In such a case, a GSI range must be determined for each rock mass and reported separately, or a weighted average could be used to provide a single range. For the purpose of this study, since only one site displayed such changes in rock mass characteristic, the GSI for each was weighted based on the estimated percent composition of the slope to determine an overall average GSI range. The same methodology was applied to adjust the RMR value for S070. Through visual inspection alone it is not possible to determine the appropriate values for each of the RMR parameters. Some measurements of the rock face were required but were duplicate measurements from the determination of CRHRS and Q-Slope.

An appropriate RMR score was determined for each slope and adjusted to fit the RMR_{89}' requirements for direct comparison to GSI using Equation (3-6. Figure 3-4 presents the correlation between GSI, RMR_{89}', and GRMP PF for each of the slopes included in this study. Vertical error bars correspond to the representative bounds of the GSI range selected for each of the slopes. The computed GSI value using RMR_{89}' and Equation (3-6 proved very effective and fell within the representative GSI range for each of the slopes included in this study. The average percent difference of RMR_{89}' to the median GSI value was 9% which is not significant from a practical geotechnical engineering perspective.

The only significant deviation from the trend presented in Figure 3 was S042-North-S and S042-South-S. This is attributed to the same reasoning as in Figure 3-3a and

Figure 3-3b for Q-Slope, where the rating system has no capacity to capture the increase in rockfall event volume. While Q-Slope can account for different failure mechanisms, GSI and RMR lack this capacity as well. Overall, with the exception of S042, a reasonable correlation between GSI and the GRMP PF resulted from this analysis with an R^2 value of 0.54.
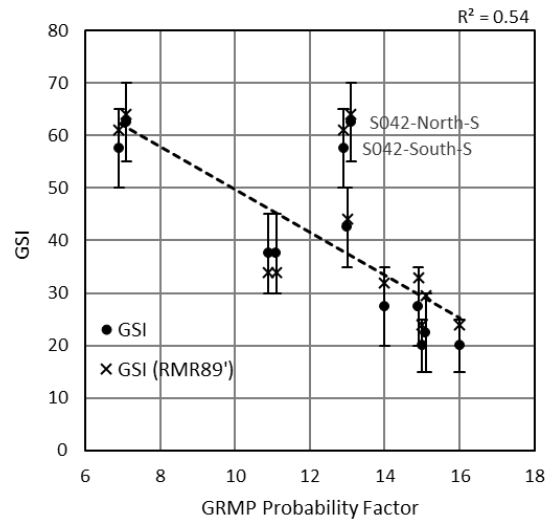
Figure 3-4: Correlation between and observed GSI, GSI from RMR$_{89}$', and the prescribed GRMP probability factor for each slope.

3.4.4 Summary of Results

The comparison between the GRMP rating system and other industry accepted rock mass and rock slope rating systems is intended to gauge the effectiveness of each at quantifying risk from rockfall geohazards along linear infrastructure. From the results of this study a range in correlation strengths were obtained. Major outliers for each correlation were largely justifiable after a detailed review of key categories for each rating system that lead to a deviation from the generated trend. A strong correlation was

derived between the GRMP RL and RHRS which gives credit to TEC's GRMP and consultants taking part in the program. For the poor correlation derived between the GRMP RL and the CRHRS values, it is unclear which rating system is better suited for Alberta rock slopes. While the simplicity of the GRMP RL may be a limitation of TEC's current system, the complexity of the CRHRS does not lend itself to easy implementation. Additionally, the narrow range of CRHRS scores determined for the study sites may make it more difficult for agencies to prioritize sites. It is also possible that the poor correlation between CRHRS and the GRMP RL is a result of the GRMP's simplicity. When considering S042, the slope must be viewed from a distance and little data regarding past rockfall events is available. This may lead the GRMP scorers to select more conservative PF or CF values, resulting in a higher RL. From an asset management perspective, a slope with a high RL would trigger additional monitoring of the slope's performance and ultimately determine if adjustment to the rating is required. Since the CRHRS is actively in use as a GAM assessment tool in Colorado, a clear conclusion cannot be drawn of the CRHRS applicability to GAM from the twelve Alberta rock slopes assessed in this study. However, the results from this limited study indicate that the CRHRS ranking does not provide adequate differentiation for rockfall hazards for highway related sites in Alberta. The correlation resulting between Q-Slope and the GRMP PF was marginal when looking at both the Q-Slope score and difference between the actual slope angle and calculated β angle (Figure 3-3a and Figure 3-3b, respectively). It is unclear if Q-Slope would hold up as an effective preliminary assessment tool in a comprehensive GAM program. A reasonable correlation between the GRMP PF and GSI was achieved considering GSI and RMR do not consider the failure mechanisms at work

within a rock slope, giving credit to GSI's strength as a rock mass characterization tool. Although, like Q-Slope, its applicability as a condition assessment tool for GAM remains in question. A range of values for each asset adds unnecessary complexity for an agency to assign priority for resource allocation.

3.5 Conclusion

This paper presents the results of a variety of rock mass and rock slope rating systems applied to rockfall geohazards present along highway corridors in Alberta, Canada. The applicability of each for use as a tool for slope condition assessment were tested as alternative methods for TEC to implement as part of a GAM program. The RHRS clearly aligned well with TEC's existing GRMP methodology. The RHRS and its modified versions are used extensively by American Departments of Transportation and have demonstrated value as effective preliminary assessment tools for rockfall geohazards. The poor correlation between the CRHRS and GRMP risk level (RL) was not unexpected, due to the relatively high complexity of the rating system compared to the simplicity of the GRMP RL. The increased complexity provides many outlets for deviation from a trend that may be improved with inclusion of lower activity slopes to better define a range of slopes which do not require attention through monitoring or rehabilitation measures. However, the CRHRS did not provide a clear ranking for prioritizing resource allocation for these sites in Alberta. Q-Slope, GSI, and RMR are not formally considered preliminary assessment tools for the application of GAM but still resulted in moderately acceptable correlations to the GRMP probability factor (PF). Outliers for each methodology could be explained with reasoning pertaining to site-specific characteristics e.g., varying failure mechanisms and rockfall event volumes

(S042 and C018), presence of rockfall mitigation measures (S018), or slope heights extending beyond the rating system's input ranges (C018 and S042 for Q-Slope). It should be noted that the RHRS (and subsequently the CRHRS) is the only rating system discussed in this paper which includes a methodology for estimating the cost of rockfall remedial measures. This is an important aspect when considering a rating systems' applicability to an agency GAM program.

Even though the GRMP RL does not incorporate a measure of risk exposure as mentioned in Section 3.2.1, from the correlation derived with the RHRS ratings it appears that the technical expertise of TEC and its consultants has inherently accounted for this limitation to some degree. The limitations of Q-Slope, GSI, and RMR pertaining to their applicability to GAM are evident since they do not carry the capacity to measure consequence and, subsequently, risk. However, when considering likelihood of failure alone, Q-Slope could be employed as a tool to determine PF if varying rockfall event volumes are considered through their failure mechanism and not strictly volume. Selection of an appropriate Discontinuity Orientation Factor (O-factor) proved to be the most challenging aspect when implementing Q-Slope due to the ambiguity of discontinuity orientation descriptions. Careful consideration must be made by the scorer to maintain consistency throughout an asset inventory when applying Q-Slope. GSI should be considered as a solid baseline methodology to determine the likelihood of a rockfall occurring. Its correlation with the GRMP PF gives credit to TEC's PF at capturing the reality of low-quality rock masses bearing a greater likelihood of rock block detachment. Overall, Alberta's GRMP system held up as a viable condition assessment tool to be used within a GAM program against other comprehensive rock slope and rock

mass rating systems, which require more in-depth and explicit geological ratings and measured values. The GRMP RL and RHRS are considered short-listed as viable tools for quantifying risk. Q-Slope and GSI may be short-listed for use as viable tools to assess likelihood or probability of rockfall occurrence, supplementary to the GRMP PF, with GSI better-suited for implementation through visual inspection alone.

3.6 Acknowledgements

3.7 References

American Association of State Highway Transportation Officials (AASHTO). 2020. *Transportation Asset Management Guide*. Available from: https://www.tamguide.com/ (accessed March 2023).

Agriculture and Irrigation, Alberta Climate Information Service (ACIS). 2022. Data provided by Agriculture and Irrigation, Alberta Climate Information Service (ACIS) https://acis.alberta.ca (accessed December 2022)

Aksoy, C.O. 2008. Review of rock mass rating classification: historical developments, applications, and restrictions. *Journal of mining science*, 44(1): 51–63.

Alberta Transportation and Economic Corridors (TEC). 2022. Highway traffic counts, traffic volume data map. Electronic dataset. http://www.transportation.alberta.ca/mapping/ (accessed September 2022)

AMEC Earth & Environmental. 2006. *Geohazards Review: Highway 40 / Highway 541 Corridor, Southwestern Alberta*. Report submitted to Alberta Infrastructure and Transportation.

AMEC Environment and Infrastructure. 2015. *Southern Region Geohazard Assessment, 2014 Annual Inspection Report, Site S42: Highway 742:02, Spray Lakes Rock Fall.*
http://www.transportation.alberta.ca/PlanningTools/GMS/Annual%20Landslides%20Assessments/Reg-Southern%20(CMA517,%20CRR)/Inspection%20Sites/25291_02%20or%20742_02%20(S042)%20-%20Spray%20Lakes%20Rockfall/Reports/2014%20S42%20Inspection%20Report.pdf

AMEC. 2006. Geohazards Review - *Highway 40/Highway 541 Corridor, Site 28 - Lipsett Ridge Rock Cut.*
http://www.transportation.alberta.ca/PlanningTools/GMS/Annual%20Landslides%20Assessments/Reg-Southern%20(CMA517,%20CRR)/Expired%20Sites/040_12%20(S074-1%20to%205)%20-%20Lineham%20Creek%20to%20Lipsett%20Geohazards/040_10%20(S074-5)%20-%20Lipsett%20Ridge%20Rock%20cut/Reports/2006%20S074-5%20Inspection%20Report.pdf

AMEC. 2009a. *Site S018 - Galatea Rockfall, Highway 40:12, Kananaskis River Valley, Alberta*, Site Data - Summary Binder, Section A - File Review.
http://www.transportation.alberta.ca/PlanningTools/GMS/Annual%20Landslides%20Assessments/Reg-Southern%20(CMA517,%20CRR)/Inspection%20Sites/040_12%20(S018)%20-%20Galatea%20Creek%20Through-Cut/Reports/Section%20A/2009%20S18%20Section%20A%20Report.pdf

AMEC. 2009b. *Southern Region Geohazard Assessment Program, Highway 541:02, East of Fir Creek Rock Cut Site, June 2009 Inspection Report.*
http://www.transportation.alberta.ca/PlanningTools/GMS/Annual%20Landslides%20Assessments/Reg-Southern%20(CMA517,%20CRR)/Expired%20Sites/541_02%20(S070-1%20to%208)%20-%20Eyrie%20Gap%20and%20Fir%20Creek%20Geohazard%20Sites/541_02%20(S070-6)%20-%20East%20of%20Fir%20Creek/Reports/2009%20S070-6%20%20Inspection%20Report.pdf

Anderson, S.A., Schaefer, V.R., and Nichols, S.C. 2016. *Taxonomy for geotechnical assets, elements, and features* (No. 16-5659).

Baecher, G.B., Christian, J.T. 2003. *Reliability and Statistics in Geotechnical Engineering.* John Wiley & Sons.

Bar, N. and Barton, N. 2017. The Q-slope method for rock slope engineering. *Rock Mechanics and Rock Engineering*, 50(12): 3307–3322.

Bar, N., Barton, N.R., and Ryan, C.A. 2016. Application of the Q-slope method to highly weathered and saprolitic rocks in Far North Queensland. In *ISRM International Symposium-EUROCK 2016.*

Barton, N. and Bar, N. 2015. Introducing the Q-slope method and its intended use within civil and mining engineering projects. In *ISRM Regional Symposium-EUROCK 2015.*

Barton, N. and Grimstad, E. 2014. Forty years with the Q-system in Norway and abroad. *Fjellsprengningsteknikk, Bergmekanikk, Geoteknikk*, vol 4.1–4.25.

Barton, N., Lien, R., and Lunde, J. 1974. Engineering classification of rock masses for the design of tunnel support. *Rock Mechanics*, 6(4): 189–236.

Bernhardt, K.L.S., Loehr, J.E., and Huaco, D. 2003. Asset management framework for geotechnical infrastructure. *Journal of Infrastructure Systems*, 9(3): 107–116. American Society of Civil Engineers.

Bieniawski, Z.T. 1973. Engineering classification of jointed rock masses. *The Civil Engineer*, South African Institution of Civil Engineering (SAICE), 1973(12): 335–343.

Bieniawski, Z.T. 1989. *Engineering rock mass classifications: a complete manual for engineers and geologists in mining, civil, and petroleum engineering*. John Wiley & Sons.

Bieniawski, Z.T. 1993. Classification of rock masses for engineering: the RMR system and future trends. In *Rock Testing and Site Characterization*. 553-573, Elsevier.

Budetta, P. 2004. Assessment of rockfall risk along roads. *Natural Hazards and Earth System Sciences*, 4(1): 71–81.

Colorado Department of Transportation. 2020. Laboratory Manual of Test Procedures, Determining the Durability of Shales for Use as Embankments, CP-L 3104. https://www.codot.gov/business/designsupport/materials-and-geotechnical/manuals/2020-laboratory-manual-of-test-procedures/lmtp

Google Earth Pro 7.3. 2022. Central and southern Alberta. Image © 2022 Google LLC. (Accessed 20 December 2022).

Higgins, J.D., Andrew, R.D., Turner, K.A., and Schuster, R.L. 2012. Rockfall types and causes. In *Rockfall Characterization and Control*, 21-55.

Hoek, E. 1994. Strength of rock and rock masses. *ISRM News Journal*, 2(2): 4–16.

Hoek, E., Kaiser, P.K., and Bawden, W.F. 1995. *Support of Underground Excavations in Hard Rock*. Balkema, Rotterdam, Netherlands.

Hoek, E., and Brown, E.T. 1997. Practical estimates of rock mass strength. *International Journal of Rock Mechanics and Mining Sciences*, 34(8): 1165–1186.

Hoek, E. and Brown, E.T., 2019. The Hoek–Brown failure criterion and GSI – 2018 edition. *Journal of Rock Mechanics and Geotechnical Engineering*, 11(3): 445-463.

Hutchinson, D.J. and Diederichs, M. 1996. The cablebolting cycle - underground support engineering. *CIM Bulletin*, 89(1001). Sudbury, Ontario, Canada.

Justice, S.M. 2015. *Application of a Hazard Rating System for Rock Slopes Along a Transportation Corridor Using Remote Sensing*. Michigan Technological University.

Klohn Crippen Berger. 2018a. *Southern Region GRMP Site Inspection Report, S020 Highwood House Rock Cut.* http://www.transportation.alberta.ca/PlanningTools/GMS/Annual%20Landslides%20Assessments/Reg-Southern%20(CMA517,%20CRR)/Inspection%20Sites/541_02%20(S020)%20-%20Highwood%20House%20Rock%20Cut/Reports/2018%20S020%20Inspection%20Report.pdf

Klohn Crippen Berger. 2018b. *CON0017608 Central Region GRMP – Call-Out Report, C018 Hwy 837:02 Call-Out Report.* http://www.transportation.alberta.ca/PlanningTools/GMS/Annual%20Landslides%20Assessments/Reg-Central%20Region%20(CMA511-516)/Inspection%20Sites/837_02%20(C18)%20-%20Red%20Deer%20River%20Scour%201.9km%20from%20SH575/Reports/Call%20Out%20Reports/2018%20C018%20Call%20Out%20Report.pdf

Klohn Crippen Berger. 2019a. *Southern Region Geohazard Risk Management Plan, Hwy 1A:02, km 12.52 to 11.91 Call-Out Report.* http://www.transportation.alberta.ca/PlanningTools/GMS/Annual%20Landslides%20Assessments/Reg-Southern%20(CMA517,%20CRR)/Inspection%20Sites/001A-02%20(S057)%20-%20Rock%20fall%20sites%20near%20Exshaw/Reports/Call%20Out%20Reports/2019%20S057%20Call%20Out.pdf

Klohn Crippen Berger. 2019b. *Southern Region GRMP Site Inspection Report, S042 - I & II Spray Lakes Rockfall.* http://www.transportation.alberta.ca/PlanningTools/GMS/Annual%20Landslides%20Assessments/Reg-Southern%20(CMA517,%20CRR)/Inspection%20Sites/25291_02%20or%20742_

02%20(S042)%20-
%20Spray%20Lakes%20Rockfall/Reports/2019R%20S042%20Inspection%20Re
port.pdf

Klohn Crippen Consultants Ltd. 2001. *Alberta Transportation Central Region, Site C018 Annual Inspection Report.*
http://www.transportation.alberta.ca/PlanningTools/GMS/Annual%20Landslides
%20Assessments/Reg-Central%20Region%20(CMA511-
516)/Inspection%20Sites/837_02%20(C18)%20-
%20Red%20Deer%20River%20Scour%201.9km%20from%20SH575/Reports/20
01%20C018%20Inspection%20Report.pdf

Macciotta, R. 2019. Review and latest insights into rock fall temporal variability associated with weather. *Proceedings of the Institution of Civil Engineers-Geotechnical Engineering*, 172(6): 556-568.

Macciotta, R. and Martin, C.D. 2019. Preliminary approach for prioritizing resource allocation for rock fall hazard investigations based on susceptibility mapping and efficient three-dimensional trajectory modelling. *Bulletin of Engineering Geology and the Environment*, 78(4): 2803-2815.

Macciotta, R., Gräpel, C., and Skirrow, R. 2020. Fragmented rockfall volume distribution from photogrammetry-based structural mapping and discrete fracture networks. *Applied Sciences*, 10(19): 6977.

Macciotta, R., Grapel, C., Duxbury, J., Keegan, T., and Skirrow, R. 2018. Explicit estimation of rock slope failure likelihood for hazard assessment and safety engineering near Canmore, AB. In *Proceedings of the 7th Canadian Conference on Geohazards: Geohazards* (Vol. 7).

Macciotta, R., Gräpel, C., Keegan, T., Duxbury, J., and Skirrow, R. 2019. Quantitative risk assessment of rock slope instabilities that threaten a highway near Canmore, Alberta, Canada: managing risk calculation uncertainty in practice. *Canadian Geotechnical Journal*, 57(3): 337-353.

Marinos, P., and Hoek, E. 2000. GSI: A Geologically Friendly Tool for Rock Mass Strength Estimation. *ISRM International Symposium*.

Marinos, P.G., Marinos, V., and Hoek, E. 2007. The Geological Strength Index (GSI): A Characterization Tool for Assessing Engineering Properties for Rock Masses. In *The International Workshop on Rock Mass Classification in Underground Mining*.

Marinos, V., Marinos, P., and Hoek, E. 2005. The geological strength index: applications and limitations. *Bulletin of Engineering Geology and the Environment*, 64(1): 55–65.

McHechan, M. E. 1995. *Rocky Mountain Foothills and Front Ranges in Kananaskis Country, West of Fifth Meridian, Alberta.* Scale 1:100,000. Geological Survey of Canada, "A" Series Map 1865A. Open access from: https://ftp.maps.canada.ca/pub/nrcan_rncan/publications/STPublications_Publicat ionsST/204/204897/gscmap-a_1865a_e_1995_mg01.pdf

Pierson, L.A. 1992. *Rockfall Hazard Rating System.* Transportation Research Record 1343

Pierson, L.A. and Van Vickle, R. 1993. *Rockfall Hazard Rating System: Participant's Manual*. Federal Highways Administration. SA-93-057.

Pierson, L.A., Turner, A.K., Turner, K.A., and Schuster, R.L. 2012. Implementation of rock slope management systems. In *Rockfall Characterization and Control*, 73-112.

Pratt, C., Macciotta, R. and Hendry, M. 2019. Quantitative relationship between weather seasonality and rock all occurrences north of Hope, BC, Canada. *Bulletin of Engineering Geology and the Environment*, 78(5): 3239-3251.

Price, R. A. 1970. *Geology, Canmore (west half), west of Fifth Meridian, Alberta.* Scale 1:50,000. Geological Survey of Canada, "A" Series Map 1266A. Open access from: https://ftp.maps.canada.ca/pub/nrcan_rncan/publications/STPublications_Publicat ionsST/108/108954/gid_108954.zip

Rodriguez, J., Macciotta, R., Hendry, M.T., Roustaei, M., Gräpel, C., and Skirrow, R. 2020. UAVs for monitoring, investigation, and mitigation design of a rock slope with multiple failure mechanisms—a case study. *Landslides*, 17(9): 2027–2040.

Romana, M., Tomás, R., and Serón, J.B. 2015. Slope Mass Rating (SMR) geomechanics classification: thirty years review. *13th ISRM International Congress of Rock Mechanics*, OnePetro, Quebec, Canada. 10 pp.

Rose, B.T. 2005. *Tennessee rockfall management system.* Virginia Polytechnic Institute and State University.

Roustaei, M., Macciotta R., Hendry, M., Rodriguez, J., Gräpel, C., and Skirrow, R. 2020. Characterisation of a rock slope showing three weather-dominated failure modes. In *Proceedings of the 2020 International Symposium on Slope Stability in Open Pit Mining and Civil Engineering.* Australian Centre for Geomechanics, Perth. 427–438.

Russell, C.P., Santi, P., and Higgins, J.D. 2008. Modification and Statistical Analysis of the Colorado Rockfall Hazard Rating System. Prepared for Colorado Department of Transportation.

Santi, P.M., Russell, C.P., Higgins, J.D., and Spriet, J.I. 2008. Modification and statistical analysis of the Colorado rockfall hazard rating system. *Engineering Geology*, 104(1–2): 55–65.

Stewart, J. S., Rose, B., Marshall, J. R. 1924. *Upper Elk and Upper Highwood Rivers, British Columbia and Alberta.* Scale 1:253,440. Geological Survey of Canada, Multicoloured Geological Map. Open access from: https://ftp.maps.canada.ca/pub/nrcan_rncan/publications/STPublications_Publicat ionsST/106/106832/gscmcm_1980_e_1924_mn01.pdf

Tappenden, K.M. and Skirrow, R.K. 2020. Vision for Geotechnical Asset Management at Alberta Transportation. *2020 Canadian Geotechnical Conference (GeoVirtual).*

Walkinshaw, J.L. and Santi, P.M. 1996. *Landslides: Investigation and Mitigation*. Chapter 21-Shales and Other Degradable Materials. Transportation Research Board Special Report, 247.

Wolf, R.E., Bouali, E.H., Oommen, T., Dobson, R.J., Vitton, S., Brooks, C., and Lautala, P. 2015. *Sustainable Geotechnical Asset Management Along the Transportation Infrastructure Environment Using Remote Sensing: Final Report.* Michigan Technological University, Houghton, MI, USA.

Wollenberg-Barron T., Macciotta R., Gräpel C., Tappenden K., Skirrow R. 2022. Use of rock slope rating systems with remote sensing for Geotechnical Asset Management and preliminary application at a rock slope in Southern AB. In *Proceedings of the 8th Canadian Conference on Geotechnique and Natural Hazards:Geohazards 8, Quebec City, Musée de la civilisation*, 12-15 June, 2022. Canadian Geotechnical Society.

Wyllie, D.C. 2014. *Rock fall engineering*. CRC Press.

Chapter 4

Combining Change Detection and Slope Condition Assessment Tools to Enhance Geotechnical Asset Management in Alberta

Contributions made to this Chapter:

The work presented in this chapter, which includes literature review, development of a methodology, analysis, discussion of results, and writing of the text was carried out by the M.Sc. Recipient.

Dr. Renato Macciotta reviewed all parts of the work and provided guidance during the development of the methodology and analysis of the results. The other authors reviewed the text and provided recommendations for edits and additional discussion.

A version of this Chapter is being prepared for submission to the Canadian Geotechnical Journal with the following citation:

Wollenberg-Barron, T.D.G., Macciotta R., Mirhadi, N., Gräpel, C., Tappenden, K.M., and Skirrow, R.K. 2023. Combining Change Detection and Slope Condition Assessment Tools to Enhance Geotechnical Asset Management in Alberta. University of Alberta Geotechnical Centre [Unpublished].

Abstract

Alberta Transportation and Economic Corridors (TEC) is currently working towards the development of a formalized geotechnical asset management (GAM) program, which requires linking rockfall geohazard condition assessment tools with rock slope performance. Integrating the use of remote sensing technologies with condition

assessment tools may provide transportation agencies with a methodological basis to aid in the prioritization of capital expenditure for rockfall geohazard sites. Presented in this paper is a methodology to develop a direct correlation between slope condition assessments and slope performance metrics derived from change detection. The methodology is demonstrated using an initial database of change detection results for three rockfall geohazard sites in Alberta, Canada where a suite of rock slope and rock mass rating systems were applied, including Alberta's current condition assessment tool, the Geohazards Risk Management Program (GRMP) Risk Level rating. Rockfall metrics including annual failure volumes and annual frequencies for events greater than or equal to 1 m^3 were derived from the change detection results and compared with the results of the rock slope and rock mass rating tools for each of the study sites. Strong correlations were achieved between each rating system and the rockfall metrics derived from the change detection results. This methodology provides a direct correlation between practical condition assessment tools and rock slope performance monitoring techniques to be used along transportation corridors to improve prioritization of maintenance and remediation based on a quantified level of hazard.

4.1 Introduction

Alberta Transportation and Economic Corridors' (TEC) Geohazard Risk Management Program (GRMP) includes more than 250 actively monitored geohazard sites along the provincial highway network. Managing the risk imposed by geohazard sites requires monitoring through robust and cost-effective strategies to maintain a safe and efficient transportation network. In recent years, remote sensing techniques such as Unmanned Aerial Vehicle (UAV) photogrammetry and Light Detection and Ranging (LiDAR)

combined with a subsequent change detection analysis have become part of the state of practice in slope risk management due to how they allow for an improved understanding of slope deformation processes.

The results of change detection analyses completed for three rockfall geohazard sites within TEC's geotechnical asset inventory are presented in this paper. Five rock mass and rock slope rating systems were previously applied to each of these sites, in addition to TEC's current condition assessment tool: the GRMP Risk Level (RL) rating, to compare and assess the applicability of each for use as condition assessment tools as part of a geotechnical asset management (GAM) program (Wollenberg-Barron et al. 2023). The results of a previous study provided a shortlist of the rock slope and rock mass rating systems deemed most viable, which included: Alberta's GRMP RL rating (AMEC 2006), the Rockfall Hazard Rating System (RHRS) (Pierson 1992), the Q-Slope system (Barton and Bar 2015), and the Geological Strength Index (GSI) (Hoek 1994).

The integration of change detection analyses with the results of condition assessment tools can provide transportation agencies with an additional methodology to aid in the prioritization of capital expenditure for geohazard sites. The challenge which presents itself is how to combine the results of change detection with condition assessment results in a way that can benefit transportation agencies, such as TEC, in planning and prioritizing candidate mitigation projects to achieve agency strategic objectives as part of a GAM program. The approach presented in this paper can provide a direct correlation between practicable condition assessment tools applied to rock slopes along transportation corridors, and quantified levels of hazard and slope maintenance requirements as part of TEC's GAM program.

4.1.1 Geotechnical Asset Management

GAM emerged from Transportation Asset Management (TAM) due to the interrelated performance and impact of geotechnical assets on transportation infrastructure. Geotechnical assets can be defined as physical and independent assets present within a highway right-of-way which contribute to the operation of the transportation corridor (Tappenden and Skirrow 2020) The basis for a GAM program is generally defined by its governing agency's strategic goals, including but not limited to the management of risk within a transportation system. The assessment of each asset's condition within an asset inventory is necessary in determining how an agency's resources will be used to the greatest benefit when maintaining and remediating geotechnical assets throughout their lifetime in order to reduce their risk. Consistent documentation is essential to a comprehensive management program; each asset identified within a target area must be cataloged with its physical characteristics but also some measure of its cost, performance, and impact of failure (Bernhardt et al. 2003). The development and management of an asset inventory is a continuous process; following the initial assessment and identification of an unstable asset, continued monitoring of its performance is required to maintain an adequate resource allocation to accommodate changing conditions. This gives rise to the need for robust analytical tools capable of monitoring the performance of a geotechnical asset, forecasting its future condition, and planning for ongoing maintenance and future capital investment.

TEC is currently working towards the development of a formalized GAM program to enhance their ability to monitor the condition and deterioration of

geotechnical assets. The analysis presented in this paper was conducted to provide input for the continuous development of TEC's GAM program.

4.1.2 Remote Sensing Techniques

Rock slope performance at the study sites was quantified with the aid of remote sensing techniques. Remotely piloted and automated aerial vehicles, otherwise known as UAVs, have become increasingly popular for use in photogrammetric remote sensing. Recent technological advances have made UAVs cost effective and resulted in increased use of UAVs in geotechnical engineering (Salvini et al. 2013, Lucieer et al. 2014, Agüera-Vega et al. 2016, Rodriguez et al. 2020, Macciotta and Hendry 2021).

Imagery gathered via UAVs provide multiple perspectives of targets stored with position and orientation information for photogrammetry algorithms to construct detailed terrain surfaces, including point clouds. A variety of photogrammetry software is available to generate point clouds including those used in this research: Pix4Dmapper (Pix4D S.A. 2023) and 3DM Analyst (Adam Technology 2023a). A DJI Phantom 4 Pro was utilized for the collection of slope imagery throughout the course of this research, equipped with a 12 (earlier campaigns) to 17 (more recent campaigns) megapixel camera supported by a gimble to reduce vibration and increase stability during imagery collection. The UAV's internal GPS has a hovering accuracy of ± 1.5 m so ground control points (GCPs) with measured coordinates are essential for optimizing the accuracy of location and orientation information captured with each photo.

Point clouds generated via UAV photogrammetry are rendered with true colour images of the target, enhancing the ability to identify geological and structural features of rock slopes. Photogrammetry is dependent on optical imagery, requiring a clear view of the

target. Poor lighting and weather factors can impact the quality of imagery. Vegetation obscuring the ground surface also limits the quality of surface data. Other environmental factors may also impact the effectiveness of the UAV platform which is unable to operate in high winds.

LiDAR is a range-based imaging tool that uses the reflection of light to determine a target's location, measuring the time between a laser signal's emission to return (Lato 2010). LiDAR can be deployed via ground-based or airborne platforms for static (ground-based) and dynamic (via airplane, helicopter, satellite, and terrestrial or nautical vehicles) data collection. Unlike photogrammetry, LiDAR lacks the capacity to capture the true colour of a target and must be supplemented with photos to differentiate vegetation and identify some geological and structural features. While the upfront cost of LiDAR equipment is greater than that of a UAV setup, objects can be scanned relatively quickly to generate point clouds without the need for additional software.

The quality of LiDAR data depends on two major attributes: density and accuracy (Lato 2010). Generally, these attributes are controlled by the equipment, skill of the operator, and data processing experience and techniques utilized. Point density is controlled by the equipment used and highly dependent on the distance from the target. Additionally, for static LiDAR platforms, surface roughness may result in occlusion patterns (i.e., missing data) depending on the viewpoint of the device (Lague et al. 2013). This is less of a concern for dynamic platforms, including UAVs where multiple perspectives of an object are captured throughout the flight path. Other environmental factors like temperature and humidity can also impact LiDAR accuracy. For this research ground-based LiDAR data was captured using an Optech ILRIS-LR device which has a

maximum range of approximately 3,000 m (under ideal conditions) and an accuracy of

± 7 mm.

4.2 Study Sites

The rock slopes included in this study had been identified as rockfall hazards by TEC and

their consultants through the GRMP. Remote sensing data was collected at each site

utilizing either ground-based LiDAR or UAV photogrammetry on a 0.5- to 2-year

frequency, over a period of at least three years. Slope inspections and the application of

rock slope and rock mass rating systems as initial condition assessment tools were

conducted on November 12, 2021 for site C018, and between September 24 and 25, 2022

for sites S020 and S042. Due to the opposing slope aspects at the S042 site (S042-North

and S042-South), separate LiDAR scanning datums were required to capture the entire

slope. The locations and representative photographs for each of the study sites are shown

in Figure 4-1.
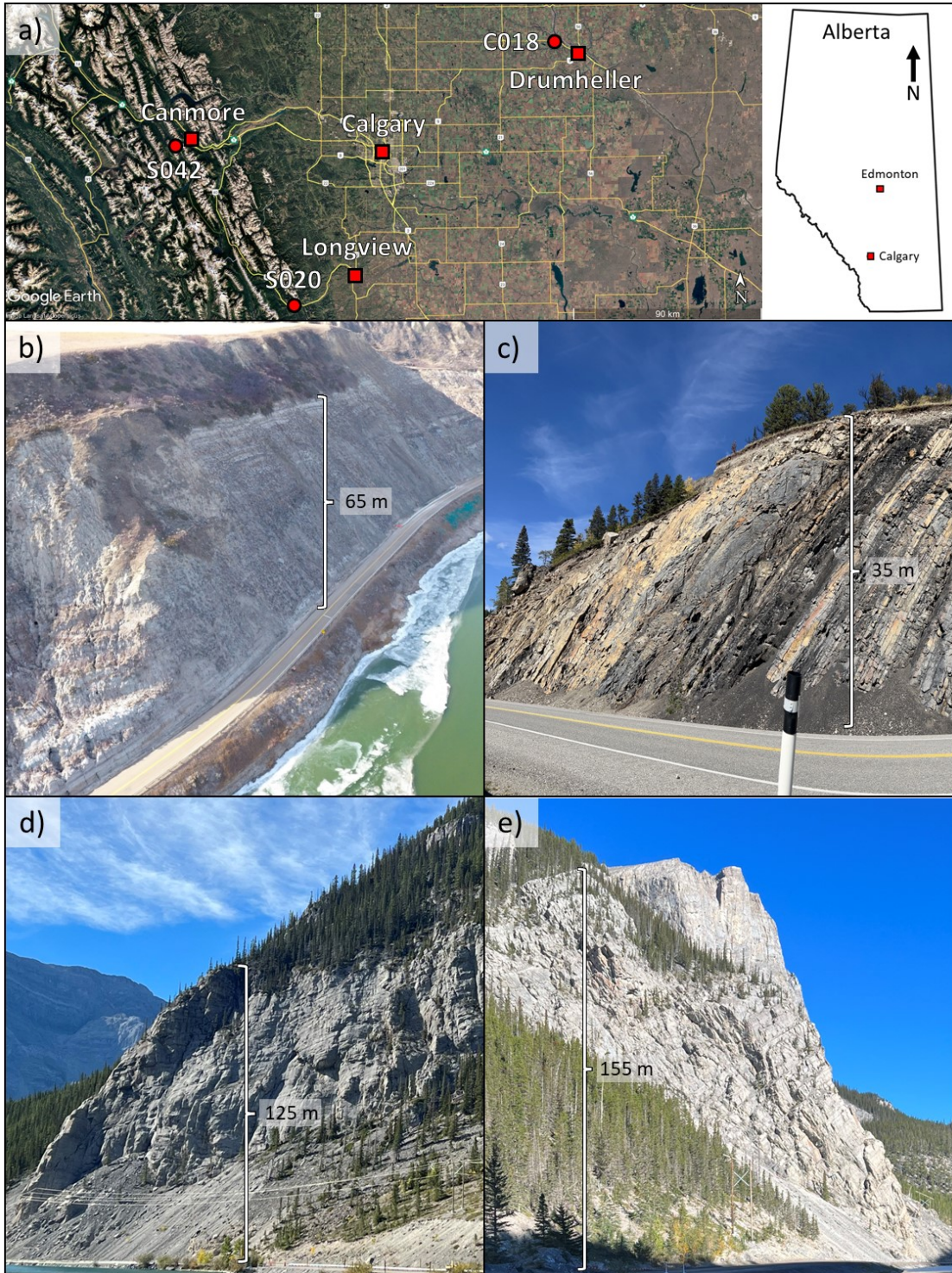
Figure 4-1: a) Location of rock slope case studies (red circles) with map of Alberta and populated centres (red squares) as reference (Google Earth 2022). Slope photos and approximate slope heights of b) C018, c) S020, d) S042-North, and e) S042-South.

70

4.2.1 C018 – Red Deer River Valley Slope Instability

The Red Deer River Valley Slope Instability, denoted as the C018 site within TEC's

GRMP Central Region, is located along Highway 837:02 approximately 14 km

Northwest of Drumheller, Alberta. The weighted average annual daily traffic (WAADT)

at this location is approximately 290 vehicles per day (vpd) (TEC 2022). The average

daily air temperature recorded near C018 ranges from lows of -17.9 °C in the winter to

highs of 24.5 °C in the summer, and the average annual precipitation of combined rainfall

and snow in the area is 370 mm (ACIS 2022). The slope is part of the Horseshoe Canyon

formation comprising feldspathic sandstone interbedded with siltstone, bentonitic

mudstone, carbonaceous mudstone, concretionary sideritic layers, and laterally

continuous coal seams (Roustaei et al 2020). The active portion of the C018 site is

approximately 60 m high and extends approximately 500 m along the highway adjacent

to the Red Deer River.

The implementation of a biannual remote sensing program utilizing UAV

photogrammetry at the C018 site began in 2017 following a debris flow. Other major

events occurred throughout 2017 and 2018 including a fall of frozen weathered rock, a

translational slide, and additional rockfalls, prompting the installation of jersey barriers to

effectively widen the catchment area, and reducing highway traffic to one lane. The

highly disaggregated and dispersive nature of the sedimentary deposits at the C018 site

leads to a variety of complex failure mechanisms. When temperatures are above zero,

erosional processes trigger rockfalls or sliding wedges, often preceded by precipitation

events which weaken the dispersive slope material and increase the potential for debris

flows. When temperatures are below zero the predominant failure mode is falls of frozen weathered rock.

To compare the varying risk associated with different slope failure mechanisms and rockfall block volumes, three GRMP RLs were developed by TEC and their consultants for the C018 site (KCB 2018a). These RLs set event volume thresholds for events greater than 0.5 m^3 (C018-L), less than 0.5 m^3 (C018-S), and for earth slide events. To capture the impact of increased failure event volume on the applicable rating systems, a volume of 10 m^3 was selected to represent an event greater than 0.5 m^3 based on TEC's experience with previous failures at the site.

4.2.2 S020 – Highwood House Rockfall Hazard

The Highwood House Rockfall Hazard, denoted as the S020 site within TEC's GRMP Southern Region, is located along Highway 541:02, approximately 800 m east of the junction between Highways 40, 541, and 940. The WAADT at this location is approximately 620 vpd (TEC 2022). The average daily air temperature recorded near the S020 site ranges from lows of -15.9 °C in the winter to highs of 19.7 °C in the summer. The average annual precipitation of combined rainfall and snow near the S020 site is 492 mm (ACIS 2022). The slope comprises interbedded coal, shale, mudstone, and sandstone with sub-vertical bedding planes. Geological maps of the area indicate the slope is composed of Mesozoic sandstone, shale, and coal (Stewart et al. 1924). KCB (2018b) noted that the mudstone and sandstone were notably less weathered than the coal and shale. The S020 site extends approximately 150 m along the highway and the slope is approximately 35 m high. The west side of the slope reaches a height of approximately 50 m where an extended zone of brow erosion has developed.

Due to the relatively high volume of rockfalls present in the ditch and the presence of boulders perched along the brow of the slope (KCB 2018b), a remote sensing program was initiated to assess failure modes and monitor slope performance. Remote sensing data was collected from the S020 site between 2020 and 2022 on an annual basis via drone photogrammetry. Rockfalls at the S020 site are likely attributed to both erosion of the surficial soils and differential weathering leading to undercutting of the rock mass.

4.2.3 S042 – Spray Lakes Rockfall

The Spray Lakes Rockfall, denoted as the S042 site within TEC's GRMP Southern Region, is located on Highway 742 (Spray Lakes Road) approximately 5 km southwest of Canmore, Alberta. The WAADT at this location is approximately 1420 vpd (TEC 2022). The average daily air temperature recorded near the S042 site ranges from lows of - 14.1 °C in the winter to highs of 20.7 °C in the summer. The average annual precipitation of combined rainfall and snow near the S042 site is 384 mm (ACIS 2022). The S042 site is part of the Mount Rundle range which comprises Paleozoic limestones, dolomitic limestones, dolostones, and shales (Macciotta et al. 2019). The north portion of S042 (S042-North), with an eastern slope aspect, extends approximately 200 m while the south portion (S042-South), with a southern slope aspect, extends approximately 110 m. The slope has a maximum height of approximately 155 m. A talus slope exists along the base of the slope which narrows significantly at the corner of the two opposing slope aspects.

A call-out inspection was made at the S042 site in 2013 following a relatively large rockfall event, with an estimated volume of 15 m^3, that narrowly missed a vehicle and group of people travelling along Highway 742 (AMEC 2015). A remote sensing

program utilizing ground-based LiDAR was initiated in 2018 for the S042 site which has continued annually. Macciotta et al (2019 and 2020) presented a kinematic analysis which found that wedge failure is the most probable failure mechanism at S042 while planar sliding and flexural toppling are marginally possible from the north slope. Similar to the C018 site, AMEC (2015) introduced two RLs for the S042 site following the rockfall event in 2013. These distinguished the relative difference in risk for small and frequent falls of loose blocks (S042-S), and large and infrequent rockfalls (S042-L). Large rockfall blocks volumes were defined by KCB (2019) as greater than 15 m^3 based on structural analyses. The small rockfall block volume was selected as less than 0.3 m^3 following the observations and analysis presented in Macciotta et al. (2019). With the application of the additional rating systems to the S042 site (Wollenberg-Barron et al. 2023), up to four ratings for the S042 site exist. These account for both the north and south slopes as well as the two rockfall block volume thresholds, i.e., S042-North-S, S042-North-L, S042-South-S, and S042-South-L.

4.3 Change Detection Methodology

Change detection is a process of detecting the variation between two temporally independent topographic models (Deane et al. 2020). Before measuring the change, point clouds generated through LiDAR or photogrammetry must first be aligned considering topographic changes that may have occurred over time. This is achieved by either matching areas considered stable or matching the entire slope but limiting the degree of overlap. The latter applies to slopes with only isolated movements. The first survey of the target area is generally used as the reference and each subsequent survey is aligned to the first to monitor cumulative change.

Several methods of change detection are available, including DEM of difference (DoD), direct cloud-to-cloud comparison (C2C) (Girardeau-Montaut et al. 2005), cloud-to-mesh or cloud-to-model distance (C2M), and multi-scale model-to-model cloud comparison (M3C2) (Lague et al. 2013). Both the C2C and M3C2 methodologies are available within the CloudCompare V2.12 software (CloudCompare 2022). There are obvious limitations regarding the C2C since the direction of the distance computation is dependent on the point spacing and surface roughness of each cloud (DiFancesco et al. 2020). The M3C2 change detection method works by first sub-sampling core points from the reference cloud. Then, normal vectors are calculated for points which fall within a specified diameter around each core point. Finally, an average distance between the two clouds is calculated along the previously determined core point vectors, within a specified cylindrical diameter. Some limitations arise with complex topography and surface roughness where the distance can be overestimated due to normal misorientation (Lague et al. 2013). M3C2 has become a widely used method for change detection in a variety of fields, including rock slopes (Macciotta and Martin 2019, Rodriguez et al. 2020, DiFrancesco et al. 2020, Deane et al. 2020).

Slope imagery collected from UAV platforms requires pre-processing by photogrammetry software to generate point clouds. Both Pix4Dmapper and 3DM Analyst with 3DM CalibCam (Adam Technology 2023b) were used over the course of the remote sensing programs at the C018 and S020 sites to construct point clouds from UAV imagery. LiDAR data collected with the Optech ILRIS-LR, or similar ground-based LiDAR system, requires minimal pre-processing to generate a point cloud.

CloudCompare V2.12 (CloudCompare 2022) was utilized for all the subsequent

analysis steps. Each point cloud was visually inspected in detail to confirm adequate

point density, cloud completeness, or presence of any anomalies. The density of each

cloud was measured in CloudCompare using the Compute Geometric Features tool. The

CloudCompare Statistical Outlier Removal (SOR) filter was utilized to remove outlier

points and reduce cloud noise. The SOR filter tends to exacerbate any occlusion patterns

present especially for surfaces with a high degree of surface roughness. This was

mitigated by selecting SOR filter parameters iteratively, observing if undesirable point

removal occurs after each application. Point cloud alignment was completed in a multi-

stage process. First, vegetation present within the areas of interest was identified, cross

referenced and verified with photos, and removed from each point cloud. Then, the Align

(point pairs picking) tool was used to select equivalent stable locations (i.e., without slope

movement or rockfall detachment) between the reference and each aligned cloud. This

provides a 'rough' alignment of the clouds so that the Fine Registration (ICP) tool can be

used. An initial fine registration was completed over the entire slope surface. A second

round of fine registration was conducted isolating sections of each slope which are

considered 'stable' and aligning those to mitigate the loss of potential slope movements

in other areas. If poor point cloud registration persisted after multiple alignment attempts,

the clouds were split into sections and individually aligned. It is important to note that

point clouds generated through photogrammetry require scale adjustment during the

alignment process if GCPs are not established during each UAV scan. In this case, each

aligned cloud was scaled to the reference cloud. Once the alignment process was

completed, the M3C2 plugin was utilized to generate change detection clouds for each pair of reference and aligned clouds.

The limit of detection (LoD) for each analysis was estimated via two methods. The first was set as 2 times the standard deviation of the measured change across the slope for areas identified as stable (Deane et al. 2020). The second method used Equation 4-1 presented in Lague et al. (2013) for a 95% confidence interval ($LOD_{95\%}$).

$$LOD_{95\%}(d) = \pm 1.96 \left(\sqrt{\frac{\sigma_1(d)^2}{n_1} + \frac{\sigma_2(d)^2}{n_2}} + reg \right) \tag{4-1}$$

$\sigma_1(d)$ and $\sigma_2(d)$ correspond to the standard deviations, or local roughness, measured within a diameter d and across several points equal to n_1 and n_2 on the reference and aligned point clouds, respectively. The registration error (reg) between each cloud pair was estimated using the CloudCompare Root Mean Square (RMS) value resulting after the final fine registration. The RMS value is essentially an approximation of the registration error between the cloud pairs but computed on less points.

Once the change detection process was completed for the study areas, individual rockfall events were identified and their volumes were estimated by taking the average change multiplied by the impacted area. If it was not possible to isolate individual rockfalls occurring across the slopes, the 2.5D Volume tool within CloudCompare was utilized to estimate the total volume change within specified areas. The 2.5D Volume tool works by rasterizing point pairs between the reference and aligned cloud and summing the product of the columnal distances over a specified grid spacing. As noted by DiFancesco et al. (2020) this method, while robust, is highly sensitive to the grid spacing and other input parameters. For this reason, use of the 2.5D Volume tool was limited to

slope movements that could not be reasonably attributed to isolated rockfall events (e.g., zones of extended erosion).

4.4 Change Detection Results

Two metrics were selected from the change detection results to quantify slope performance: the average annual failure volume from the currently available remote sensing periods, and the frequency of failure events greater than or equal to 1 m^3 from failure volume-cumulative frequency plots developed for each study site. Annual failure volumes provide a measure of the required cleanup effort for slope maintenance, while frequency of events greater than or equal to 1 m^3 provides an indirect measure of the hazard of falling material impacting vehicles or blocking the road. Failure volume-cumulative frequency relationships are commonly used tools for calculating failure frequencies from rock slopes (Macciotta et al. 2019, 2020) and were developed from individual event volumes extracted from the change detection analyses performed. These plots provide a quantitative volume-failure likelihood for each of the study sites. The following sections provide the detailed results of the change detection analyses conducted at each site.

4.4.1 The C018 Site

Change detection results from December 2017 to May 2018 for the C018 site were previously published by Rodriguez et al. (2020) and Roustaei et al. (2020), and additional change detection analyses were conducted on subsequent point clouds. A total of 9 change detection analyses were conducted for the C018 site. The density of the point clouds generated of the C018 site ranged from approximately 500 to 20 points/m^2 which

corresponds to an approximate point spacing between 4 and 100 mm, respectively. The

wide range of cloud densities is attributed to the densification of the earlier point clouds

(Rodriguez et al. 2020). However, the range of point cloud densities was not found to

have a significant impact on the change detection results, while the lower density clouds

were less computationally expensive. The LoD for the C018 site change detection

analysis was determined for each set of reference and aligned clouds following the

methodology presented in Section 4.3. A homogenized LoD of 0.2 m was applied to each

change detection analysis in order to assess the cumulative slope change across multiple

years of change detection. The results of the change detection analysis and progressive

material loss between 2018 and 2022 at the C018 site is presented in Figure 4-2.
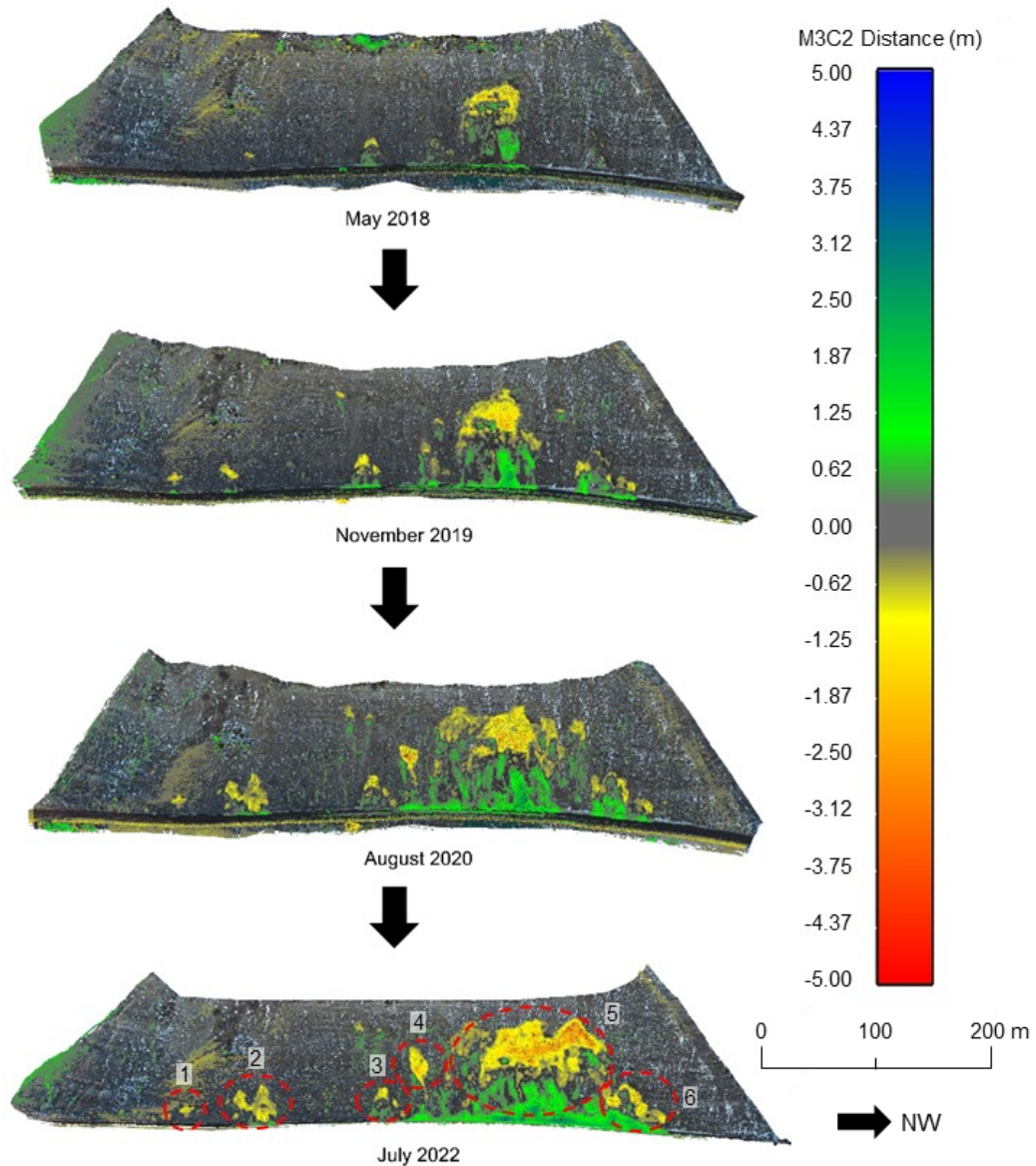
Figure 4-2: Results of the change detection analyses for the C018 site with the six active zones highlighted. Each change detection is relative to December 2017.

To estimate the volumes of change from each of the change detection analyses conducted for the C018 site, CloudCompare's 2.5D Volume tool was applied to six active zones (noted on the July 2022 change detection in Figure 4-2) corresponding to areas of the greatest measured change. Due to the highly disaggregated nature of the rock mass comprising the C018 site, it was not feasible to isolate individual detachments from the

slope. The six active zones have shown material loss since December 2017 and are the

main contributors of material falling and reaching the highway. The highest degree of

material loss occurred from zone 5 where the depth of material loss, normal to the slope

surface, has reached approximately 3 m. Zones 3 to 6, comprising almost half of the slope

length, are considered the most active areas, where surficial erosion has led to

progressive failures. The flanks of the landslide in zone 5 have enlarged on both sides,

especially towards the northwest, and the crown has progressively retrogressed up slope.

The active zones show no signs of slowing, and the volume of material deposited in the

ditch is expected to increase as the failure area progresses up slope. The cumulative

material loss measured at the C018 site for each change detection period, relative to the

December 2017 point cloud, is presented in Table 4-1. The average annual failure volume

calculated for the C018 site is approximately 696 m^3 from the currently available remote

sensing period.

Table 4-1: Cumulative material loss by zone at the C018 site relative to December 2017.

Aligned scan date	Cumulative material loss (m^3)						
	Zone 1	Zone 2	Zone 3	Zone 4	Zone 5	Zone 6	Total
18-May	6.0	36.9	45.6	14.3	706.9	48.7	858.5
18-Nov	9.7	49.3	46.5	18.9	720.0	58.9	903.2
19-Aug	18.5	62.0	63.6	21.6	920.5	147.5	1233.7
19-Nov	19.4	57.5	60.0	14.0	1042.9	161.5	1355.2
20-Aug	23.1	178.8	74.3	170.7	1427.9	235.7	2110.5
21-May	19.6	164.3	70.1	137.4	1859.4	233.3	2484.1
21-Nov	18.1	157.9	65.0	126.9	1920.2	256.5	2544.6
22-Apr	17.9	153.3	68.2	161.2	1947.1	233.0	2580.7
22-Jul	22.8	181.6	77.7	142.3	2087.6	390.2	2902.2

Failure volume-frequency relationships for changes detected at the C018 site were estimated utilizing the change measured at each of the six active zones between each of the available point clouds. While these measured changes do not directly correspond to isolated detachments from the slope, they act as an approximation of the progressive material loss over the current monitoring period. It is likely that some of these measured volumes are a combination of several smaller events occurring throughout the period between capture of remote sensing data. The largest of the measured incremental changes was approximately 432 m^3, occurring between August 2020 and November 2021. While quite large, this volume is reasonable considering the two debris flows in 2017, which triggered the initiation of a remote sensing program at the C018 site, had an estimated combined volume of 1,300 m^3 (Rodriguez et al. 2020). The volume-frequency plots developed for the C018 site are presented in Figure 4-3. The frequency for an event greater than or equal to 1 m^3 was estimated by applying a best-fit trendline to Figure 4-3b which resulted in a frequency of approximately 8.0 events per year.
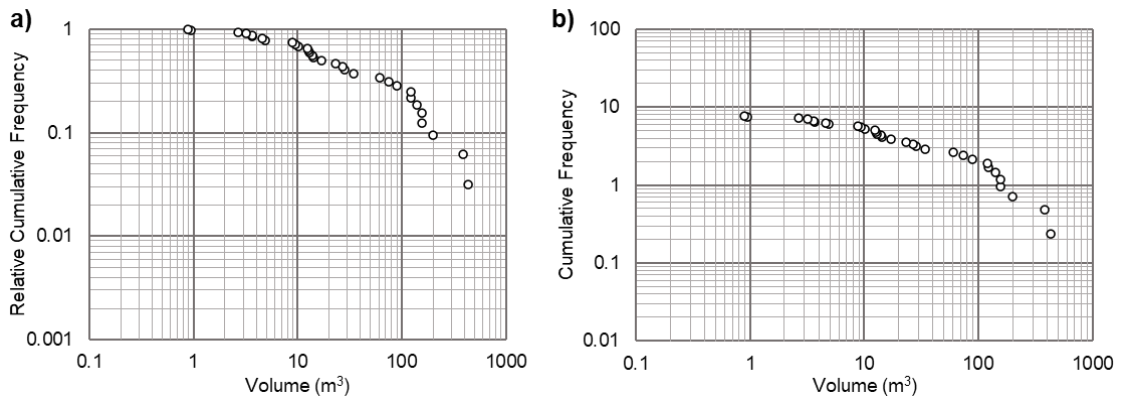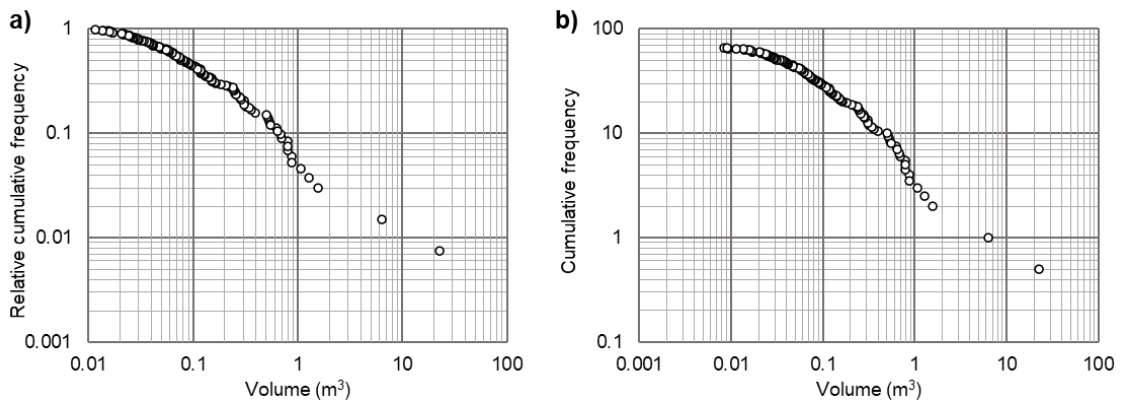

Figure 4-3: a) Relative and b) absolute cumulative frequency of detected volumes changes from the active zones of the C018 site.

4.4.2 The S020 Site

A total of 2 change detection analyses were completed for the S020 site. The density of

the point clouds generated of the S020 site ranged from 84 to 28 points/m^2, which equates

to a point spacing of approximately 24 to 72 mm, respectively. The LoD of the change

detection results for the S020 site was determined through both methods described in

Section 4.3. The average of the two methods, which resulted in a LoD of approximately

15 cm, was then applied to both analyses.

The change detection analyses from 2020 to 2021 and 2020 to 2022 are presented

in Figure 4-4a and Figure 4-4b, respectively. Two boulders which are perched within the

surficial colluvial soil along the brow that are highlighted in Figure 4-4a are expected to

eventually fall. However, no movement from them was detected during the current

monitoring period. Erosion of the block-in-matrix colluvial soil across the brow of the

slope appears to be a prominent rockfall failure mechanism at the S020 site. Additionally,

highlighted in Figure 4-4b is the presence of a slickensided discontinuity surface, which

likely contributed to a rockfall event detected between 2021 and 2022 with an estimated

volume of approximately 6.3 m^3. Other potential failure mechanisms identified include

weathering of the interbedded coal seams, leading to reduced confinement of the

surrounding, more competent rock, producing further rockfalls and block toppling along

joints nearly parallel to the slope face.
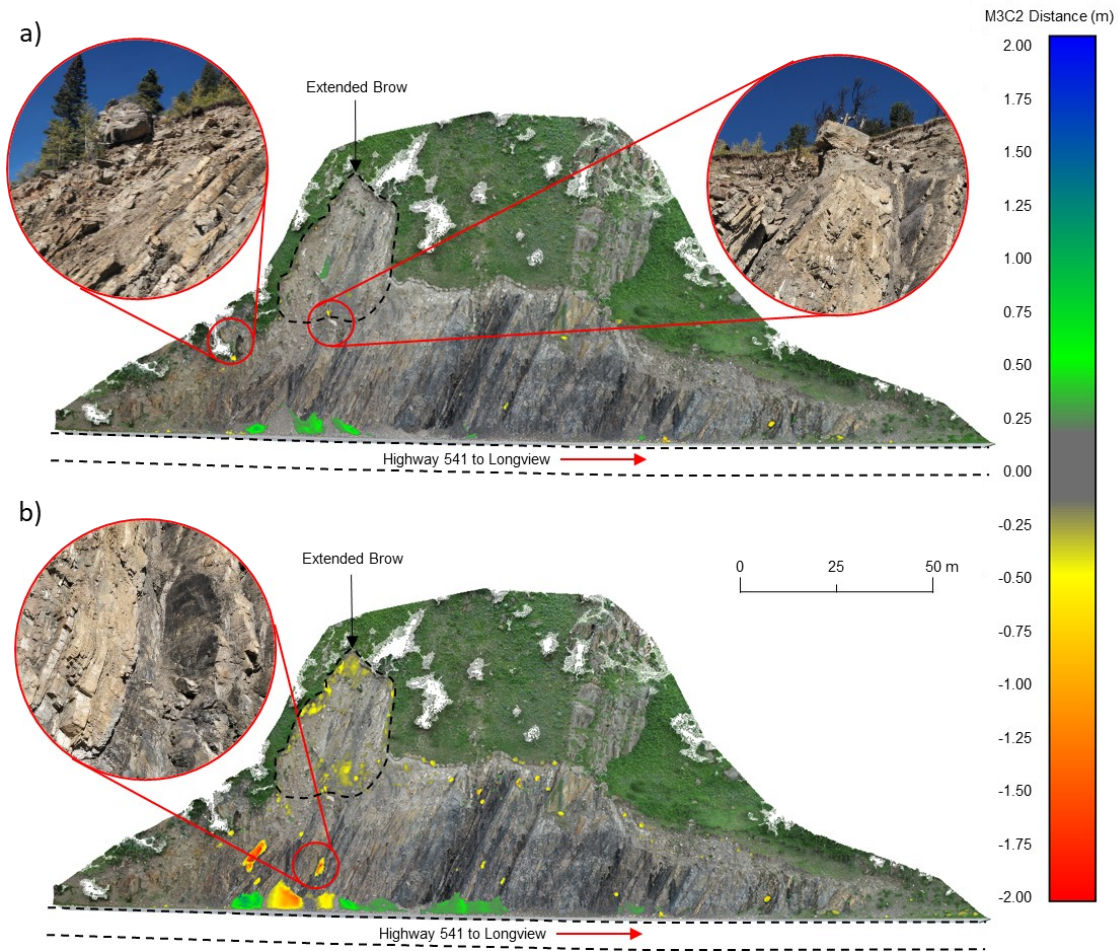
Figure 4-4: Results of the change detection analyses conducted for the S020 site from a) 2020 to 2021, highlighting two boulders perched at the brow of the slope and b) 2020 to 2022, highlighting slickenside rock surface exposed after recent rockfall.

Rockfall and erosion detected across the S020 slope and brow, for both the 2021 and 2022 change detection, were identified and individual volume estimations were completed for each. For the zone of extended brow erosion above the western portion of the slope, denoted as the Extended Brow for further discussion in this paper, an aggregated volume calculation was conducted utilizing CloudCompare's 2.5D volume tool since it was not possible to determine which, if any, of these changes were attributed

to isolated events versus cumulative erosion. It should be noted that rockfalls and erosional movements identified across the rest of the slope were assumed to be isolated events equal to their measured volume. I.e., the possibility of progressive erosion throughout the period of change detection was neglected; however this was considered a reasonable assumption due to the blocky nature of the exposed rock slope. The largest individual rockfall event had an estimated volume of approximately 22.5 m^3, which likely filled that portion of the ditch upon failure. The measured material loss for each change detection period conducted for the S020 slope is presented in Table 4-2. The average annual failure volume calculated for the S020 site is approximately 76 m^3 from the currently available remote sensing period. The negative value presented for the material loss from the Extended Brow between 2020 and 2021 indicates that more material was retained within the Extended Brow than debris discharged towards the highway below. Note that the volume discharged from the Extended Brow in 2022, however, greatly outweighs the combined volume measured from the rest of the S020 site.

Table 4-2: Change detection volumes and number of detected events for the S020 site.

Change Detection Period	Measured Material Loss (m^3)				Number of Events
	Slope	Brow	Extended Brow	Total	
2020-2021	2.1	3.6	-3.9	1.9	33
2020-2022	37.5	14.6	99.3	151.4	100

A review of precipitation data from weather stations near the S020 site was conducted to understand the drastic difference in rockfall volumes between the 2021 and 2022 change detection results. In Figure 4-5 the daily and cumulative precipitation spanning the current remote sensing period is presented. The 2021 UAV survey was completed in May

of 2021, while the 2020 and 2022 scans were conducted in July. The difference in cumulative precipitation between the consecutive remote sensing dates was found to be approximately 390 mm. This is possibly a result of the early capture of remote sensing data in 2021, with approximately 180 mm of cumulative precipitation between May and July of 2021, but more likely a result of several large precipitation events which occurred during the summer months of 2021 and 2022. Two of these events produced more than 50 mm of precipitation in 24 hours. This suggests that the occurrence of intense precipitation events is another major factor contributing to failure frequency and volumes at the S020 site, and would explain the large volume of displaced material between spring of 2021 and 2022.
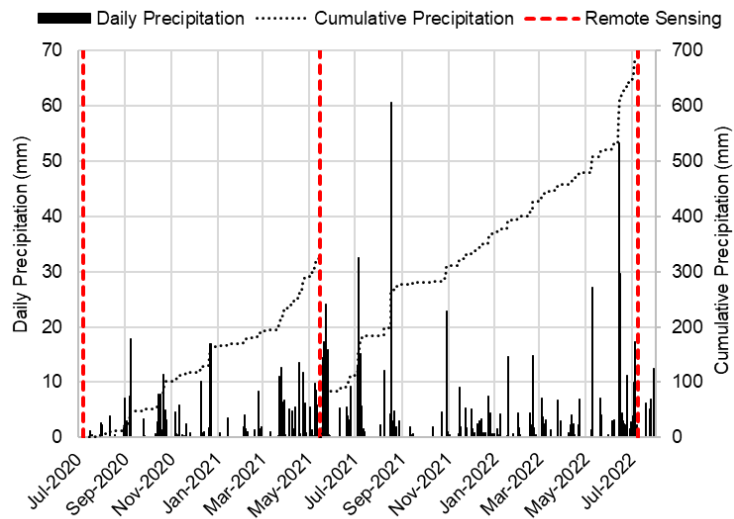
Figure 4-5: Recorded precipitation near the S020 site compared to the collection dates of remote sensing data.

The individual event volumes extracted from the change detection analysis conducted for the S020 site were used to develop the failure volume-frequency plots presented in Figure 4-6. It should be noted that the material losses due to surficial erosion

detected within the Extended Brow were excluded from this figure, as they could not be attributed to individual event volumes. A best-fit trendline was applied to the section of the curve crossing 1 m³ in Figure 4-6b to determine an appropriate event frequency. The frequency for events greater than or equal to 1 m³ at the S020 site was estimated at 4.7 per year.
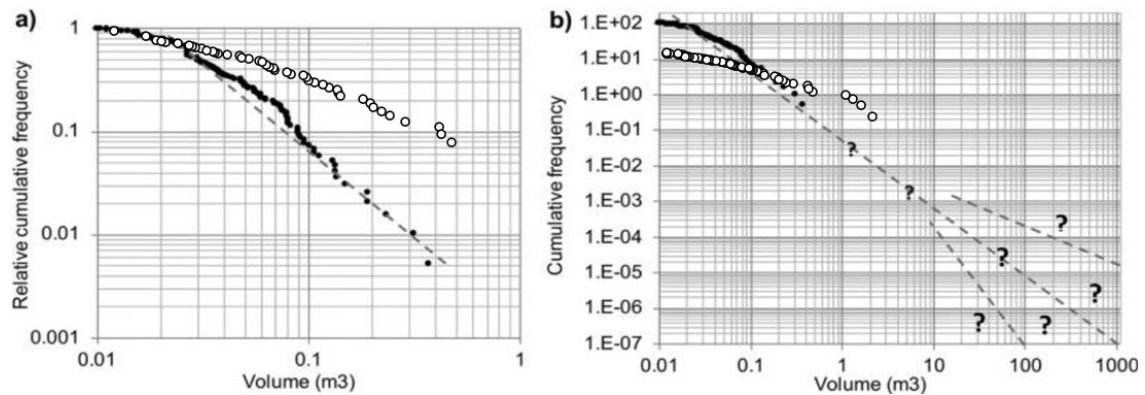

Figure 4-6: a) Relative and b) absolute cumulative frequency of detected volumes changes from the active zones of the S020 site.

4.4.3 The S042 Site

A total of 5 change detection analyses were performed for the S042 site, two for the north slope and three for the south slope. The densities of the point clouds gathered for the S042 site ranged from approximately 300 to 1400 points per m² which corresponds to a point spacing between 1.4 mm and 6.7 mm, respectively. Similar to the S020 site, the LoD of the change detection results for the S042 site was determined through both methods described in Section 4.3. The largest of the two methods resulted in an average LoD of approximately 20 cm which was applied to each analysis to assess the cumulative slope change over the current monitoring period.

The change detection results between 2018 and 2022 for both S042-North and

S042-South are presented in Figure 4-7a and Figure 4-7b, respectively. Compared to the

two previously discussed slopes, a relatively small number of rockfalls were detected

from the S042 site. This is attributed to the higher quality of rock comprising the S042

site compared to both the C018 and S020 sites. From the current period of change

detection results, it is difficult to discern the prominent failure mechanisms present;

wedge failures are the most likely, occurring between the prominent bedding plane and

intersecting discontinuities. Erosion of the talus slope, undercutting larger blocks which

eventually fall is another mechanism present which results in material reaching the

highway. While the rock mass comprising S042-South appears to be of slightly lower

quality than S042-North, the large rockfall event in 2013, with an estimated volume of 15

m^3, originated from the north slope. Its approximate location is highlighted in Figure

4-7a. The two largest rockfalls detected during this analysis period originated from S042-

South, as highlighted in Figure 4-7b; the events occurred between 2020 and 2022, and

have volumes estimated at 2.10 m^3 and 0.42 m^3. The final resting place of these rockfalls

could not be confirmed, nor the degree of disaggregation they experienced during the fall.

While other slope movements greater than 1 m^3 were detected, they originated from the

talus slope (previous rockfall events that were contained on the talus) rather than as

detachments from the S042 rock face.
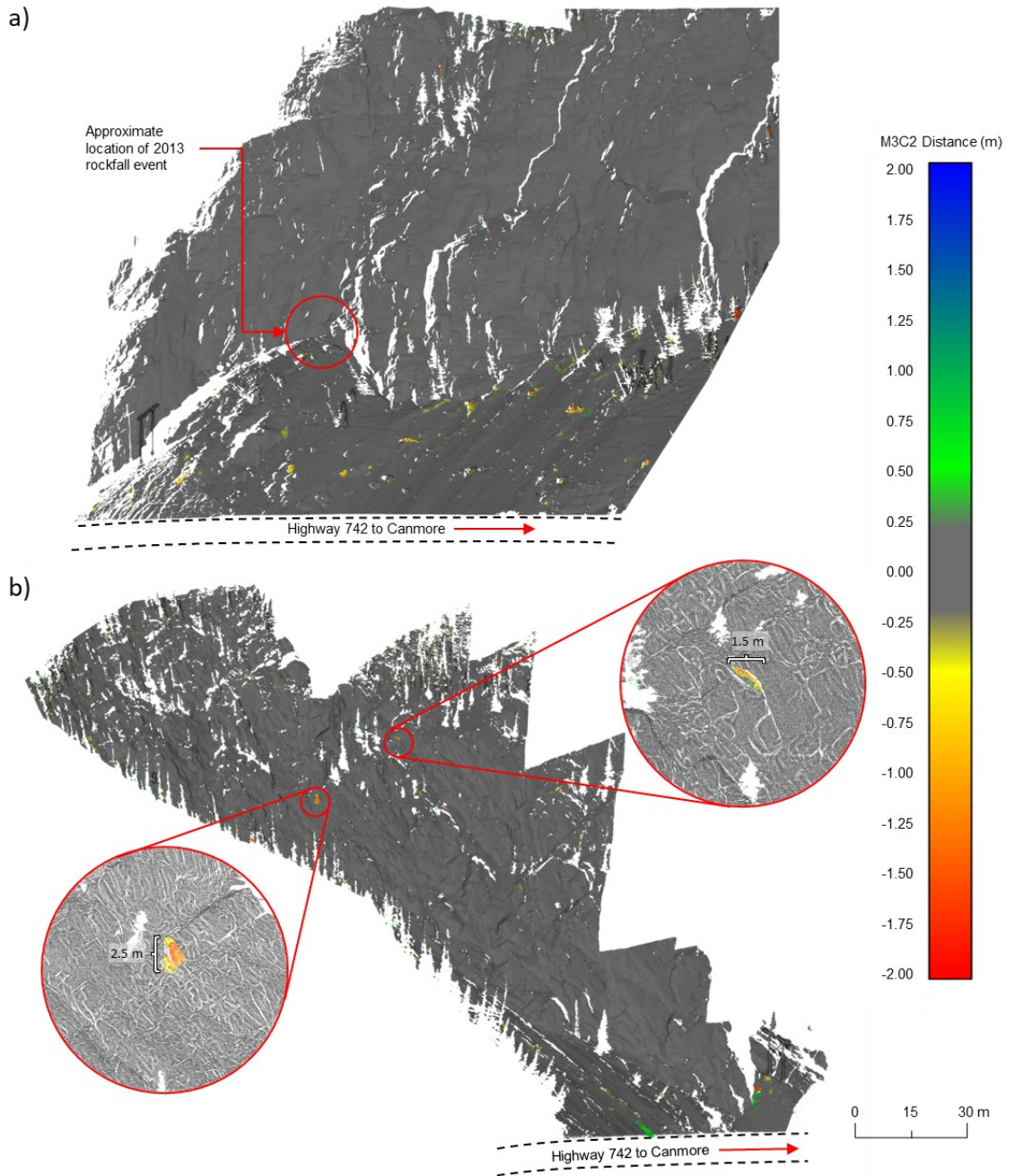
Figure 4-7: Results of the change detection analyses for the S042 site from 2018 to 2022 for a) S042-North, highlighting the approximate location of the 2013 rockfall event and b) S042-South highlighting location of two largest detected rockfalls (Modified from Wollenberg-Barron et al. 2023).

To account for all potential slope movements which could impact Highway 742, the change detection results for both the rock slope and talus slope were reviewed for movements. Only movements detected within the talus slope which appear to have reached the highway below were included in the volume calculations.
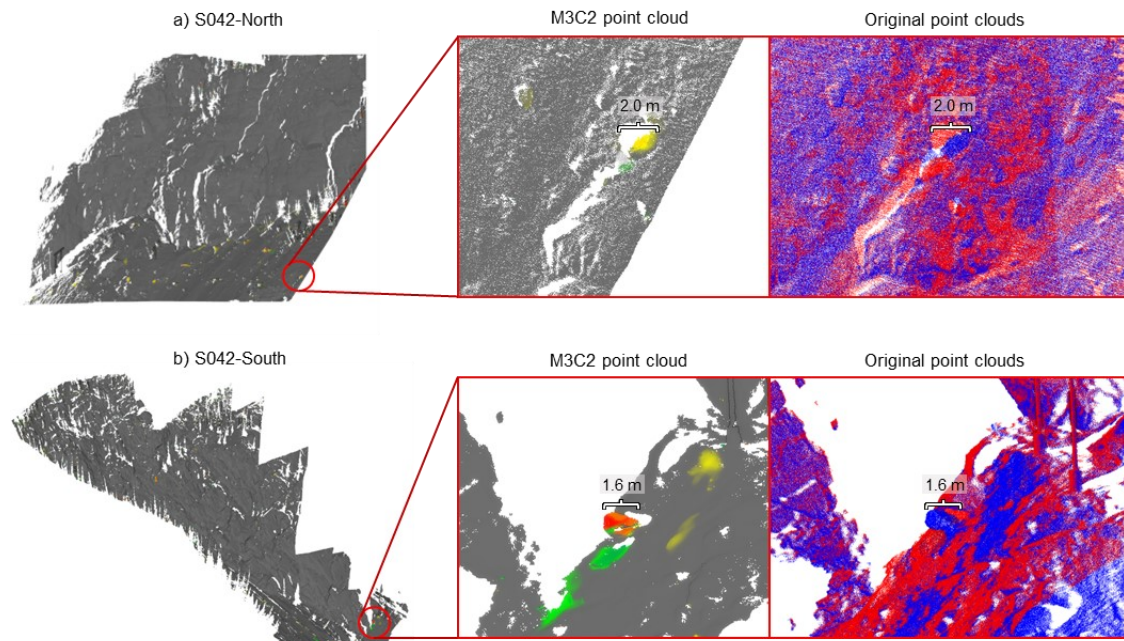
Figure 4-8: Technique used to determine if talus slope movements reached the highway. Examples from a) S042-North and b) S042-South utilizing both the M3C2 point clouds and original point clouds. The 2018 and 2022 point clouds are displayed in blue and red, respectively.

The individual volume estimation methodology described in Section 4.3 was utilized for each of the detected movements. The measured material loss for each change detection period conducted for the S042 site is presented in Table 4-3. While more events and a greater total volume were detected originating from S042-North, most of the volume was attributed to movements from the extensive talus slope. The largest rockfall from the slope at S042-North was measured to be approximately 0.12 m^3. It should be

90

noted that none of the events detected within the 4-year monitoring period were close to the 15 m^3, large rockfall threshold introduced in Section 4.2.3. Considering the large rockfall event in 2013 which originated from S042-North, the current period of change detection results fails to capture the return period of large rockfall events (greater than 15 m^3) at the S042 site. The average annual combined failure volumes over the current monitoring period, combining slope detachments and talus slope movements for the S042 site, were approximately 1.7 m^3 and 0.9 m^3 for the north and south slope, respectively.

Table 4-3: Change detection volumes and number of detected events for the S042 site.

Slope	Change Detection Period	Total measured change (m^3)			Number of events
		Slope	Talus	Total	
S042-North	2018-2021	0.24	4.23	4.47	21
	2018-2022	0.13	2.87	3.00	23
S042-South	2018-2020	0.02	0.10	0.12	5
	2018-2021	0.42	0.43	0.85	7
	2018-2022	2.19	0.48	2.67	8

A failure volume-frequency relationship was previously developed for the S042 site (Macciotta et al. 2019), and the results of the current change detection analysis are overlain in Figure 4-9 for comparison. The previously developed failure volume-frequency relationship utilized rockfall blocks which were present along the toe of the talus slope and therefore, had reached the highway. The relationship developed from the change detection results presented herein is of detachments from the slope and movements within the talus slope which had no distinct endpoint, unlike the examples shown in Figure 4-8 which were likely to have reached the highway. The difference between the two could be interpreted as a quantifiable effectiveness of the talus slope for

reducing a rock block's energy, or an indication of larger rockfall blocks breaking up before reaching the highway. Importantly, the difference between the two plots also results from the limitations imposed by the LoD of the change detection analysis performed, as rockfall blocks less than 20 cm were not detected (it is noted that blocks of this and lower volumes would be the most commonly found on the road). A best-fit trendline was applied to the section of the curve crossing 1 m^3 in Figure 4-9b to determine an appropriate event frequency. The frequency for events greater than or equal to 1 m3 at the S042 site was estimated at 0.7 events per year.

Figure 4-9: a) Relative and b) absolute cumulative frequency of detected slope movements from the S042 site change detection (white circles) overlain on previously developed failure volume-frequency plots (black dots) (modified from Macciotta et al. 2019).

4.5 Slope Performance and Condition Ratings

The GRMP RL rating, RHRS, Q-Slope system, and GSI were shortlisted as the most viable options for TEC to implement as part of a formalized GAM program for slope condition rating (Wollenberg-Barron et al. 2023). The GRMP RL is the product of two qualitative factors: a probability factor (PF), ranging from 1 to 20, and consequence factor (CF), ranging from 1 to 10. Each is selected from tables developed to address a

variety of geohazard types including earth slides and debris flows, rockfalls, erosion, and voids-dispersive soil sites (AMEC 2006). Q-Slope and GSI have no capacity to quantify the consequence of failure, and are only representative of the likelihood of failure. Similarly, the failure metrics derived from the change detection results presented in this paper carry the same limitation and therefore were compared to the GRMP PF and not RL.

Table 4-4: Failure metrics derived from change detection results and previously developed condition assessment tool results in Wollenberg-Barron et al. (2023).

| Study Site | *Average annual failure volume (m³) | ≥ 1 m³ annual event frequency | GRMP Rating | | | RHRS | Q-Slope | GSI |
			PF	CF	RL			
C018-S	696.0	8.0	15	6	90	413	0.00083	15 - 25
C018-L	696.0	8.0	16	9	144	512	0.00083	15 - 25
S020	76.2	4.7	14	5	70	394	0.036	20 - 35
S042-North-S	1.7	0.7	13	4	52	293	0.098	55 - 70
S042-North-L	1.7	0.7	7	7	49	358	0.098	55 - 70
S042-South-S	0.9	0.7	13	4	52	287	0.099	50 - 65
S042-South-L	0.9	0.7	7	7	49	352	0.099	50 - 65

*Detected by change detection techniques limited by the respective LoD assigned to each slope.

Correlations were developed between each of the condition assessment tool results and change detection results. Since four individual ratings were developed for each of the RHRS, Q-Slope, and GSI at the S042 site, results for each of the condition assessment tools applied to S042 site with minimal difference in value were labelled following the nomenclature introduced for the S042 site in Section 4.2.3 in the following figures, i.e., either S042-North and S042-South or S042-S and S042-L.

In Figure 4-10 the calculated average annual failure volume was plotted against the GRMP PF, RHRS, Q-Slope, and GSI values for each of the study sites. The average annual failure volume, across the x-axis, was plotted on a logarithmic scale to accentuate the relatively large range of failure volumes from the three study sites. Trendlines were applied to determine a coefficient of determination (R^2) for each. The resulting R^2 values indicate a strong correlation between the annual average failure volumes and each of the condition assessment tools. The lowest R^2 was 0.54 for the correlation with the GRMP PF, shown in Figure 4-10a, which is attributed to the variation in GRMP PF between the rockfall volume thresholds assigned to the S042 site. This deviation is not unexpected as the GRMP PFs and RLs for the S042 site were previously identified as a prominent outlier in the analysis of condition assessment tools presented in Wollenberg-Barron et al. (2023). The other R^2 values presented in Figure 4-10b, Figure 4-10c, and Figure 4-10d for RHRS, Q-Slope, and GSI, respectively, ranged from 0.73 to 0.95. This gives credit to the robustness of the RHRS, Q-Slope, and GSI as rock slope and rock mass rating systems.
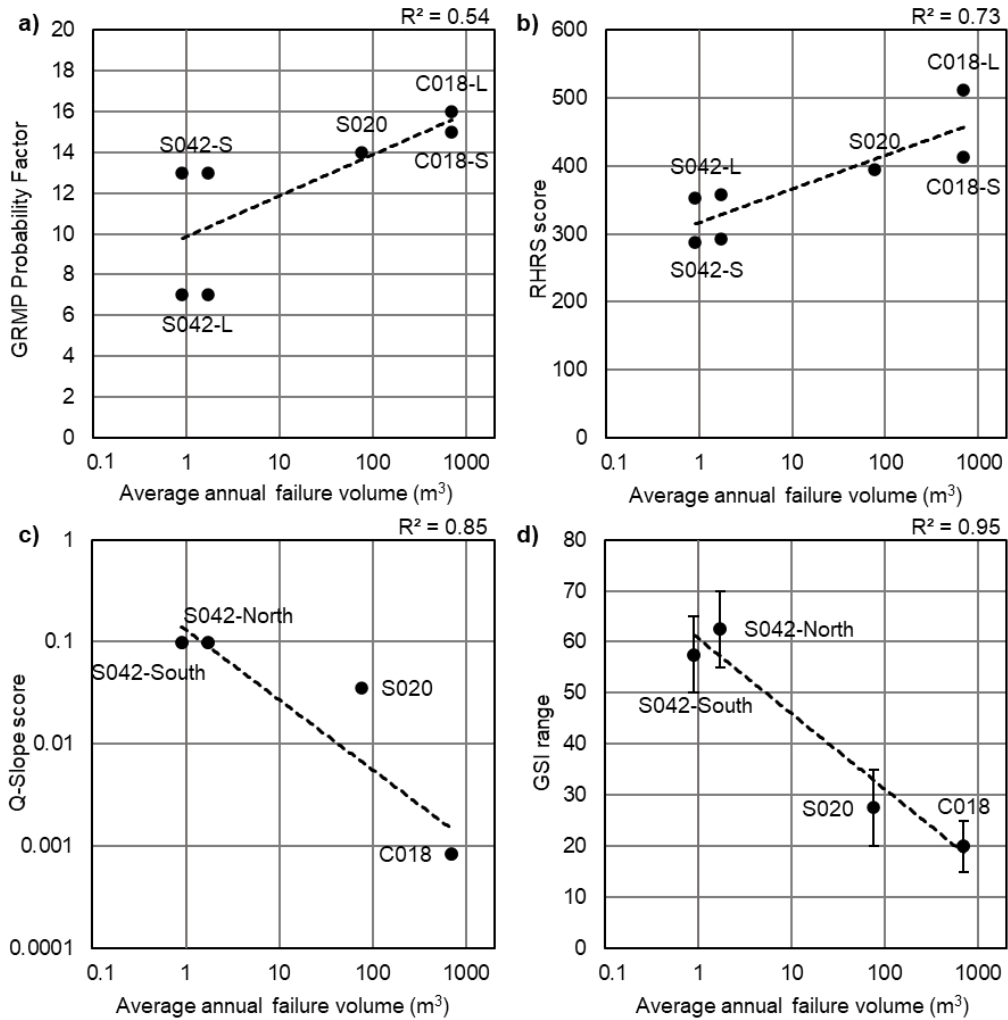
Figure 4-10: Correlations derived from the measured annual average failure volume and shortlisted condition assessment tools, including a) the GRMP PF, b) the RHRS, c) Q-Slope, and d) GSI.

The annual frequency for events greater than or equal to 1 m³ was plotted against the GRMP PF, RHRS, Q-Slope, and GSI values for each study site in Figure 4-11. Like Figure 4-10, trendlines were added to determine the R^2 of each which resulted in relatively high values ranging from 0.61 to 0.94. The R^2 for the correlation between the GRMP PF and annual event frequency, presented in Figure 4-11a, was slightly greater than that of Figure 4-10a, with a value of 0.61. This may be a result of fewer data points

used to develop Figure 4-11a since events from both S042-North and S042-South were combined to develop a more representative failure volume-frequency plot for the S042 site.
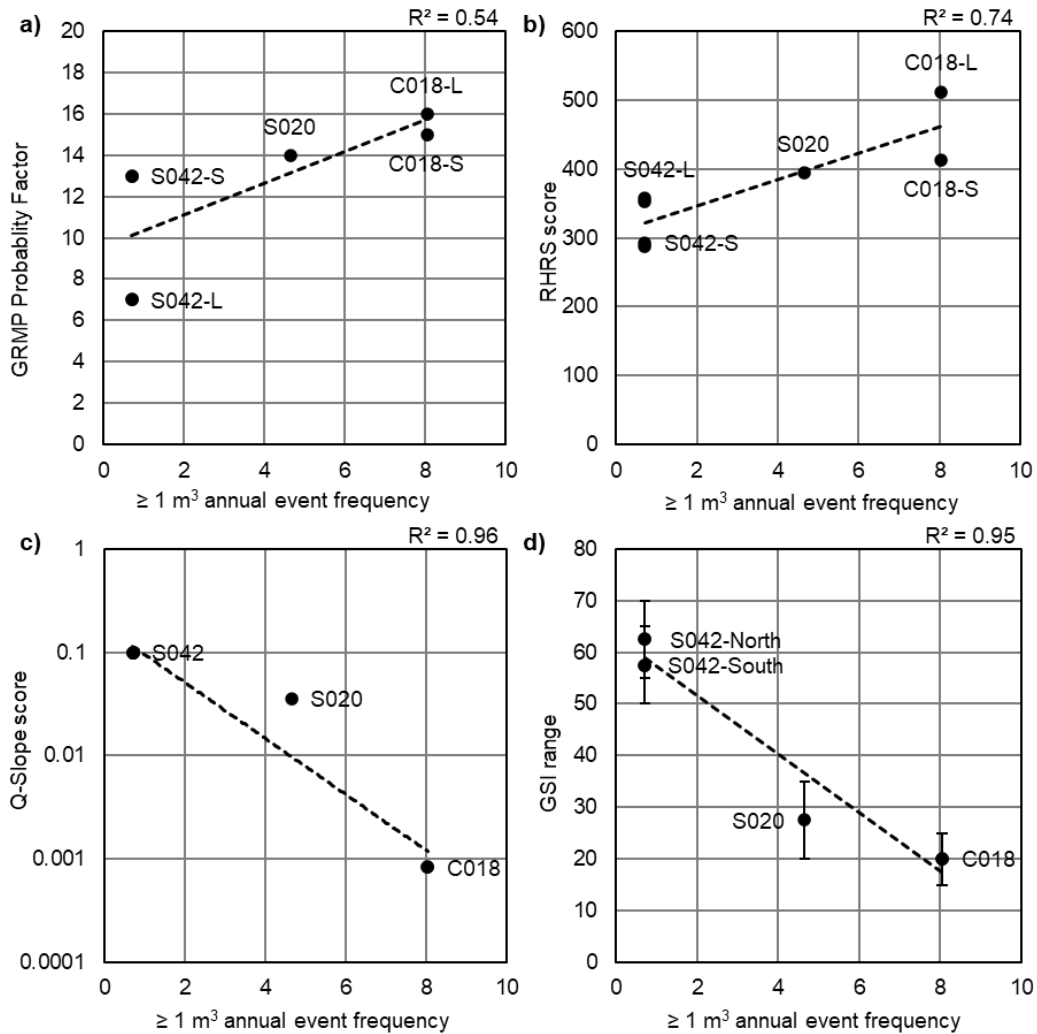
Figure 4-11: Correlations derived from the estimated annual frequency for events greater than or equal to 1 m³ and each shortlisted condition assessment tool, including a) the GRMP PF, b) the RHRS, c) Q-Slope, and d) GSI.

Comparing the R2 values from Figure 4-10 and Figure 4-11, the use of annual event frequencies (Figure 4-11) derived from failure volume-frequency relationships appears to be a slightly more robust failure metric, although more laborious to derive.

Annual failure volumes (Figure 4-10) are more easily extracted from change detection

results and may be updated annually to reflect the changing condition of a site.

The above results clearly show a correlation between the observed frequency and

condition of discontinuities and levels of disaggregation/weathering of the slope

materials, and the frequency and volumes of failure. The methodology illustrated at these

three sites can be deployed at a larger suite of rock slope sites to strengthen the

correlations presented here and allow calculation of confidence intervals for these same

correlations. Furthermore, the continued gathering of remote sensing and rating

information can be leveraged to quantify rock slope deterioration curves as a means of

geologically specific forecast modelling.

4.6 Conclusion

In this paper, the change detection analyses and results of three rockfall geohazard sites

in Alberta are presented. Failure metrics derived from these results were successfully

combined with the results of several established condition assessment tools to illustrate a

method to enhance TEC's ability to assess the performance of rockfall geohazard sites

along Alberta's transportation corridors as part of a GAM program.

The change detection results for the C018 site indicate that the erosional processes

of the highly disaggregated rock mass which has led to debris flows, rockfalls, and

rockslides have an estimated average annual failure volume of 696 m^3, and will continue

to progress. The progressive deterioration observed from the change detection of the

C018 site indicates that additional large failure events, such as debris flows, are likely to

occur if remedial measures are not put in place. This assessment is corroborated by the

results presented in Figure 4-10 and Figure 4-11, indicating a much higher likelihood of

failure for the C018 site than the S020 or S042 sites. Note that this assessment is independent of the consequence of failure, which must be considered to assess the overall risk.

With two years of remote sensing data available for the S020 site, it appears that intense precipitation events during the summer months are major contributors to both erosion of the brow and rockfall events at the site; however continued monitoring is encouraged to improve the understanding of the weather effects on the performance of this slope. An average annual failure volume of 76 m^3 was estimated for the S020 site, with the largest failure event measured at approximately 22.5 m^3. The assigned ratings for the S020 site indicate that it has a high likelihood of rockfall events which is substantiated by the change detection results. Considering the relatively large volume of debris originating from the Extended Brow at the S020 site, continued erosion is anticipated which should be mitigated. Regular clearing of the ditch is recommended to maintain its effectiveness and continuation of the remote sensing program at the S020 site is also recommended to monitor the effects of intense precipitation events and to establish more reliable annual failure volumes.

The change detection analyses conducted for the S042 site yielded relatively little slope change compared to the other study sites. The largest rockfall detected from the slope at the S042 site was an estimated volume of 2.1 m^3 and the average annual failure volumes were only 1.7 m^3 and 0.9 m^3 for north and south slope, respectively. This is counterintuitive with field observations of blocks regularly found at the toe of the slope; however, the change detection results also suggest that most of these blocks likely originate from the talus slope, and the frequent sizes of blocks observed at the toe tend to

be smaller than the limits of detection for the site. The S042 site is a challenging case for the application of condition assessment tools due to its significant height and limited access. The results from Figure 4-10 and Figure 4-11 may be utilized to assist TEC and its consultants in the selection of rockfall volume thresholds and GRMP PFs for the S042 site which are more representative of the likelihood of failure indicated by the change detection results. The failure volumes detected from the S042 site were much lower than the large rockfall event in 2013 which originated from S042-North, with an estimated volume of 15 m^3. This implies that the return period for this failure volume is much greater than the current remote sensing monitoring period. The remote sensing program for the S042 site should be continued to provide further insight into the frequency of relatively large volume events. Although, from the results presented in this paper, the scanning frequency could be reduced to once every two years without significantly impacting its value.

The methodology developed and presented in this paper may be adopted by transportation agencies to improve the long-term monitoring of rockfall geohazards to both validate their assigned condition assessment ratings and justify the need for capital expenditures for sites with the greatest quantified likelihood of failure. The analytical processes presented herein may also be used as a basis for the future development of geologically specific deterioration curves through continued monitoring and the incorporation of financial data pertaining to both maintenance and remedial measures for rockfall geohazards.

4.7 Acknowledgements

4.8 References

Adam Technology. 2023a. 3DM Analyst. Belmont, Australia.

Adam Technology. 2023b. 3DM CalibCam. Belmont, Australia.

Agriculture and Irrigation, Alberta Climate Information Service (ACIS). 2022. Data provided by Agriculture and Irrigation, Alberta Climate Information Service (ACIS) https://acis.alberta.ca (December 2022)

Agüera-Vega, F., Carvajal-Ramírez, F., and Martínez-Carricondo, P. 2017. Accuracy of digital surface models and orthophotos derived from unmanned aerial vehicle photogrammetry. *Journal of Surveying Engineering*, *143*(2):04016025.

Alberta Transportation and Economic Corridors (TEC). 2022. Highway traffic counts, traffic volume data map. Electronic dataset. http://www.transportation.alberta.ca/mapping/ (September 2022)

AMEC Earth & Environmental. 2006. *Geohazards Review: Highway 40 / Highway 541 Corridor, Southwestern Alberta.* Report submitted to Alberta Infrastructure and Transportation.

AMEC Environment and Infrastructure. 2015. *Southern Region Geohazard Assessment, 2014 Annual Inspection Report, Site S42: Highway 742:02, Spray Lakes Rock Fall.* http://www.transportation.alberta.ca/PlanningTools/GMS/Annual%20Landslides%20Assessments/Reg-Southern%20(CMA517,%20CRR)/Inspection%20Sites/25291_02%20or%20742_02%20(S042)%20-%20Spray%20Lakes%20Rockfall/Reports/2014%20S42%20Inspection%20Report.pdf

Barton, N. and Bar, N. 2015. Introducing the Q-slope method and its intended use within civil and mining engineering projects. In *ISRM Regional Symposium-EUROCK 2015*. OnePetro.

Bernhardt, K.L.S., Loehr, J.E., and Huaco, D. 2003. Asset management framework for geotechnical infrastructure. *Journal of infrastructure systems*, 9(3): 107–116. American Society of Civil Engineers.

CloudCompare [GNU GPL software] (2.12). 2022. Retrieved from http://www.cloudcompare.org/

Deane, E., Macciotta, R., Hendry, M.T., Gräpel, C., and Skirrow, R. 2020. Leveraging historical aerial photographs and digital photogrammetry techniques for landslide investigation—a practical perspective. *Landslides*, 17(8): 1989–1996.

DiFrancesco, P.M., Bonneau, D., and Hutchinson, D.J. 2020. The implications of M3C2 projection diameter on 3D semi-automated rockfall extraction from sequential terrestrial laser scanning point clouds. *Remote Sensing*, *12*(11): 1885.

Girardeau-Montaut, D., Roux, M., Marc, R., and Thibault, G. 2005. Change detection on points cloud data acquired with a ground laser scanner. *International Archives of Photogrammetry, Remote Sensing and Spatial Information Sciences*, *36*(part 3), p.W19.

Google Earth Pro 7.3. 2022. Central and southern Alberta. Image © 2022 Google LLC. [Accessed 20 December 2022.]

Hoek, E. 1994. Strength of rock and rock masses. *ISRM News Journal*, 2(2): 4–16.

Klohn Crippen Berger. 2018a. *CON0017608 Central Region GRMP – Call-Out Report, C018 Hwy 837:02 Call-Out Report.* http://www.transportation.alberta.ca/PlanningTools/GMS/Annual%20Landslides%20Assessments/Reg-Central%20Region%20(CMA511-516)/Inspection%20Sites/837_02%20(C18)%20-%20Red%20Deer%20River%20Scour%201.9km%20from%20SH575/Reports/Call%20Out%20Reports/2018%20C018%20Call%20Out%20Report.pdf

Klohn Crippen Berger. 2018b. *Southern Region GRMP Site Inspection Report, S020 Highwood House Rock Cut.* http://www.transportation.alberta.ca/PlanningTools/GMS/Annual%20Landslides%20Assessments/Reg-Southern%20(CMA517,%20CRR)/Inspection%20Sites/541_02%20(S020)%20-%20Highwood%20House%20Rock%20Cut/Reports/2018%20S020%20Inspection%20Report.pdf

Klohn Crippen Berger. 2019. *Southern Region GRMP Site Inspection Report, S042 - I & II Spray Lakes Rockfall.* http://www.transportation.alberta.ca/PlanningTools/GMS/Annual%20Landslides%20Assessments/Reg-Southern%20(CMA517,%20CRR)/Inspection%20Sites/25291_02%20or%20742_02%20(S042)%20-%20-%20Spray%20Lakes%20Rockfall/Reports/2019R%20S042%20Inspection%20Report.pdf

Lague, D., Brodu, N., and Leroux, J. 2013. Accurate 3D comparison of complex topography with terrestrial laser scanner: Application to the Rangitikei canyon (NZ). *ISPRS Journal of Photogrammetry and Remote Sensing*, 82: 10-26.

Lato, M.J. 2010. *Geotechnical applications of LiDAR pertaining to geomechanical evaluation and hazard identification*. Library and Archives Canada. Canada, Ottawa.

Lucieer, A., de Jong, S.M., and Turner, D. 2014. Mapping landslide displacements using Structure from Motion (SfM) and image correlation of multi-temporal UAV photography. *Progress in Physical Geography: Earth and Environment*, 38(1): 97–116.

Macciotta, R. and Hendry, M. 2021. Remote sensing applications for landslide monitoring and investigation in Western Canada. *Remote Sensing*, 13(3): 366

Macciotta, R. and Martin, C.D. 2019. Preliminary approach for prioritizing resource allocation for rock fall hazard investigations based on susceptibility mapping and efficient three-dimensional trajectory modelling. *Bulletin of Engineering Geology and the Environment*, 78(4): 2803-2815.

Macciotta, R., Gräpel, C., Skirrow, R. 2020. Fragmented rockfall volume distribution from photogrammetry-based structural mapping and discrete fracture networks. *Applied Sciences*, 10: 6977.

Macciotta, R., Gräpel, C., Keegan, T., Duxbury, J., and Skirrow, R. 2019. Quantitative risk assessment of rock slope instabilities that threaten a highway near Canmore, Alberta, Canada: managing risk calculation uncertainty in practice. *Canadian Geotechnical Journal,* 57(3): 337-353.

Pierson, L.A. 1992. *Rockfall Hazard Rating System*. Transportation Research Record 1343.

Pix4D S.A. 2023. Pix4Dmapper Pro. Lausanne, Switzerland.

Rodriguez, J., Macciotta, R., Hendry, M.T., Roustaei, M., Gräpel, C., and Skirrow, R. 2020. UAVs for monitoring, investigation, and mitigation design of a rock slope with multiple failure mechanisms—a case study. *Landslides*, 17(9): 2027–2040.

Roustaei, M., Macciotta, R., Hendry, M., Rodriguez, J., Grapel, C., and Skirrow, R. 2020. Characterisation of a rock slope showing three weather-dominated failure modes. In *Proceedings of the 2020 International Symposium on Slope Stability in Open Pit Mining and Civil Engineering*. Australian Centre for Geomechanics, Perth, 427–438.

Salvini, R., Francioni, M., Riccucci, S., Bonciani, F., and Callegari, I. 2013. Photogrammetry and laser scanning for analyzing slope stability and rock fall runout along the Domodossola–Iselle railway, the Italian Alps. *Geomorphology*, 185: 110-122.

Stewart, J. S., Rose, B., Marshall, J. R. 1924. *Upper Elk and Upper Highwood Rivers, British Columbia and Alberta.* Scale 1:253,440. Geological Survey of Canada, Multicoloured Geological Map. Open access from: https://ftp.maps.canada.ca/pub/nrcan_rncan/publications/STPublications_Publicat ionsST/106/106832/gscmcm_1980_e_1924_mn01.pdf

Wollenberg-Barron, T.D.G., Macciotta R., Tappenden, K.M., and Skirrow, R.K. 2023. *Comparison of Rating Systems for Alberta Rock Slopes, and Assessment of Applicability for Geotechnical Asset Management*. University of Alberta Geotechnical Centre [Unpublished].

Chapter 5

Conclusion and Future Research Recommendations

This thesis provides a methodological basis from which results of initial condition assessment tools can be compared with metrics derived from performance monitoring via remote sensing, and subsequent change detection analysis, which may be used to assist transportation agencies with the risk ranking of rockfall geohazards as part of a GAM program.

The development of this methodology was achieved by first conducting a narrative literature review which focused on the concepts, state of practice, framework of asset management and GAM, industry accepted rock slope and rock mass rating systems which could be used as initial condition assessment tools, and remote sensing techniques commonly used for rock slopes and the associated methodologies to conduct change detection analyses.

A critical aspect for the success of this thesis required the understanding of asset management and how the supplementary research material could be best applied to asset management. A GAM framework has been developed and implemented by several US Departments of Transportation (DOT) who have been influential in developing a comprehensive framework of GAM from defining of an agency's goals and registering assets into an inventory, to assessing their condition, continued monitoring and forecasting, through program optimization and addressing both short- and long-term goals of the program. The development of a successful geotechnical asset inventory

requires the use of robust analytical tools to assess, catalog, and subsequently rank the relative condition of assets within an inventory.

The next stage of the literature review focused on the tools available to geotechnical practitioners for assessing the initial condition of rockfall geohazards. With the goal in mind to limit the time and specialized tools required on site to apply the rating systems, following the current methodology of Alberta Transportation and Economic Corridors' (TEC) regional slope tours. TEC's Geohazards Risk Management Program (GRMP) Risk Level (RL) rating was included as a baseline condition assessment since the sites included in the study were pre-existing geohazards in TEC's asset inventory. The Rockfall Hazard Rating System (RHRS) was a clear front-runner for inclusion in the study due to its successful implementation throughout the United States. A multitude of RHRS versions were considered for inclusion in the research, each with varying complexity and certain categories tailored for use in their perspective US state transportation department and subsequent geological setting. The original version was included as a reliable initial condition assessment tool widely accepted by transportation agencies across North America as well as Europe. The results of the literature review indicated that the Modified Colorado RHRS (CRHRS) represented a complex, modernized version of the RHRS which aligned with Alberta's geological setting. To round out the suite of tools, several widely accepted geotechnical rock slope assessment tools were accepted into the study which, indicated by the literature review, were the Geological Strength Index (GSI), Q-Slope, and the Rock Mass Rating (RMR) system.

The selected suite of rock slope and rock mass rating systems (initial condition assessment tools) were successfully applied to eight rockfall geohazards existing within

TEC's geotechnical asset inventory. Each of the selected initial condition assessment tools was directly compared to TEC's rockfall geohazard rating method, the GRMP RL. Some of the selected tools lacked the capacity to quantify the consequence of a failure event, in which case they were compared to the GRMP Probability Factor (PF) instead of the overall Risk Level (RL) rating. Correlations were derived for each of the condition assessment tool results and the corresponding GRMP RL or PF assigned to the geotechnical asset. The results of the correlations indicated that although TEC's GRMP rating system is relatively simplistic, it is viable as an initial condition assessment tool to be used within a comprehensive GAM program. The GRMP RL correlated strongly with the RHRS results for the study sites. The RHRS is a rigorously tested method for assessing rockfall geohazards and is considered a practical alternative to the GRMP RL for rock slopes in Alberta. The GRMP PF correlated reasonably well with both Q-Slope and GSI (validated with RMR). While only a measure of likelihood of failure, Q-Slope and GSI have clear limitations for use as a condition assessment tool. In addition, Q-Slope requires additional time and measurements of a rock mass to effectively apply, making it less practical for use by TEC in Alberta. As a result of this work, RHRS, Q-Slope, and GSI were shortlisted as viable condition assessment tools to be included within further study and possibly implemented along with TEC's GRMP RL rating for rockfall geohazards within Alberta's geological setting.

Following the application of potential condition assessment tools to a variety of rockfall geohazards in Alberta, change detection was performed for the S020 and S042 sites and a methodology was successfully developed correlating the results of initial condition assessment tools with failure metrics derived from change detection results.

106

Failure metrics were selected from the change detection results considering two levels of extraction complexity, from an aggregated annual failure volume to an estimated event frequency for a 1 m^3 volume of rock. Annual failure volumes are a clear indicator of the degree of activity presented at a rockfall site. Failure volume-frequency plots are regularly used to estimate return periods of rockfall events. Event for highly weathered rock masses, like that of the C018 site, the methodology proved viable to develop an approximate failure volume-frequency plot for movements detected throughout the remote sensing monitoring period without distinctly individual movement volumes. Utilizing slope changes detected between scans it was possible to construct an event volume-frequency plot which aligned with the initial correlation. The comparison of the initial condition assessment tool results and the failure metrics derived from the change detection results was successfully employed at three relatively high event likelihood rockfall geohazard sites within TECs asset inventory. This analysis resulted in robust correlations between both selected failure metrics and the short-listed condition assessment tools which illustrated the success of the methodology to combine rating systems and change detection results. This has initiated a database of rockfall geohazards for which TEC can include additional sites where remote sensing techniques have been employed for advanced performance monitoring. The inclusion of additional datapoints will further strengthen the correlations developed and presented in this thesis and provides TEC with an additional tool where relatively high risk rockfall geohazards from across the province can be added with relative ease, following an established methodology, correlated based on quantified performance, and subsequently prioritized for remedial measures as part of a formalized GAM program.

5.1 Recommendations for Further Research

This thesis provides a detailed review of asset management, viable condition assessment tools, and remote sensing techniques from which change detection can be performed. The results of this research provide a methodological basis from which TEC assess the ranking of rockfall geohazards across the province. The following list provides recommendations for further research to build upon the methodology developed in this thesis and assist TEC in the development of a formalized GAM program for rockfall geohazards:

- Develop a more detailed, temporal breakdown of slope changes detected at each of the study sites to analyze the potential for different failure mechanisms and the impact of weather effects. This should also include statistical forecasting of weather effects as a step towards understanding the impacts of climate change.

- Continued monitoring of the C018, S020, and S042 sites and include additional rockfall sites, such as the Grande Prairie region Highway 40 rock fall sites, within the established database to strengthen the derived correlations.

- Include rating system results for before and after the implementation of remedial measures at a rockfall geohazard site, such as rockfall fences, mesh drapes, scaling of the slope, or installation or rock bolts, to quantify the impact of said remedial measures. This will provide valuable insight into which condition assessment tools are able to capture the remedial measures reduction in the likelihood of failure or risk. In addition, the inclusion of economic data pertaining to the cost to install the remedial measure is a critical step in the development of site-specific deterioration curves.

- Development of geologically specific deterioration curves may be advanced with the use of the correlations developed as part of this thesis. With the incorporation of economic data pertaining to remedial measures and maintenance efforts, the changes in year-to-year condition assessment tool results may provide insight necessary to develop site specific deterioration curves. It may also be possible to aggregate rockfall sites within the same geologic setting to determine broader, geologically specific deterioration curves for TEC to implement within regions of Alberta where rockfalls are more prevalent, such as the Kananaskis region along Highway 40 or Grande Prairie region, also along Highway 40.

- Development of a revised GRMP RL rating for rockfall geohazards. Although the GRMP RL and PF correlated well with the shortlisted condition assessment tools, the methodology has clear limitations and relies on the knowledge of the practitioners applying the rating system. The GRMP PF and consequence factors (CF) table would benefit from revisions which incorporated aspects of the RHRS or CRHRS for the consequence to include a measure of exposure. The GRMP PF table could incorporate aspects of GSI, RMR, or Q-Slope to reduce the ambiguity of the scoring selection.

- Conduct a literature review of the modelling tools available for efficiently estimating and extracting the volumes of point clouds. To continue with this line of research, it would be beneficial to TEC and their consultants to develop a standardized methodology for the extraction of rockfall event volumes from point clouds. While methods within CloudCompare exist, the author found that they

were time consuming and carried some degree of uncertainty in their
repeatability.

- Conduct similar research to provide a summary of the available condition
  assessment tools and performance monitoring techniques but focusing on other
  prominent geohazard categories found along transportation corridors such as earth
  slides and debris flows or erosion sites. The eventual goal being an assessment of
  alternative tools for TEC to implement as part of a comprehensive GAM program.

Bibliography

Abellán, A., Calvet, J., Vilaplana, J.M., and Blanchard, J. 2010. Detection and spatial prediction of rockfalls by means of terrestrial laser scanner monitoring. *Geomorphology*, 119(3-4): 162-171.

Adam Technology. 2023a. 3DM Analyst. Belmont, Australia.

Adam Technology. 2023b. 3DM CalibCam. Belmont, Australia.

Agriculture and Irrigation, Alberta Climate Information Service (ACIS). 2022. Data provided by Agriculture and Irrigation, Alberta Climate Information Service (ACIS) https://acis.alberta.ca (accessed December 2022)

Agüera-Vega, F., Carvajal-Ramírez, F., and Martínez-Carricondo, P. 2017. Accuracy of digital surface models and orthophotos derived from unmanned aerial vehicle photogrammetry. *Journal of Surveying Engineering*, *143*(2):04016025.

Aksoy, C.O. 2008. Review of rock mass rating classification: historical developments, applications, and restrictions. *Journal of mining science*, 44(1): 51–63.

Alberta Transportation and Economic Corridors (TEC). 2022. Highway traffic counts, traffic volume data map. Electronic dataset. http://www.transportation.alberta.ca/mapping/ (accessed September 2022)

AMEC Earth & Environmental. 2006. *Geohazards Review: Highway 40 / Highway 541 Corridor, Southwestern Alberta*. Report submitted to Alberta Infrastructure and Transportation.

AMEC Environment and Infrastructure. 2015. *Southern Region Geohazard Assessment, 2014 Annual Inspection Report, Site S42: Highway 742:02, Spray Lakes Rock Fall.* http://www.transportation.alberta.ca/PlanningTools/GMS/Annual%20Landslides%20Assessments/Reg-Southern%20(CMA517,%20CRR)/Inspection%20Sites/25291_02%20or%20742_02%20(S042)%20-%20Spray%20Lakes%20Rockfall/Reports/2014%20S42%20Inspection%20Report.pdf

AMEC. 2006. Geohazards Review - *Highway 40/Highway 541 Corridor, Site 28 - Lipsett Ridge Rock Cut.* http://www.transportation.alberta.ca/PlanningTools/GMS/Annual%20Landslides%20Assessments/Reg-Southern%20(CMA517,%20CRR)/Expired%20Sites/040_12%20(S074-

1%20to%205)%20-
%20Lineham%20Creek%20to%20Lipsett%20Geohazards/040_10%20(S074-
5)%20-%20Lipsett%20Ridge%20Rock%20cut/Reports/2006%20S074-
5%20Inspection%20Report.pdf

AMEC. 2009a. *Site S018 - Galatea Rockfall, Highway 40:12, Kananaskis River Valley, Alberta*, Site Data - Summary Binder, Section A - File Review.
http://www.transportation.alberta.ca/PlanningTools/GMS/Annual%20Landslides
%20Assessments/Reg-
Southern%20(CMA517,%20CRR)/Inspection%20Sites/040_12%20(S018)%20-
%20Galatea%20Creek%20Through-
Cut/Reports/Section%20A/2009%20S18%20Section%20A%20Report.pdf

AMEC. 2009b. *Southern Region Geohazard Assessment Program, Highway 541:02, East of Fir Creek Rock Cut Site, June 2009 Inspection Report*.
http://www.transportation.alberta.ca/PlanningTools/GMS/Annual%20Landslides
%20Assessments/Reg-
Southern%20(CMA517,%20CRR)/Expired%20Sites/541_02%20(S070-
1%20to%208)%20-
%20Eyrie%20Gap%20and%20Fir%20Creek%20Geohazard%20Sites/541_02%2
0(S070-6)%20-%20East%20of%20Fir%20Creek/Reports/2009%20S070-
6%20%20Inspection%20Report.pdf

American Association of State Highway Transportation Officials (AASHTO). 2020. *Transportation Asset Management Guide*. Available from: https://www.tamguide.com/ (accessed March 2023).

Anderson, S.A., Schaefer, V.R., and Nichols, S.C. 2016. *Taxonomy for geotechnical assets, elements, and features* (No. 16-5659).

Baecher, G.B., Christian, J.T. 2003. *Reliability and Statistics in Geotechnical Engineering.* John Wiley & Sons.

Bar, N. and Barton, N. 2017. The Q-slope method for rock slope engineering. *Rock Mechanics and Rock Engineering*, 50(12): 3307–3322.

Bar, N., Barton, N.R., and Ryan, C.A. 2016. Application of the Q-slope method to highly weathered and saprolitic rocks in Far North Queensland. In *ISRM International Symposium-EUROCK 2016.*

Barton, N. and Bar, N. 2015. Introducing the Q-slope method and its intended use within civil and mining engineering projects. In *ISRM Regional Symposium-EUROCK 2015.*

Barton, N. and Grimstad, E. 2014. Forty years with the Q-system in Norway and abroad. *Fjellsprengningsteknikk, Bergmekanikk, Geoteknikk*, vol 4.1–4.25.

Barton, N., Lien, R., and Lunde, J. 1974. Engineering classification of rock masses for the design of tunnel support. *Rock Mechanics*, 6(4): 189–236.

Bernhardt, K.L.S., Loehr, J.E., and Huaco, D. 2003. Asset management framework for geotechnical infrastructure. *Journal of Infrastructure Systems*, 9(3): 107–116. American Society of Civil Engineers.

Bieniawski, Z.T. 1973. Engineering classification of jointed rock masses. *The Civil Engineer*, South African Institution of Civil Engineering (SAICE), 1973(12): 335–343.

Bieniawski, Z.T. 1989. *Engineering rock mass classifications: a complete manual for engineers and geologists in mining, civil, and petroleum engineering*. John Wiley & Sons.

Bieniawski, Z.T. 1993. Classification of rock masses for engineering: the RMR system and future trends. In *Rock Testing and Site Characterization*. 553-573, Elsevier.

Brawner, C.O. and Wyllie, D. 1976. Rock slope stability on railway projects. *American Railway Engineering Association*, Bulletin 656: 449–474.

Budetta, P. 2004. Assessment of rockfall risk along roads. *Natural Hazards and Earth System Sciences*, 4(1): 71–81.

Cambridge Systematics, Texas Transportation Institute and Parsons Brinckerhoff. 2006. Performance measures and targets for transportation asset management (Vol. 551). Transportation Research Board.

CloudCompare [GNU GPL software] (2.12). 2022. Retrieved from http://www.cloudcompare.org/

Colorado Department of Transportation. 2020. Laboratory Manual of Test Procedures, Determining the Durability of Shales for Use as Embankments, CP-L 3104. https://www.codot.gov/business/designsupport/materials-and-geotechnical/manuals/2020-laboratory-manual-of-test-procedures/lmtp

Deane, E., Macciotta, R., Hendry, M.T., Gräpel, C., and Skirrow, R. 2020. Leveraging historical aerial photographs and digital photogrammetry techniques for landslide investigation—a practical perspective. *Landslides*, 17(8): 1989–1996.

Dehghanisanij, M., Flintsch, G.W., and Verhoeven, J. 2012. Framework for Aggregating Highway Asset Performance Measures: Application to Resource Allocation Across Assets. *Transportation Research Record*, 2271(1): 37-44.

DiFrancesco, P.M., Bonneau, D., and Hutchinson, D.J. 2020. The implications of M3C2 projection diameter on 3D semi-automated rockfall extraction from sequential terrestrial laser scanning point clouds. *Remote Sensing*, *12*(11): 1885.

Federal Highway Administration (FHWA). 1999. Asset Management Primer. Office of Asset Management, Washington, D.C.

Fish, M. and Lane, R. 2002. Linking New Hampshire's rock cut management system with a geographic information system. *Transportation Research Record*, SAGE Publications, 1786(1): 51–59.

Gigli, G. and Casagli, N. 2011. Semi-automatic extraction of rock mass structural data from high resolution LIDAR point clouds. *International Journal of Rock Mechanics and Mining Sciences*, 48(2): 187–198.

Girardeau-Montaut, D., Roux, M., Marc, R., and Thibault, G. 2005. Change detection on points cloud data acquired with a ground laser scanner. *International Archives of Photogrammetry, Remote Sensing and Spatial Information Sciences*, *36*(part 3), p.W19.

Google Earth Pro 7.3. 2022. Central and southern Alberta. Image © 2022 Google LLC. (Accessed 20 December 2022).

Grussing, M.N., Uzarski, D.R., and Marrano, L.R. 2006. Condition and reliability prediction models using the Weibull probability distribution. In *Applications of Advanced Technology in Transportation*, 19-24.

Hadjin, D.J. 2002. New York State Department of Transportation rock slope rating procedure and rockfall assessment. *Transportation Research Record*, SAGE Publications, 1786(1): 60–68.

Haneberg, W.C., Norrish, N.I., and Findley, D.P. 2006. Digital Outcrop Characterization for 3-D Structural Mapping and Rock Slope Design Along Interstate 90 Near Snoqualmie Pass, Washington. In *Proceedings, 57th annual highway geology symposium*. Breckenridge, Colorado, USA.

Higgins, J.D., Andrew, R.D., Turner, K.A.. and Schuster, R.L. 2012. Rockfall types and causes. In *Rockfall Characterization and Control*, 21-55.

Hoek, E. 1994. Strength of rock and rock masses. *ISRM News Journal*, 2(2): 4–16.

Hoek, E. and Bray, J.D. 1981. *Rock slope engineering*. CRC press.

Hoek, E., and Brown, E.T. 1997. Practical estimates of rock mass strength. *International Journal of Rock Mechanics and Mining Sciences*, 34(8): 1165–1186.

Hoek, E. and Brown, E.T., 2019. The Hoek–Brown failure criterion and GSI – 2018 edition. *Journal of Rock Mechanics and Geotechnical Engineering*, 11(3): 445-463.

Hoek, E., Kaiser, P.K., and Bawden, W.F. 1995. *Support of Underground Excavations in Hard Rock*. Balkema, Rotterdam, Netherlands.

Hutchinson, D.J. and Diederichs, M. 1996. The cablebolting cycle - underground support engineering. *CIM Bulletin*, 89(1001). Sudbury, Ontario, Canada.

Justice, S.M. 2015. *Application of a Hazard Rating System for Rock Slopes Along a Transportation Corridor Using Remote Sensing*. Michigan Technological University.

Klohn Crippen Berger. 2018a. *Southern Region GRMP Site Inspection Report, S020 Highwood House Rock Cut.* http://www.transportation.alberta.ca/PlanningTools/GMS/Annual%20Landslides%20Assessments/Reg-Southern%20(CMA517,%20CRR)/Inspection%20Sites/541_02%20(S020)%20-%20Highwood%20House%20Rock%20Cut/Reports/2018%20S020%20Inspection%20Report.pdf

Klohn Crippen Berger. 2018b. *CON0017608 Central Region GRMP – Call-Out Report, C018 Hwy 837:02 Call-Out Report.* http://www.transportation.alberta.ca/PlanningTools/GMS/Annual%20Landslides%20Assessments/Reg-Central%20Region%20(CMA511-516)/Inspection%20Sites/837_02%20(C18)%20-%20Red%20Deer%20River%20Scour%201.9km%20from%20SH575/Reports/Call%20Out%20Reports/2018%20C018%20Call%20Out%20Report.pdf

Klohn Crippen Berger. 2019a. *Southern Region Geohazard Risk Management Plan, Hwy 1A:02, km 12.52 to 11.91 Call-Out Report.* http://www.transportation.alberta.ca/PlanningTools/GMS/Annual%20Landslides%20Assessments/Reg-Southern%20(CMA517,%20CRR)/Inspection%20Sites/001A-02%20(S057)%20-%20Rock%20fall%20sites%20near%20Exshaw/Reports/Call%20Out%20Reports/2019%20S057%20Call%20Out.pdf

Klohn Crippen Berger. 2019b. *Southern Region GRMP Site Inspection Report, S042 - I & II Spray Lakes Rockfall.* http://www.transportation.alberta.ca/PlanningTools/GMS/Annual%20Landslides%20Assessments/Reg-Southern%20(CMA517,%20CRR)/Inspection%20Sites/25291_02%20or%20742_02%20(S042)%20-%20Spray%20Lakes%20Rockfall/Reports/2019R%20S042%20Inspection%20Report.pdf

Klohn Crippen Consultants Ltd. 2001. *Alberta Transportation Central Region, Site C018 Annual Inspection Report.*
http://www.transportation.alberta.ca/PlanningTools/GMS/Annual%20Landslides%20Assessments/Reg-Central%20Region%20(CMA511-516)/Inspection%20Sites/837_02%20(C18)%20-%20Red%20Deer%20River%20Scour%201.9km%20from%20SH575/Reports/2001%20C018%20Inspection%20Report.pdf

Kromer, R., Lato, M., Hutchinson, D.J., Gauthier, D. and Edwards, T., 2017. Managing rockfall risk through baseline monitoring of precursors using a terrestrial laser scanner. *Canadian Geotechnical Journal*, 54(7): 953-967.

Kromer, R.A., Hutchinson, D.J., Lato, M.J., Gauthier, D. and Edwards, T. 2015. Identifying rock slope failure precursors using LiDAR for transportation corridor hazard management. *Engineering Geology*, 195: 93-103.

Lague, D., Brodu, N., and Leroux, J. 2013. Accurate 3D comparison of complex topography with terrestrial laser scanner: Application to the Rangitikei canyon (NZ). *ISPRS Journal of Photogrammetry and Remote Sensing*, 82: 10-26.

Lato, M.J. 2010. *Geotechnical applications of LiDAR pertaining to geomechanical evaluation and hazard identification*. Library and Archives Canada. Canada, Ottawa.

Lato, M., Diederichs, M.S., Hutchinson, D.J. and Harrap, R. 2009. Optimization of LiDAR scanning and processing for automated structural evaluation of discontinuities in rockmasses. *International Journal of Rock Mechanics and Mining Sciences*, 46(1): 194-199.

Lucieer, A., de Jong, S.M., and Turner, D. 2014. Mapping landslide displacements using Structure from Motion (SfM) and image correlation of multi-temporal UAV photography. *Progress in Physical Geography: Earth and Environment*, 38(1): 97–116.

Macciotta, R. 2019. Review and latest insights into rock fall temporal variability associated with weather. *Proceedings of the Institution of Civil Engineers-Geotechnical Engineering*, 172(6): 556-568.

Macciotta, R. and Hendry, M. 2021. Remote sensing applications for landslide monitoring and investigation in Western Canada. *Remote Sensing*, 13(3): 366.

Macciotta, R. and Martin, C.D. 2019. Preliminary approach for prioritizing resource allocation for rock fall hazard investigations based on susceptibility mapping and efficient three-dimensional trajectory modelling. *Bulletin of Engineering Geology and the Environment*, 78(4): 2803-2815.

Macciotta, R., Gräpel, C., and Skirrow, R. 2020. Fragmented rockfall volume distribution from photogrammetry-based structural mapping and discrete fracture networks. *Applied Sciences*, 10(19): 6977.

Macciotta, R., Grapel, C., Duxbury, J., Keegan, T., and Skirrow, R. 2018. Explicit estimation of rock slope failure likelihood for hazard assessment and safety engineering near Canmore, AB. In *Proceedings of the 7th Canadian Conference on Geohazards: Geohazards* (Vol. 7).

Macciotta, R., Gräpel, C., Keegan, T., Duxbury, J., and Skirrow, R. 2019. Quantitative risk assessment of rock slope instabilities that threaten a highway near Canmore, Alberta, Canada: managing risk calculation uncertainty in practice. *Canadian Geotechnical Journal*, 57(3): 337-353.

Macciotta, R., Hendry, M., Cruden, D.M., Blais-Stevens, A., and Edwards, T. 2017. Quantifying rock fall probabilities and their temporal distribution associated with weather seasonality. *Landslides*, 14(6): 2025-2039.

Maerz, N.H., Otoo, J., Kassebaum, T. and Boyko, K. 2012. Using LIDAR in highway rock cuts. In *Proceedings of the 63rd Annual Highway Geology Symposium,* 7-10.

Maerz, N.H., Youssef, A., and Fennessey, T.W. 2005. New risk–consequence rockfall hazard rating system for Missouri highways using digital image analysis. *Environmental & Engineering Geoscience*, Association of Environmental & Engineering Geologists, 11(3): 229–249.

Marinos, P., and Hoek, E. 2000. GSI: A Geologically Friendly Tool for Rock Mass Strength Estimation. *ISRM International Symposium*.

Marinos, P.G., Marinos, V., and Hoek, E. 2007. The Geological Strength Index (GSI): A Characterization Tool for Assessing Engineering Properties for Rock Masses. In *The International Workshop on Rock Mass Classification in Underground Mining*.

Marinos, V., Marinos, P., and Hoek, E. 2005. The geological strength index: applications and limitations. *Bulletin of Engineering Geology and the Environment*, 64(1): 55–65.

McHechan, M. E. 1995. *Rocky Mountain Foothills and Front Ranges in Kananaskis Country, West of Fifth Meridian, Alberta.* Scale 1:100,000. Geological Survey of Canada, "A" Series Map 1865A. Open access from: https://ftp.maps.canada.ca/pub/nrcan_rncan/publications/STPublications_Publicat ionsST/204/204897/gscmap-a_1865a_e_1995_mg01.pdf

Miller, S.M. 2003. Development and implementation of the Idaho highway slope instability and management system (HiSIMS). Prepared for Idaho Transporation Department.

Oppikofer, T., Jaboyedoff, M., Blikra, L., Derron, M.H. and Metzger, R. 2009. Characterization and monitoring of the Åknes rockslide using terrestrial laser scanning. *Natural Hazards and Earth System Sciences*, 9(3): 1003-1019.

Otoo, J.N., Maerz, N.H., Xiaoling, L., and Duan, Y. 2011. 3-D Discontinuity Orientations Using Combined Optical Imaging And LiDAR Techniques. In *45th U.S. Rock Mechanics / Geomechanics Symposium*. San Francisco, California.

Pierson, L.A. 1992. *Rockfall Hazard Rating System.* Transportation Research Record 1343

Pierson, L.A. and Van Vickle, R. 1993. *Rockfall Hazard Rating System: Participant's Manual*. Federal Highways Administration. SA-93-057.

Pierson, L.A., Turner, A.K., Turner, K.A., and Schuster, R.L. 2012. Implementation of rock slope management systems. In *Rockfall Characterization and Control*, 73-112.

Pix4D S.A. 2023. Pix4Dmapper Pro. Lausanne, Switzerland.

Pratt, C., Macciotta, R., and Hendry, M. 2019. Quantitative relationship between weather seasonality and rock all occurrences north of Hope, BC, Canada. *Bulletin of Engineering Geology and the Environment*, 78(5): 3239-3251.

Price, R. A. 1970. *Geology, Canmore (west half), west of Fifth Meridian, Alberta.* Scale 1:50,000. Geological Survey of Canada, "A" Series Map 1266A. Open access from: https://ftp.maps.canada.ca/pub/nrcan_rncan/publications/STPublications_PublicationsST/108/108954/gid_108954.zip

Riquelme, A., Cano, M., Tomás, R., and Abellán, A. 2017. Identification of Rock Slope Discontinuity Sets from Laser Scanner and Photogrammetric Point Clouds: A Comparative Analysis. *Procedia Engineering*, 191: 838–845.

Riquelme, A.J., Abellán, A., and Tomás, R. 2015. Discontinuity spacing analysis in rock masses using 3D point clouds. *Engineering Geology*, 195: 185–195.

Riquelme, A.J., Abellán, A., Tomás, R., and Jaboyedoff, M. 2014. A new approach for semi-automatic rock mass joints recognition from 3D point clouds. *Computers & Geosciences*, 68: 38–52.

Riquelme, A.J., Tomás, R., and Abellán, A. 2016. Characterization of rock slopes through slope mass rating using 3D point clouds. *International Journal of Rock Mechanics and Mining Sciences*, 84: 165–176.

Rodriguez, J., Macciotta, R., Hendry, M.T., Roustaei, M., Gräpel, C., and Skirrow, R. 2020. UAVs for monitoring, investigation, and mitigation design of a rock slope with multiple failure mechanisms—a case study. *Landslides*, 17(9): 2027–2040.

Romana, M. 1985. New adjustment ratings for application of Bieniawski classification to slopes. In *Proceedings of the international symposium on role of rock mechanics*, Zacatecas, Mexico, 49–53.

Romana, M., Tomás, R., and Serón, J.B. 2015. Slope Mass Rating (SMR) geomechanics classification: thirty years review. *13th ISRM International Congress of Rock Mechanics*, OnePetro, Quebec, Canada. 10 pp.

Rose, B.T. 2005. *Tennessee rockfall management system.* Virginia Polytechnic Institute and State University.

Roustaei, M., Macciotta R., Hendry, M., Rodriguez, J., Gräpel, C., and Skirrow, R. 2020. Characterisation of a rock slope showing three weather-dominated failure modes. In *Proceedings of the 2020 International Symposium on Slope Stability in Open Pit Mining and Civil Engineering.* Australian Centre for Geomechanics, Perth. 427–438.

Russell, C.P., Santi, P., and Higgins, J.D. 2008. *Modification and Statistical Analysis of the Colorado Rockfall Hazard Rating System*. Prepared for Colorado Department of Transportation.

Salvini, R., Francioni, M., Riccucci, S., Bonciani, F., and Callegari, I. 2013. Photogrammetry and laser scanning for analyzing slope stability and rock fall runout along the Domodossola–Iselle railway, the Italian Alps. *Geomorphology*, 185: 110-122.

Santi, P.M., Russell, C.P., Higgins, J.D., and Spriet, J.I. 2009. Modification and statistical analysis of the Colorado rockfall hazard rating system. *Engineering Geology*, 104(1–2): 55–65.

Shah, J., Jefferson, I., Ghataora, G., and Hunt, D. 2014. Resilient geotechnical infrastructure asset management. In *Geo-Congress 2014: Geo-characterization and Modeling for Sustainability*, 3769-3778.

Shakoor, A. 2005. *Development of a rockfall hazard rating matrix for the State of Ohio*. Prepared for Ohio Department of Transporation Office of Research and Development.

Stanley, D.A. and Pierson, L.A. 2013. Geotechnical Asset Management of Slopes: Condition Indices and Performance Measures. *Geo-Congress 2013*. ASCE, San Diego, California, USA, 1651–1660.

Stewart, J. S., Rose, B., Marshall, J. R. 1924. *Upper Elk and Upper Highwood Rivers, British Columbia and Alberta.* Scale 1:253,440. Geological Survey of Canada, Multicoloured Geological Map. Open access from: https://ftp.maps.canada.ca/pub/nrcan_rncan/publications/STPublications_Publicat ionsST/106/106832/gscmcm_1980_e_1924_mn01.pdf

Stover, B.K. 1992. *Highway Rockfall Research Report: Colorado Gelogical Survey, 37*. Special Publication. 27 pp.

Sturzenegger, M. and Stead, D. 2009. Quantifying discontinuity orientation and persistence on high mountain rock slopes and large landslides using terrestrial remote sensing techniques. *Natural Hazards and Earth System Sciences*, 9(2): 267-287.

Tappenden, K.M. and Skirrow, R.K. 2020. Vision for Geotechnical Asset Management at Alberta Transportation. *2020 Canadian Geotechnical Conference (GeoVirtual)*.

Thompson, P.D. 2017. *Geotechnical Asset Management Plan*. Prepared for Alaska Department of Transportation and Public Facilities.

Vandewater, C.J., Dunne, W.M., Mauldon, M., Drumm, E.C., and Bateman, V. 2005. Classifying and Assessing the Geologic Contribution to Rockfall Hazard. *Environmental & Engineering Geoscience*, Association of Environmental & Engineering Geologists, 11(2): 141–154.

Vessely, M. 2013. Risk Based Methods for Management of Geotechnical Features in Transportation Infrastructure. *Geo-Congress 2013*. ASCE, San Diego, California, USA. pp. 1625–1632.

Vessely, M., Robert, W., Richrath, S., Schaefer, V.R., Smadi, O., Loehr, E., and Boeckmann, A. 2019. *Geotechnical Asset Management for Transportation Agencies, Volume 1: Research Overview* (No. Project 24-46).

Walkinshaw, J.L. and Santi, P.M. 1996. *Landslides: Investigation and Mitigation*. Chapter 21-Shales and Other Degradable Materials. Transportation Research Board Special Report, 247.

Wolf, R.E., Bouali, E.H., Oommen, T., Dobson, R.J., Vitton, S., Brooks, C., and Lautala, P. 2015. *Sustainable Geotechnical Asset Management Along the Transportation Infrastructure Environment Using Remote Sensing: Final Report.* Michigan Technological University, Houghton, MI, USA.

Wollenberg-Barron T., Macciotta R., Gräpel C., Tappenden K., Skirrow R. 2022. Use of rock slope rating systems with remote sensing for Geotechnical Asset Management and preliminary application at a rock slope in Southern AB. In *Proceedings of the 8th Canadian Conference on Geotechnique and Natural Hazards:Geohazards 8, Quebec City, Musée de la civilisation*, 12-15 June, 2022. Canadian Geotechnical Society.

Wollenberg-Barron, T.D.G., Macciotta R., Tappenden, K.M., and Skirrow, R.K. 2023. Comparison of Rating Systems for Alberta Rock Slopes, and Assessment of Applicability for Geotechnical Asset Management. University of Alberta Geotechnical Centre [Unpublished].

Woods, A., Macciotta, R., Hendry, M.T., Stewart, T. and Marsh, J. 2021. Updated understanding of the deformation characteristics of the Checkerboard Creek rock slope through GB-InSAR monitoring. *Engineering Geology*, 28:105974.

Wyllie, D.C. 2014. *Rock fall engineering*. CRC Press.

Appendix A

GRMP Risk Level Rating – Table B – Geohazard Risk Level Factors – Rock Fall

Probability Factor (ranked on a scale of 1 to 20)	
1	Inactive, very low probability of fall occurrence
3	Inactive, low probability of fall occurrence.
5	Inactive, moderate probability of fall occurrence.
7	Inactive, high probability of fall occurrence (e.g., seasonal, following freeze/thaw cycles) and/or a fall has occurred in the past.
9	Active, falls occur after exceptional weather (e.g., the melting of greater than average snow accumulations or exceptionally intense precipitation), fall frequency is in the order of once a decade.
11	Active, one or two falls occur each year triggered by annually recurring weather conditions.
13	Active, several falls occur each year and/or the frequency of falls is increasing in comparison to equivalent time periods in previous years.
15	Active, many falls occur each year and/or the area producing rock falls is expanding. Ongoing or persistent rock falls during specific times of the year.
20	Active, a large volume of rock is surrounded by open cracks. Toppling or sliding of the displacing mass is accelerating. Sites where rapid movement of a large fall is possible.

Consequence Factor (ranked on a scale of 1 to 10)	
1	Rock fall contained by ditch if cleaned as required to maintain capacity.
2	Rock fall onto roadway removable by maintenance crews by hand or with shovels. Road closure not required. Minor damage to the road surface that can be repaired during annual patching and sealing of the road. Minor to no damage to vehicles being struck by falling rocks or striking rocks deposited onto road.
3	Rock fall onto road that could damage a vehicle (e.g., flat tire, dent body of vehicle). Rocks bounce or roll onto the road surface but likely not with a trajectory that would pass through the windows or windshield of a passing vehicle.

4	Individual rocks or the total volume of rocks deposited on the road large enough to: • Damage vehicles or cause accidents if struck by traffic or damage vehicles and injure occupants if they strike a moving vehicle. • Cause partial closure of the road or require a detour lane prior to cleanup. • Damage to the road surface may require temporary repair in order to re-open road.
6	Individual rocks or the total volume of rocks deposited on the road large enough to: • Damage/destroy vehicles and severely injure occupants if struck by traffic or damage/destroy vehicles and severely injure/kill occupants if they strike a moving vehicle. • Cause complete closure of the road, with a rough detour/diversion possible within hours to days. • Require days to weeks required to restore the road to normal service. • Possibly significant damage to the road surface that requires immediate repair.
8	Same as weighting of 6, but with several days required to develop a rough detour/diversion around the rockfall site.
10	Individual rocks or the total volume of rocks deposited on the road large enough to: • Damage/destroy vehicles and severely injure occupants if struck by traffic. • Bury vehicles if they strike a moving vehicle. • Cause complete closure of the road, with a temporary, rough detour or diversion possible in days to weeks. • Require complete reconstruction or rerouting of the road after the rockfall.

Appendix B

GSI and J$_n$ Determination Figures

C018 – Red Deer River Valley Slope Instability – GSI and Joint Set Number

Jn: 20 (Crushed rock, earthlike)

S018 – Galatea Creek Rock Cut – GSI and Joint Set Number

Jn: 9 (Three joint set)

S020 – Highwood House Rockfall Hazard – GSI and Joint Set Number — Jn: 12 (Three joint sets plus random joints)

S042 – Spray Lakes Rockfall (North) – GSI and Joint Set Number — Jn: 9 (Three joint sets)

125

S042 – Spray Lakes Rockfall (South) – GSI and Joint Set Number

Jn: 9 (Three joint sets)

GEOLOGICAL STRENGTH INDEX FOR JOINTED ROCKS (Hoek and Marinos, 2000)

From the lithology, structure and surface conditions of the discontinuities, estimate the average value of GSI. Do not try to be too precise. Quoting a range from 33 to 37 is more realistic than stating that GSI = 35. Note that the table does not apply to structurally controlled failures. Where weak planar structural planes are present in an unfavourable orientation with respect to the excavation face, these will dominate the rock mass behaviour. The shear strength of surfaces in rocks that are prone to deterioration as a result of changes in moisture content will be reduced if water is present. When working with rocks in the fair to very poor categories, a shift to the right may be made for wet conditions. Water pressure is dealt with by effective stress analysis.

SURFACE CONDITIONS / DECREASING SURFACE QUALITY →

- VERY GOOD — Very rough, fresh unweathered surfaces
- GOOD — Rough, slightly weathered, iron stained surfaces
- FAIR — Smooth, moderately weathered and altered surfaces
- POOR — Slickensided, highly weathered surfaces with compact coatings or fillings or angular fragments
- VERY POOR — Slickensided, highly weathered surfaces with soft clay coatings or fillings

STRUCTURE / DECREASING INTERLOCKING OF ROCK PIECES

- INTACT OR MASSIVE - intact rock specimens or massive in situ rock with few widely spaced discontinuities — 90 / 80 / N/A / N/A
- BLOCKY - well interlocked undisturbed rock mass consisting of cubical blocks formed by three intersecting discontinuity sets — 70 / 60
- VERY BLOCKY - interlocked, partially disturbed mass with multi-faceted angular blocks formed by 4 or more joint sets — 50
- BLOCKY/DISTURBED/SEAMY - folded with angular blocks formed by many intersecting discontinuity sets. Persistence of bedding planes or schistosity — 40 / 30
- DISINTEGRATED - poorly interlocked, heavily broken rock mass with mixture of angular and rounded rock pieces — 20
- LAMINATED/SHEARED - Lack of blockiness due to close spacing of weak schistosity or shear planes — N/A / N/A / 10

155 m

S057 – Hwy 1A, Exshaw, Site A – GSI and Joint Set Number

Jn: 15 (Four or more joint sets, random, heavily jointed)

GEOLOGICAL STRENGTH INDEX FOR JOINTED ROCKS (Hoek and Marinos, 2000)

From the lithology, structure and surface conditions of the discontinuities, estimate the average value of GSI. Do not try to be too precise. Quoting a range from 33 to 37 is more realistic than stating that GSI = 35. Note that the table does not apply to structurally controlled failures. Where weak planar structural planes are present in an unfavourable orientation with respect to the excavation face, these will dominate the rock mass behaviour. The shear strength of surfaces in rocks that are prone to deterioration as a result of changes in moisture content will be reduced if water is present. When working with rocks in the fair to very poor categories, a shift to the right may be made for wet conditions. Water pressure is dealt with by effective stress analysis.

SURFACE CONDITIONS / DECREASING SURFACE QUALITY →

- VERY GOOD — Very rough, fresh unweathered surfaces
- GOOD — Rough, slightly weathered, iron stained surfaces
- FAIR — Smooth, moderately weathered and altered surfaces
- POOR — Slickensided, highly weathered surfaces with compact coatings or fillings or angular fragments
- VERY POOR — Slickensided, highly weathered surfaces with soft clay coatings or fillings

STRUCTURE / DECREASING INTERLOCKING OF ROCK PIECES

- INTACT OR MASSIVE - intact rock specimens or massive in situ rock with few widely spaced discontinuities — 90 / 80 / N/A / N/A
- BLOCKY - well interlocked undisturbed rock mass consisting of cubical blocks formed by three intersecting discontinuity sets — 70 / 60
- VERY BLOCKY - interlocked, partially disturbed mass with multi-faceted angular blocks formed by 4 or more joint sets — 50
- BLOCKY/DISTURBED/SEAMY - folded with angular blocks formed by many intersecting discontinuity sets. Persistence of bedding planes or schistosity — 40 / 30
- DISINTEGRATED - poorly interlocked, heavily broken rock mass with mixture of angular and rounded rock pieces — 20
- LAMINATED/SHEARED - Lack of blockiness due to close spacing of weak schistosity or shear planes — N/A / N/A / 10

15 m

S057 – Hwy 1A, Exshaw, Site B – GSI and Joint Set Number

Jn: 12 (Three joint sets plus random joints)

S070 – East of Fir Creek Rock Cut – GSI and Joint Set Number

Jn: 12 (One joint set plus random joints)

GEOLOGICAL STRENGTH INDEX FOR JOINTED ROCKS (Hoek and Marinos, 2000)

From the lithology, structure and surface conditions of the discontinuities, estimate the average value of GSI. Do not try to be too precise. Quoting a range from 33 to 37 is more realistic than stating that GSI = 35. Note that the table does not apply to structurally controlled failures. Where weak planar structural planes are present in an unfavourable orientation with respect to the excavation face, these will dominate the rock mass behaviour. The shear strength of surfaces in rocks that are prone to deterioration as a result of changes in moisture content will be reduced if water is present. When working with rocks in the fair to very poor categories, a shift to the right may be made for wet conditions. Water pressure is dealt with by effective stress analysis.

		SURFACE CONDITIONS	VERY GOOD Very rough, fresh unweathered surfaces	GOOD Rough, slightly weathered, iron stained surfaces	FAIR Smooth, moderately weathered and altered surfaces	POOR Slickensided, highly weathered surfaces with compact coatings or fillings or angular fragments	VERY POOR Slickensided, highly weathered surfaces with soft clay coatings or fillings
STRUCTURE			DECREASING SURFACE QUALITY ⟹				
INTACT OR MASSIVE - intact rock specimens or massive in situ rock with few widely spaced discontinuities		DECREASING INTERLOCKING OF ROCK PIECES	90 / 80			N/A	N/A
BLOCKY - well interlocked undisturbed rock mass consisting of cubical blocks formed by three intersecting discontinuity sets				70 / 60			
VERY BLOCKY- interlocked, partially disturbed mass with multi-faceted angular blocks formed by 4 or more joint sets					50		
BLOCKY/DISTURBED/SEAMY - folded with angular blocks formed by many intersecting discontinuity sets. Persistence of bedding planes or schistosity					40 / 30		
DISINTEGRATED - poorly interlocked, heavily broken rock mass with mixture of angular and rounded rock pieces						20	
LAMINATED/SHEARED - Lack of blockiness due to close spacing of weak schistosity or shear planes			N/A	N/A			10